PARTICLE DIFFUSION

IN A TURBULENT AIR JET

SABIR MOHAMED SALIH

Thesis submitted for the Degree of

Doctor of Philosophy

University of Edinburgh

December 1976

CONTENTS

ACKNOWLEDGEMENT

The author wishes to express his especial indebtedness to Dr W D McComb for his supervision and constant encouragement, without which this work could not have reached this stage.

The author also wishes to acknowledge his sincere gratitude to all members of the staff and colleagues of the Mechanical Engineering Department and the Fluid Mechanics Section of the Physics Department and all friends whose help and good wishes helped the completion of this work. Special appreciation is expressed to Dr G O Goudie for his useful discussions and help in the early stages of the work.

The author is also grateful to the Technical staff of the Mechanical Engineering Department under the guidance of the late Mr D Pringle and recently, of Mr G Smith, for their efficient response to making the experimental apparatus in a working condition.

The effort by Mrs Ruth Gosden in typing the manuscript in a good presentable form despite the shortage of time is much appreciated.

Finally, the author wishes to acknowledge his genuine gratitude to Professor J L King for the use of facilities in the Department of Mechanical Engineering during the period of this research and for his helpful advice and to the Sudan Government for financing the scholarship.

ABSTRACT

In this work an experimental apparatus was designed to produce a solid particle-laden, round, free air jet. It was tested for axisymmetry and similarity of the velocity profiles with a pitot-tube and a hot wire anemometer and the results confirmed measurements by previous investigators. The apparatus was also tested with particles and found to perform within the design limits. A laser Doppler anemometer (LDA) was used in the real-fringe forward-scattering mode to determine the size of the particles used and the result was verified by photomicrography. The LDA burst signal visibility was related to the number of scattering-centres in the probe volume by Farmer (1972). This relationship was used to measure the number of particles at radial positions across the jet relative to that at the centre-line. Firstly, the visibility was measured directly from a storage oscilloscope trace and secondly, an electronic signal processing technique was developed. Measurements for titanium dioxide particles, which are expected to follow closely the fluid flow, were found to agree quite well with the classical results of heat and tracer gas diffusion. Measurements with tungsten metal particles, which are heavy and so their inertia is expected to resist diffusion, were in good agreement with theoretical predictions. The analytical result was obtained from a numerical solution of the theory developed by Davidson and McComb (1975). This theory, which is for monodisperse particles was derived in detail and a crude generalisation to the case of polydisperse particles was then given.

CHAPTER I

INTRODUCTION

1.1. GENERAL

The importance of fluid flow as a means of transferring or transporting properties of the fluid or some foreign contaminants, has been realised since the early days of Boussinesq (1877). Depending on the nature of the transportable quantity the problem can be divided into two categories.

1) When the contaminant is momentum, heat or tracer element that does not introduce any new dynamical properties to the fluid.

2) When the fluid is transporting some elements with finite sizes and the particle inertia can no longer be neglected as it will tend to resist diffusion.

This last case can be divided into two types depending on the number of particles present in the flow field.

2a) Where the particles are only few in number so that the characteristics of the flow field as a whole are not affected.

2b) Where the particles are so many that multiphase systems have to be considered as the particle fluid mixture can no longer be treated as a Newtonian fluid.

Types (1) and (2a) are those with which the present work is concerned and they will be referred to henceforth as tracer elements and heavy particles respectively. One or more aspects

of these types are encountered in many and diverse disciplines and fields of technique. The fields of interest vary from engineering equipment and processes, such as pneumatic conveyors, dust collectors, atomized fuel injection systems to environmental condition studies of air pollution, stack plume formation and meteorology.

The main objective of the present work is to measure the concentration of discrete solid particles in a round, free, aerosol jet. In the first part of the work measurement is confined to small particles which behave like tracer elements. Titanium dioxide particles are used and they are introduced into the jet through a partially fluidized bed. The second part of the work deals with heavy tungsten metal powder particles. These are introduced into the jet in the same manner as for the previous particles. Measurement is made by analysing the Laser Doppler Anemometer (LDA) signal. The results are presented, compared with previous work and the theoretical results of Davidson and McComb (1975) in Chapter VI.

The rest of this chapter will be devoted to a review of the work in the field of turbulent diffusion with particular reference to cases of jet flow, For simplicity of presentation the subject will be dealt with under two sub-titles, namely theoretical and experimental contributions. The theoretical analysis will be presented first and it will be divided into two parts. The first part dealing with contributions in the tracer-element field and the second will correspond to the heavy particle contributions. The heat-type transport problem will be presented

in the theoretical review in three subdivisions according to the method of approach, ie. Lagrangian, Eulerian or Phenomenological. The experimental work will be given in two parts corresponding to the tracer elements and heavy particles cases. Finally, in the last section of this chapter, a brief description of the way this thesis is presented will be given.

1.2 REVIEW OF PREVIOUS WORK

1.2.1 Theoretical Contributions

A complete review of the work on turbulent diffusion would in fact be a review of the problem of turbulence as a whole, as well as convective heat transfer and molecular diffusion. Such a review will not be attempted here, but rather a selection of contributions which will give a fair representation of the problem will be presented.

The pioneering work of Taylor (1921) is usually considered to be the basis of the study of the problem of turbulent diffusion in a Lagrangian frame of reference. He applied the theory of random functions and considered one dimensional flow. From his work it was found that the spread of turbulent diffusion in a certain direction at right angles to the direction of mean flow is proportional to the time of diffusion, if the latter is short. On the other hand, the spread is found to be proportional to the square root of long diffusion time. This spread depends on a Lagrangian correlation function that correlates the component of velocity in the specific direction to that component at an interval of time later. The result for long diffusion time is

in conformity with molecular diffusion results and this leads to the use of a coefficient of turbulent diffusion analogous to that of molecular diffusion. The main difficulty in applying this result to a practical problem lies in the fact that the Lagrangian correlation function cannot be determined unless it is related to some measurable quantities. In other words, a satisfactory relationship must exist between Lagrangian and Eulerian variables. Moreover, extension of the analysis to three dimensions to give a true description of the diffusion problem is faced by unresolvable complications. Such extensions had been suggested by Batchelor (1952). He obtained a relationship for the diffusion coefficient tensor in terms of the Lagrangian correlation-tensor. In this sense the result is of little practical use due to the difficulty of obtaining sufficient information about the correlation-tensor. Frenkiel (1953) assumed a three-dimensional Gaussian distribution of the probability of finding one fluid element at some point within a specified volume. He obtained a relationship for the concentration distribution of fluid elements as a function of the Lagrangian correlation function, the intensity of turbulence and the product of the mean velocity by the Lagrangian scale of turbulence. He applied this relationship for the two cases of long and short diffusion times. For large diffusion time he obtained a relationship corresponding to that given by Taylor for the one-dimensional case. In the case of short diffusion time the mean concentration distribution was found to be approximately Gaussian for low turbulence intensity and small transverse distances from the source.

Generally it is found that, although the treatment of the problem of turbulent diffusion in a Lagrangian frame of reference is more amenable to theoretical analysis, yet the difficulty of relating Lagrangian variables to some measurable quantities remains unsolved. In addition, the complications that arise from generalisation to three dimensions only aggravate the problem of determination of the Lagrangian variables. Two lines of thought have emerged in an attempt to resolve this situation. In the first, the coefficient of diffusion is related to a directly measurable quantity or property of the flow with a basic theoretical approach which is Lagrangian in nature. These theories are known as phenomenological theories. The second line is to treat the problem in a purely Eulerian frame of reference.

In one form of the phenomenological approach a certain property or quantity is assumed to be preserved along a certain length that characterizes the flow field. In the other form the data obtained experimentally is used as basis for the solution of the analytical problem. The 'mixing length' theory was introduced by Taylor (1915) and Prandtl (1925). Both theories are based on the assumption of the existence of an analogy with the kinetic theory of gases and that a coefficient of eddy viscosity or eddy heat conductivity similar to the viscosity and heat conductivity of molecular transport can be determined. Prandtl considered each fluid element subjected to turbulent motion had a separate entity and that a certain property is preserved along a small length, L, of the order of magnitude of

the size of the fluid element. He took momentum to be the transferrable quantity and determined an expression for the eddy diffusivity in terms of the gradient of velocity in the direction of diffusion, and the momentum mixing length. This length is assumed to be proportional to the width of the mixing zone in free turbulent flow or the distance from the wall in wall turbulent flow. The results obtained by this method are found to agree fairly well with experiment. The main objections to the theory are (1) when the gradient of velocity is zero then the coefficient of diffusion is zero - in reality the coefficient does have a value - and (2) because of pressure fluctuations to which each fluid element is subjected during its path over the mixing length, the momentum will not remain constant thus violating the main requirement. Realising these objections, Prandtl (1942) proposed a more extended expresseion for the eddy viscosity. This leads to better agreement with experiment but at the expense of considerable complications in the computations. Again generalisation of the original problem is hindered by intricate expressions. Taylor (1915) had previously followed the same arguments as Prandtl and assumed that the transferrable quantity was vorticity. He reached an expression for the coefficient of diffusivity, also of the gradient type, that would give a greater spread of the diffused quantity than that of velocity. Extension to three dimensions was faced with the fact that vorticity in three-dimensional turbulence was not a constant quantity. Taylor (1932) realised that if this effect was to be accounted for then the expressions would be intractable. So he assumed that in three dimensions also vorticity was

preserved. He obtained a differential equation for the velocity which is the same as that obtained by Prandtl if the turbulence is homogeneous and the eddy viscosity of the momentum transport theory can be reduced to a scalar quantity. Another contribution in this field was presented by Von Kármán (1930). He assumed that the mixing length can be determined in terms of quantities obtained from local flow conditions. He assumed that the characteristic length can be obtained from the ratio between two consecutive lateral derivatives of the mean velocity. This leads to a situation in which the eddy viscosity is infinite if the second derivative of the velocity is zero. Moreover, it does not offer a better agreement with experiment than the simpler Prandtl theory.

A purely phenomenological theory was proposed by Reichardt (1941 and 1949) for free turbulent flow. From experimental measurement it was found that the total momentum flow closely follows the Gaussian error curve. Reichardt used this and assumed that the rate of transfer of U_1 momentum with a velocity U_2 in the lateral direction x_2 is proportional to the change of momentum flux $<U_1^2>$ in that lateral direction. This hypothesis is found to be untrue and a number of objections are raised against it, amongst them is that it violates Newton's law of relativity. Another theory on the same lines as Reichardt's was suggested by Baron (1949). He postulated that the transport processes in free turbulence must result in Gaussian error curves for the distribution of the quantity transported. He assumed that the spread of "momentum particles" originating from

sources determines the characteristics of the turbulent flow field. The same objections raised against Reichardt's theory are valid here.

Some investigators had tried to resolve the problem of the relationship between Lagrangian and Eulerian correlations by considering the theoretical problem of turbulent diffusion in a Eulerian frame of reference. Batchelor (1949) studied the motion of the centre of mass of lumps of fluid and the relative movement of fluid particles of the lump with respect to the centre of mass. He treated the problem as a random walk process and considering the diffusion of a single particle he showed the dependence of the spread by diffusion on the velocity correlation of the particle. He suggested that in the one-dimensional case the use of a coefficient of turbulent diffusion to describe the diffusion of a marked fluid particle need not be restricted to long diffusion times, as the probability density of the displacement of the particle tends to normal distribution for all times. In this case, the diffusion equation will take the form of the known heat conduction equation, with the diffusivity increasing with time, initially linearly, then more slowly and finally tending to a constant value. In his second paper, Batchelor (1952) considered the relative diffusion of two fluid particles, which depends on their initial relative position. In this respect the treatment is not strictly Eulerian but it is a mixed Eulerian-Lagrangian analysis. Batchelor showed that the relative diffusion-tensor can initially be obtained in terms of Eulerian double velocity correlations referring to the initial

positions of the two fluid particles. In the case of short diffusion time and for large Reynolds number of a turbulent flow he found that the velocities of the two particles remain approximately constant during the diffusion and that the rate of change of mean square separation is linear in time. As the diffusion time increases the separation between the particles increases until the dependence of the relative motion of the two particles on the initial separation is lost. Then the rate of change of mean separation increases more rapidly than linearly in time and varies as 4/3 power of the length scale of the group of particles being dispersed. This result was also obtained earlier by Richardson (1926) in his studies of atmospheric diffusion. Some appreciable work has been done on atmospheric turbulence for meteorological studies. Some of those reported are by Ertel(1942), Batchelor (1950) and Lumley and Panofsky (1964).

Saffman and Turner (1956) proposed a theory for collision between small drops in a turbulent fluid. Drops smaller than the small eddies of turbulence were considered and a relationship for the collision rate, in terms of the energy dissipation and the kinematic viscosity, was developed. The result is applied to drops in atmospheric clouds to find out the effect of turbulence on initiating rainfall. Corrsin (1952) considered the condition of steady state homogeneous heat transfer in non-decaying isotropic turbulence. He examined the result of Taylor's analysis for large diffusion time in terms of Eulerian variables. Then he suggested the concept of 'reverse diffusion' of fluid

points, considering the previous dispersion of particles which later pass through the chosen point. This allows direct formulation in the Eulerian frame of reference. He combined the two analyses and obtained an expression for the turbulent heat transfer coefficient dependent only on the velocity field. He also obtained an expression for the correlation coefficient which depends only on the velocity field and the fluid physical properties. The main objection to his treatment lies in that he neglected the effect of large inhomogeneous eddies. In a later paper, Corrsin (1972) presents a proof of his previous conjecture that the statistical properties for the forward and the backward displacements in time are equal.

The Eulerian analysis appears to be simple, but as the problem passes the level of one-dimension and one fluid particle then resort to Lagrangian variables seems inevitable. The real problem of turbulent diffusion is in fact a matter of finding a satisfactory relationship between Eulerian and Lagrangian variables. Hence many attempts have been made theoretically and experimentally to determine such relationships. Uberoi and Corrsin (1953 - as reported in Hinze 1959) obtained an expression for the ratio between the Eulerian spatial micro-scale and the Lagrangian micro-scale in terms of the Eulerian turbulence component of velocity and the Reynolds number based on that velocity and the Eulerian spatial micro-scale. Experimental measurements by these authors showed such a wide scatter that only qualitative proof of the relationship can be obtained. Another experimental effort in this respect was given by Michelson (1955 - as reported by Hinze 1959). His results show that in general the

shape of Eulerian and Lagrangian correlation coefficients is the same. His results are unreliable because his method of measurement was not sufficiently sensitive to small variations in the shape of the coefficients and he did not account for the effect of the unknown molecular diffusion. Bush (1965) gave an approximation of the ratio of the Lagrangian time scale to the Eulerian integral length scale as inversely proportional to the turbulence intensity. Kofoed-Hansen and Wandel (1967) report a detailed study of the relation berween Eulerian and Lagrangian averages for application in meteorology. Shlien and Corrsin (1972) measured the Lagrangian velocity autocorrelation. They experimented with a heated wire placed along the centre-line of a wind tunnel with induced isotropic grid turbulence. They found that the mean temperature profile behind the heated wire was Gaussian, supporting earlier results that the probability density of lateral displacements of fluid particles approximately represents the temperature profile. They found that the Lagrangian velocity micro-scale is much larger than the Eulerian micro-scale of turbulent velocity observed in a frame moving with the mean flow, which was measured by Comte-Bellot and Corrsin (1971). The Lagrangian velocity correlation coefficient was calculated assuming self-preservation of particle velocities and its value was compared with the simplest Eulerian velocity correlation in time that is moving with the mean flow. The stationary Lagrangian time integral scale was found to be about 30% larger than that of the Eulerian.

Recent developments in the theory of turbulent diffusion

are mainly attributed to the development in the statistical theory of turbulence. It is more or less an extension or a justification of some previous intuitive assumption. These studies have given a better insight into the problem of diffusion but the complete knowledge of the statistical functions describing the turbulent motion is not yet available. This, of course, implies that all solutions presented so far are only approximate. Some of the major contributions in this field are those due to Wyld (1961), Edwards (1964), Herring (1965), Edwards and McComb (1969, 1971, 1972), Kraichnan (1959, 1968, 1972), Balescue and Senatorski (1970), Batchelor (1959, 1976), McComb (1974a, 1976) and Lumley (1976). A comprehensive account is given in the book by Leslie (1973).

When the quantity to be transported is heavy, such as discrete solid particles with appreciable inertia effect on diffusion, the fluid lump or tracer element treatment discussed above will no longer describe the problem of diffusion. In this case other means must be sought. Tchen (1947) seems to be the first to study in detail the motion of a small particle suspended in a turbulent fluid flow. He laid down a number of assumptions among them the postulate that Stokes' law of resistance is applicable. For the case of stationary flow, Tchen found that for short diffusion time the ratio of the particle to fluid coefficients of diffusion is proportional to the ratio of the mean square particle to fluid velocities. For long diffusion time both coefficients were found to have the same value. This result was modified by Hinze (1959) by assuming an exponential

type Lagrangian correlation coefficient. Hinze found that the corresponding coefficient for particle motion was not a simple exponential function. He obtained a relationship for the ratio between particle and fluid coefficient of diffusion for long diffusion time in terms of the fluid Lagrangian integral time scale. For the case of very small particle to fluid density Hinze found that the ratio of particle to fluid coefficient of diffusion is equal to the ratio of the mean square fluctuating particle to fluid velocity at all times. Friedlander (1957) also studied the behaviour of particles in a turbulent fluid. He presented a theoretical analysis utilising mathematical methods similar to those employed in calculations of Brownian motion. He related heat and mass transfer to the relative velocity between particle and fluid and an eddy diffusion described by the mean square particle displacement. He found that for small fine particles the mean square displacement measured at a given point varied little with air velocity, while for heavier particles it decreased rapidly with the main stream velocity.

More studies of the problem are reported in the literature: as examples those reported by Lumley (1957), Soo and Peskin (1958) and Peskin (1959, 1962) may be cited. Recently, Hutchinson et al (1971) presented a model for deposition of liquid or solid dispersions from turbulent gas streams. They treated the problem as a random walk in two-dimensions and applied the statistical expressions given by Chandrasekhar (1943). The particles were not assumed to move with the eddies and the dynamics of gas-particles interaction was used to determine particle parameters.

A computer simulation was used to determine these parameters. They tested their result over a wide range of particle size and flow variables and found that agreement in all cases was satisfactory. McComb (1974b) used the same arguments of the random walk process and showed that this approach leads to the result for long diffusion time given by Taylor. Davidson and McComb (1975) presented a theoretical study of small spherical particles in a round, free air jet flow. They used a perturbation method to solve the diffusion equation for heavy particles which are expected to lag the fluid flow. The conventional tracer-element result was used as the zero order solution. This last theory which forms the basis for the present work will be given in detail in Chapter II of this text.

1.2.2 Experimental Contributions

The problem of turbulent diffusion of the fluid lump or of a certain passive property or element, as in the case of heat and mass transfer, has attracted the attention of many experimenters. On the other hand, the diffusion of heavy discrete particles does not seem to receive the consideration of many workers despite the numerous fields of interest in the subject. Here some of the contributions of the first category and then the available work of the second group will be presented. Special reference will be made to measurements in free turbulent flow with air jets in particular, Some of the major contributions in other types of turbulent flow will be given.

Mean temperature distribution in the boundary layer of air

flow along a heated flat plate was measured by Elias (1929) and in turbulent pipe flow by Nunner (1956). Experiments with tracer gas were carried out by Woertz and Sherwood (1939) in pipe flow. McCarter, Stutzman and Koch (1949) measured the temperature profile in radial directions of a straight vertical duct with hot air injected at a point on the axis of the duct. They produced a Gaussian temperature profile from which the assumed constant eddy diffusion coefficient of heat was calculated. They did not consider the effect of molecular diffusion and the decaying effect of grid turbulence. In a study of the effect of turbulence produced by a grid placed at different positions upstream from the point of injection of tracer gas, Towle and Sherwood (1939) measured the concentrations of CO_2 and H_2 over the central third of a straight duct with turbulent air stream. Their result shows a concentration profile which is nearly Gaussian and a marked increase in the coefficient of diffusion at distances of more than 25 duct diameters between grid and source. For distances beyond 50 duct diameters the diffusivity maintained a constant value of the order of magnitude of that obtained without grid, indicating that the grid turbulence had already decayed at those later positions. Flint, Kada and Hanratty (1960) experimented with a foreign substance (potassium chloride in water and CO_2 and H_2 in air) injected at the centre-line of a straight pipe. Samples of the flow stream at different positions along a diameter in a plane downstream of the source plane over a time longer than the time scale of turbulence were taken and analysed for the concentration of the

diffusing substance. Their results are in agreement with a theoretical formulation based on Taylor's analysis and rough predictions for the forms of the correlation coefficients. Neilson and Gilchrist (1968) studied the erosion damage to which nozzles passing a mixiture of gas and particles are subject, and found that the interchanges of heat and work between the gas and the particles are dependent on the ratio of the mass flow rate of particles to that of gas (m_{pg}). They also found that for a straight duct the particle velocity is hardly affected by the value of m_{pg}, particularly for values less than 0.8. Townsend (1947) studied extensively the turbulent quantities in the wake of a circular cylinder. From his measurements of the turbulence characteristics he found that similarity of mean velocity distribution existed at sections greater than 90 times the width of the wake, from the cylinder while the turbulence structure needed a distance of 500 to 1000 wake widths. His results for velocity distribution are in good agreement with the mixing length theory and give a Gaussian profile. In measurements of temperature profiles in the wake of heated cylinders, Townsend (1949) found that similarity in these profiles existed in the full developed region (distances greater than 500 times wake width). The diffusion coefficient of heat and that of momentum were approximately equal with that of energy considerably smaller, but the width of the temperature wake was much larger than that of the velocity wake. Townsend (1948) also measured the intermittency factor in the wake of a cylinder. It was found that turbulence kinetic energy, and the eddy viscosity remain constant over an appreciable part of the wake width if corrected for

intermittence. Investigations in a submerged water jet were carried out by Forstall and Gaylord (1955). They measured the velocity and concentration of sodium chloride solution at different points in the mixing region using an impact tube for velocity measurement and two electric conductivity cells for concentration measurements. They concluded that material and momentum diffusion in a water jet are in agreement with those for an air jet, and that the turbulent diffusion of material in water behaves like that of temperature in air. A number of investigators are reported to have performed experimental measurements in heated jets, of whom some are Ruden (1933), Corrsin (1943) and Corrsin and Uberoi (1949). Hinze and Van der Hegge Zijnen presented results of their experiment on the transport of heat and matter in the turbulent mixing zone of an axially symmetric jet. They found that heat and matter (tracer gas) diffuse at equal rate, but faster than momentum. Velocity was measured by a total head tube, temperature by a thermo-couple, while gas concentration was measured by taking samples at the points of measurement and analysing them by a thermal conductivity method. Their result gives fair agreement with a theoretical analysis in which the coefficient of diffusion of heat and mass is composed of a constant part and a part proportional to the local velocity. The experimental result obtained by these authors is compared with the concentration measurement in the present work and is presented in Chapter VI. Thomas, Baron and Alexander (1951) measured velocity and temperature profiles in a free jet in the similarity region with a probe which combined an impact tube and a thermocouple. Their result is reported to

be in good agreement with a theoretical analysis in which a generalisation of Reichardt's hypothesis is used. The theory yielded a linear differential equation for fluxes of momentum, heat and jet fluid the solution to which is an error function. This linearity enabled them to use a superposition method. An isothermal free jet was used by Taylor, Gremmett and Comings (1951) in which momentum velocity profiles were obtained by an impact tube. This was corrected to mean velocity profile and the mass flowing across the plane of the profile per unit time was determined. They concluded that at distances greater than 15 nozzle diameters the mass flow increased linearly with distance. Alexander, Arnold, Kivnick, Comings and Hinze (1955) studied the transport of momentum and energy in a ducted jet. They obtained radial profiles of velocity and temperature in a heated round jet discharging into an insulated tank with a probe similar to that used by Thomas, Baron and Alexander (1951). The duct wall seems to have a marked effect on the velocity profile but no effect on the temperature. They confirmed that heat was more rapidly transported in turbulent systems than momentum. Heat and mass fluxes were determined from these measurements. They suggested methods of correlating their data utilising Reichardt's hypothesis that leads to transport equations which are linear in the corresponding fluxes. Hence solutions may be obtained in orthogonal functions.

An unconventional method of measurement was presented by Goldschmidt (1965) in which he used a modified constant-current hot wire anemometer for the measurement of point particle

concentration flux in turbulent shear flow. The system was used for measurement of liquid drops and the number of impacts on the wire counted by an electronic counter to give the particle number density. The probe was calibrated using two other different methods - a tapping cylinder and an isokinetic probe. The noise level of the various electronic components limit the use of the system to particle sizes that cause voltage fluctuations upon impaction ~~lower~~ greater than that level. The orientation of liquid drops as they impact on the wire seem to have some effect on the response of the counter. He reported that without considerable improvement the system cannot be used for concentration measurements of solid particles due to the fragility of the wire. This method was used by Goldschmidt and Eskinazi (1966) for the measurement of Safflower oil particles in the region of 2 micron diameter in a plane jet. Their measurement ranged from a distance of 30 to 66 times half width of the jet. They compared their results with theoretical solutions based on Gortler (1942) similarity hyperbolic function and Reichardt's inductive theory. Better agreement was reported with Reichardt's hypothesis for the concentration flux. They obtained an average value of the turbulent diffusivity of the droplets of 0.03 times the centreline mean velocity and the characteristic half velocity width.

Becker, Hottel and Williams describe in two papers a novel method utilising light-scatter technique for the study of turbulence and mixing (1965a) and its use to determine the concentration of particles in a round, free jet (1965b). In the first paper they give a description of the light-scatter technique.

One of the streams entering a mixing field is marked with a sol (a cloud of particles). Light scattered by the sol from a beam projected into the field is scattered on one side and focused on a slitted diaphragm. The slit passes to a phototube the light scattered from a short segment of the incident beam. The electrical signal produced is ideally proportional to the amount of sol in the defined control volume, and when the volume is small, to the point concentration. In the second paper, they use the previous technique to study the nozzle-fluid concentration field in an isothermal, turbulent, axisymmetric, free air jet with the nozzle air marked by an oil smoke. They compare their results with other work in which heat is used to mark the nozzle fluid and conclude that close similarity exists between concentration and temperature profiles.

Bragg and Bednarick (1974) measured the concentration distribution of flint dust in a plane air jet. The concentration data was obtained using an automatic particle counter. Their result shows that the concentration profile reaches the fully developed state at distances greater than 20 times nozzle thickness. The result was compared with a theoretical analysis assuming a constant diffusion coefficient and the agreement is fair. Another recent method of determining particle concentration in a turbulent field was introduced by Durst and Umhauer (1975). In this method, the conventional laser-Doppler system is used in conjunction with a white light source with specially designed receiver optics. A photodetector is employed to detect the amplitude of the scattered white light. Mies' theory is used

to relate the output of this photodetector to the particle size. Particle concentration is then determined by a count of the pulses given by the PM tube for white light together with velocity information given by the laser-Doppler arrangement. They performed a number of experiments in which the size distribution from two particle generators was measured. Liquid sprays as well as solid particles were the subject of investigation and the results are in good agreement with electronic microscope measurements. Durst and Zare (1975) presented the basic theory for laser-Doppler velocity measurements of large curved surfaces which totally reflect or refract the light from two laser beams intersecting at the surface, at different angles. They obtained relationships for the velocity of large moving spherical particles and bubbles. They showed that the signal could be considered as a result of a reflected or refracted fringe pattern moving across the photodetector. The theoretical study presented by these authors shows that the LDA signal also provides information on the radius of the particle. They obtained a relationship for the radius of the particle in terms of the angle between the incident laser beams and the fringe geometry. They carried out a number of experiments with a large reflection sphere moving through an air flow containing small particles. The light scattered by the small particles was collected by an on-axis photodetector while the light reflected by the sphere was collected by another off-axis detector. They also measured the velocity of air bubbles rising in a liquid. Their experimental measurements appear to verify the theoretical predictions.

They suggested that this arrangmment is suitable for measurement in two phase flows and proposed optical systems and electronic signal processing for that purpose.

In all, these contributions are mainly concerned with the measurement of turbulent diffusion parameters for the case of momentum, heat or tracer-element. Very few experimental investigations in the field of dilute concentration of heavy particles in turbulent flow have been reported in the literature. Of these few, only one experiment seems to be performed in a turbulent jet flow, the rest are generally concerned with pipe flow. Furthermore, many of these are more related to multi-phase systems where the concentration is no longer dilute and application of non-Newtonian laws is more appropriate. An example of these is given by reference to the work of Soo (1964), Rosenweig, Holland and Williams (1961), Hinkle, Orr and Dallavalle (1955), Alexander and Goldern (1951), Friedlander and Johnstone (1957), Cousins and Hewitt (1968), Cousins, Denton and Hewitt (1965).

The one experimental investigation which is close to the present field of interest is that of Lewis et al (1961), who measured the mass flow rate of ion-exchange resin particles (density $\simeq$ 1.5 gm/cm^3) of size 150-300 micron in a turbulent axisymmetric air jet with nozzle diameter 0.635 cm. The concentration measurement was obtained by taking samples of the mixture of gas and solid at different points in the radial direction and at different downstream positions from the nozzle. The sample was separated in a centrifuge and the mass of particles and air weighed. Knowing the time for collection of the sample

the mass flow was calculated. They found that at distances of 100 to 180 nozzle diameters the mass flow profiles show similarity. Their theoretical problem was treated using Tollmien's method. The experimental result showed a scatter around the theoretical result which they explained as being due to the fact that the theory presented described a single-phase flow. A more elaborate model, taking into account the interaction between the solid and the fluid phases, would have been more appropriate. This experimental result was shown to agree fairly well with the general trend of the theory presented by Davidson and McComb, although it falls out of the range considered by the theory.

It is evident from the above sections that the problem of turbulent diffusion of heavy discrete particles has not received the appropriate attention. Both theoretical and experimental contributions are scarce, but the recent development of a theoretical treatment for the problem by Davidson and McComb (1975) is in advance of experimental work. Realising these facts, and to bridge the gap between theory and experiment, the present work is embarked upon.

1.3 GENERAL ARRANGEMENT OF THE THESIS

In the last few years an important development has taken place in the laser-Doppler Anemometer (LDA) as a probe for measuring various parameters of fluid flow. This powerful instrument is used for measurement of the concentration of particles in the present work. In Chapter III of this thesis a brief review of the work on the use of LDA is given and then a

theoretical analysis of its feasibility for application to this work is considered. As mentioned earlier, Chapter II is concerned with the theoretical aspects of turbulent diffusion required for this work. A brief development of the theory in a Lagrangian frame of reference is presented with detailed derivation of the theory given by Davidson and McComb. In Chapter IV the details of the experimental apparatus from the design and testing points of view are given. Chapter V shows the experimental procedure for the determination of the particle concentrations. The results are presented, compared with other experiments and theory and discussed in Chapter VI.

CHAPTER II

THEORETICAL ASPECTS OF TURBULENT DIFFUSION

2.1 INTRODUCTION

The random motion of elements of fluid in a turbulent flow is diffusive in nature. If a transportable property or quantity is thought of as being possessed or carried by the fluid, then the problem is to determine the spread of that property or quantity after a certain time has elapsed. Two methods are usually adopted to describe the motion of the fluid. The Lagrangian method, in which the path of each individual fluid element is followed. This method is the more natural for a theoretical analysis of the problem. On the other hand, the Eulerian method, in which the properties of the fluid are considered at fixed points in space forms a natural basis for experimental measurements.

In this chapter it is intended to give a brief account of the theoretical aspects of turbulent diffusion needed for the present work. Firstly, the differential equation for turbulent diffusion is derived from the analogy with molecular diffusion. Then Taylor's (1921) analysis based on the statistical theory of turbulence is presented. This result is of little use in practice due to the difficulty of generalising it to three dimensions, together with the problem of relating Lagrangian to Eulerian correlations. Theories based on observed experimental quantites or the phenomenlogical approach, are then formulated, Again these fail to predict a quantitative form of the diffusion coefficient

as will be discussed later.

All these theories are derived on the assumption that the transferrable quantity is a marked element of fluid. Any contaminant contained in these elements, such as heat or tracer molecules are assumed not to confer any new dynamical properties on the fluid elements transporting it. Discrete aerosol particles with infinitesimal size are assumed to behave in a similar manner as tracer elements. This is obviously not true for particles heavy enough to lag behind the fluid motion. In this case the inertia of the particles will have a substantial value to retard them with respect to the fluid motion. A theoretical model that will describe such a situation is needed. From the work of Tchen (1947) for discrete particles suspended in a turbulent flow, the particle coefficient of turbulent diffusion is related to that of the marked fluid element. This relation is presented. Then conclusions are drawn from more recent work of Batchelor (1952), Hutchison et al (1971) and McComb (1974b). After that a detailed account of the work by Davidson and McComb (1975) is presented. In this work, the diffusion equation as applied to a free aerosol jet is solved using a perturbation method in which the marked fluid element result is used as a zero order solution. The first order solution is expected to give a better insight into the diffusion of heavy particles. Finally, a crude generalisation of this last approach for application to a polydisperse distribution of particles is given.

2.2 MOLECULAR DIFFUSION

From the analysis of molecular diffusion, Fick's law, which is empirical in nature, can be stated as

$$P = - D_M \frac{\partial c}{\partial y} \qquad (2.1)$$

where c = Some quantity transported by molecular diffusion

y = the distance in a specified direction

D_M = the coefficient of molecular diffusion or diffusivity

and P = the rate at which the quantity is transported across unit area normal to direction y.

Considering the diffusion of some labelled molecules of a certain gas, which are concentrated in the plane y = 0 at time t = 0, into the rest of that gas in the direction y, conservation of mass enables equation (2.1) to be written as

$$\frac{\partial c}{\partial t} = - \frac{\partial P}{\partial y} = D_M \frac{\partial^2 c}{\partial y^2} \qquad (2.2)$$

If the variance, $\langle y^2 \rangle$ is taken as the measure of the spread of the gas in the y direction ($\langle\ \rangle$ indicating the time-average of the quantity included), then D_M is related to $\langle y^2 \rangle$ through (Raudkivi and Callander 1975):

$$D_M = \frac{\langle y^2 \rangle}{2t} \qquad (2.3)$$

This means that the standard deviation of the distribution of the labelled molecules ($\langle y^2 \rangle^{\frac{1}{2}}$) increases in proportion to the square root of the time of diffusion.

For three dimensional diffusion and convection in a flow with components u, v and w in the three coordinate planes, the conservation of matter reads

$$\frac{\partial c}{\partial t} + u \frac{\partial c}{\partial x} + v \frac{\partial c}{\partial y} + w \frac{\partial c}{\partial z} = D_M \frac{\partial^2 c}{\partial x^2} + D_M \frac{\partial^2 c}{\partial y^2} + D_M \frac{\partial^2 c}{\partial z^2} \tag{2.4}$$

or in tensor notation

$$\frac{\partial c}{\partial t} + u_i \frac{\partial c}{\partial x_i} = D_M \frac{\partial^2 c}{\partial x_i \partial x_i} \tag{2.5}$$

with $i = 1, 2, 3$

$x_i = x, y, z$

and $u_i = u, v, w.$

The above case is for the situation in which D_M is a scalar.

In a steady turbulent flow the mean values of the properties do not vary with time. A slow variation of these means may be allowed for provided that they do not change significantly during an interval of time long enough to average out the fluctuations. The flow is assumed to be incompressible and the concentration and velocity components are separated into a mean and a fluctuating component according to

$$c = \bar{c} + c'$$

$$u_i = \bar{u}_i + u_i'$$

Substitution in equation (2.5) and taking averages with respect to time yields

$$\frac{\partial \bar{c}}{\partial t} + \bar{u}_i \frac{\partial \bar{c}}{\partial x_i} + \overline{u_i' \frac{\partial c'}{\partial x_i}} = D_M \frac{\partial^2 \bar{c}}{\partial x_i \partial x_i} \tag{2.6}$$

For the above situation the continuity equation can be written as

$$\frac{\partial u_i'}{\partial x_i} = 0 \tag{2.7}$$

The third term on the left-hand side of equation (2.6) can be written as

$$\langle u_i' \frac{\partial c'}{\partial x_i} \rangle = \frac{\partial}{\partial x_i} \langle c' u_i' \rangle \qquad (2.8)$$

Hence equation (2.6) becomes

$$\frac{\partial \langle c \rangle}{\partial t} + \langle u_i \rangle \frac{\partial \langle c \rangle}{\partial x_i} = - \frac{\partial}{\partial x_i} \langle c' u_i' \rangle + D_M \frac{\partial^2 \langle c \rangle}{\partial x_i \partial x_i} \qquad (2.9)$$

The term $\langle c' u_i' \rangle$ is the mean rate of transport due to turbulence of the quantity with concentration c across unit area normal to the component of velocity u_i.

Assuming the analogy to Fick's law to be valid then $\langle c' u_i' \rangle$ can be determined by

$$\langle c' u_i' \rangle = - D_T \frac{\partial \langle c \rangle}{\partial x_i} \qquad (2.10)$$

where D_T is the turbulent diffusion coefficient or the eddy diffusivity.

Substituting equation (2.10) in (2.9) the result is

$$\frac{\partial \langle c \rangle}{\partial t} + \langle u_i \rangle \frac{\partial \langle c \rangle}{\partial x_i} = \frac{\partial}{\partial x_i} \left[(D_T + D_M) \frac{\partial \langle c \rangle}{\partial x_i} \right] \qquad (2.11)$$

This is the general form of the diffusion equation obtained with analogy to molecular diffusion. It was reached by making the assumption of homogeneous and isotropic turbulence whereby the eddy diffusivity has the same value in the three coordinate directions and does not vary with the space coordinates.

Certainly, the validity of this analogy is questionable

as there are considerable differences between the motion of the macroscopic fluid and that of the individual molecules. In the former, the medium is continuous while in the latter the medium consists of discrete particles. This implies that the velocity of an element of fluid at one instant is not independent of its velocity at a later instant unless the time interval is large.

Since turbulent motion is far more effective in dispersing matter than molecular motion, the effect of molecular diffusion in equation (2.11) is usually neglected. This equation, hence becomes

$$\frac{\partial \langle c \rangle}{\partial t} + \langle u_i \rangle \frac{\partial \langle c \rangle}{\partial x_i} = D_T \frac{\partial \langle c \rangle}{\partial x_i \partial x_i} \qquad (2.12)$$

For one dimensional flow where there is only one component of mean velocity $\langle u_i \rangle = U$, then equation (2.12) reduces to

$$\frac{\partial \langle c \rangle}{\partial t} + U \frac{\partial \langle c \rangle}{\partial x} = D_T \frac{\partial^2 \langle c \rangle}{\partial x^2} \qquad (2.13)$$

The above equation (2.13) forms the basis for the turbulent diffusion problem and the attempts to solve it may be reduced to finding a suitable description for the eddy diffusivity (D_T).

2.3 LAGRANGIAN ANALYSIS

Taylor (1921) in his pioneering work on the statistical theory of turbulence obtained an expression for the variance ($\langle x_2^2 \rangle$) of a fluid particle position in one dimension. In this work the assumptions of homogeneous and isotropic turbulence

were made. A particle P assumed to be at the origin of the coordinate axes at an initial time was found to be after time t at a position x_2 from the origin. For the case of stationary flow the mean velocity U was zero and the particle was assumed to be moving with a velocity v(s). After an increment of time, t, then

$$\langle x_2^2 \rangle = \langle \left[\int_o^t v(s)ds \right]^2 \rangle \qquad (2.14)$$

As v(s) is a random variable, equation (2.14) could be replaced by a more general form, ie

$$\langle x_2^2 \rangle = \int_o^t \int_o^t \langle v(s_1)v(s_2) \rangle \, ds_1 ds_2 \qquad (2.15)$$

If a Lagrangian correlation coefficient R(h), that measures the correlation between the v-component of the particle at a certain time t and that of the same particle at an interval of time h later, is introduced, then

$$R(h) = \left\langle \frac{v(t)v(t+h)}{\langle v^2 \rangle} \right\rangle \qquad (2.16)$$

Substitution in (2.16) yields

$$\langle x_2^2 \rangle = \langle v^2 \rangle \int_o^t \int_o^t R(s_2 - s_1) \, ds_1 ds_2 \qquad (2.17)$$

Since $R(s_2 - s_1)$ is a symmetrical function of $(s_2 - s_1)$, then the integration can be taken as twice that over half the area instead of that over the whole area. Taking $s_2 - s_1 = s$ and $ds_2 = ds$ while s_1 is held constant equation (2.17) can be written as

$$\langle x_2^2 \rangle = 2 \langle v^2 \rangle \int_o^t \left[\int_o^{s_1} R(s)ds \right] ds_1 \qquad (2.18)$$

This is the form reached by Taylor (1921). Kampe de Feriet (1939) took the following step:

integrating equation (2.18) by parts yields

$$\langle x_2^2 \rangle = 2\langle v^2 \rangle \left[(s_1 \int_0^s R(s)ds)_0^t - \int_0^t s_1 R(s_1)ds_1 \right]$$

substituting the limits and renaming $s_1 = s$

$$\langle x_2^2 \rangle = 2\langle v^2 \rangle \left[t \int_0^t R(s)ds - \int_0^t sR(s)ds \right]$$

or
$$\langle x_2^2 \rangle = 2\langle v^2 \rangle \int_0^t (t - s)R(s)ds \qquad (2.19)$$

For the evaluation of the integral in equation (2.19), R(s) as a function of t must be known. Although this is a difficult function to measure, yet the following properties, about it, are known,

1) for $s = 0$, $R(s) = 1$

2) because of the assumption of the homogeneity and ergodicity of the field and the symmetry of R(s) in s, it will decrease with increasing s, hence for large values of s, R(s) will tend to zero.

Equation (2.19) will be considered for these two limiting cases:

a) when the diffusion time t is much larger than the time-scale of turbulence L_t given by

$$L_t = \int_0^\infty R(s)ds \qquad (2.20)$$

Equation (2.19) after substitution of (2.20) becomes

$$\langle x_2^2 \rangle = 2\langle v^2 \rangle L_t t - 2\langle v^2 \rangle \int_0^\infty sR(s)ds \qquad (2.21)$$

The second term on the right-hand side of equation (2.21) is constant and is negligible in comparison with the first term. It follows that

$$\langle x^2 \rangle = 2 \langle v^2 \rangle L_t t \qquad (2.22)$$

Hence for a long diffusion time the standard deviation $\langle x^2 \rangle^{\frac{1}{2}}$ is proportional to the square root of the diffusion time. This result justifies the analogy between turbulent and molecular diffusion and a relationship for the eddy diffusivity similar to that for molecular diffusion can be drawn. Comparing equations (2.22) and (2.3) the coefficient of turbulent diffusion can be given by

$$D_T = \langle v^2 \rangle L_t = \lambda_L \langle v^2 \rangle^{\frac{1}{2}} \qquad (2.23)$$

$$\text{where } \lambda_L = \langle v^2 \rangle^{\frac{1}{2}} L_t = \langle v^2 \rangle^{\frac{1}{2}} \int_0^\infty R(s)ds \qquad (2.24)$$

λ_L is a space scale in which the particle moves substantially in one direction and is known as the Lagrangian integral length scale.

b) When the diffusion time t is small compared to L_t then R(h) can be expanded in a Taylor series. Neglecting terms with more than second order in h, R(h) will be given by

$$R(h) = 1 - \frac{h^2}{2} \frac{1}{\langle v^2 \rangle} \langle (\frac{dv}{dt})^2 \rangle \qquad (2.25)$$

Introducing the Lagrangian microscale of time as

$$\frac{1}{\lambda^2} = \frac{1}{\langle v^2 \rangle} \langle (\frac{dv}{dt})^2 \rangle = \frac{d^2R(o)}{dt^2} \qquad (2.26)$$

then (2.24) becomes

$$R(h) = 1 - \frac{h^2}{2\lambda^2}$$

Equation (2.19) then reads

$$\langle x^2 \rangle = (1 - \frac{1}{12} \frac{t^2}{\lambda^2}) \langle v^2 \rangle t^2 \qquad (2.27)$$

For values of $t^2 << \lambda^2$ then

$$\langle x^2 \rangle = \langle v^2 \rangle t^2 \qquad (2.28)$$

This means that for a short diffusion time the standard deviation $\langle x^2 \rangle^{\frac{1}{2}}$ is proportional to the diffusion time and the problem of molecular diffusion can no longer be taken to describe turbulent diffusion without serious discrepancy.

2.4 THE PHENOMENOLOGICAL THEORIES

Although equation (2.23) justifies the analogy with molecular diffusion, the problem of obtaining a satisfactory coefficient of turbulent diffusion remains unsolved. This is mainly because the coefficient of diffusion is given in a Lagrangian frame of reference. Both λ_L and $\langle v^2 \rangle$ have to be determined in an Eulerian frame of reference before the value of D_T can be obtained. A relationship between Lagrangian and Eulerian correlations has not yet been found. In addition, the above analysis considers one-dimensional diffusion and its extension to describe turbulent diffusion which is a three-dimensional problem leads to unresolvable complications. In the attempt to resolve these difficulties many phenomenological theories, relating the coefficient of diffusion to some measureable Eulerian property, were suggested. Here a brief account of Prandtl's (1925) 'mixing length' theory, Taylor's (1915) 'vorticity' theory and Recchardt's (1941, 1949) 'inductive' theory for free turbulence, will be given as an example of these theories.

In the mixing length theory, a length (ℓ) similar to the mean free path in the kinetic theory of gases is introduced. It is assumed that a certain quantity of the turbulent flow is preserved through the length during the turbulent mixing process. If the value of this quantity is q with mean value $\langle q(x_2)\rangle$, a function of x_2 only, is transferred between two fluid layers x_2 and $x_2 + \ell$, then at the new layer the fluctuating value (q') of q will be

$$|q'| = |\langle q(x_2 + \ell)\rangle - \langle q(x_2)\rangle| \tag{2.29}$$

Expanding in a Taylor series and neglecting terms with more than the first order in ℓ as ℓ is assumed small, equation (2.29) then becomes

$$|q'| = \ell\left|\frac{d\langle q\rangle}{dx_2}\right| \tag{2.30}$$

Prandtl assumed that the momentum was the transferrable quantity and that a constant correlation existed between the fluctuating components of velocity in two mutually perpendicular planes. For two-dimensional parallel flow the following relationships for eddy viscosity ν_E and shear stress σ were obtained

$$\nu_E = \ell^2 \left|\frac{d\langle u\rangle}{dx_2}\right| \tag{2.31}$$

$$\sigma = \rho\ell^2 \left|\frac{d\langle u\rangle}{dx_2}\right| \frac{d\langle u\rangle}{dx_2} \tag{2.32}$$

where ρ = the density of the fluid.

Then equating the rate at which momentum is transferred by turbulence to the fluid and the difference in shearing stress between two neighbouring planes gives,

$$\frac{\partial \sigma}{\partial x_2} = \rho \frac{\partial}{\partial x_2} \left(\ell^2 \left| \frac{d<u>}{dx_2} \right| \frac{d<u>}{dx_2} \right) \tag{2.33}$$

The expression for eddy diffusivity can then be obtained by analogy to read

$$D_T = \ell_e^2 \left| \frac{d<u>}{dx_2} \right| \tag{2.34}$$

where ℓ_e = mixing length for turbulent diffusion.

Usually the value of ℓ_e is assumed equal to that for ℓ. The value of ℓ itself differs from one situation to another. For free turbulence ℓ is assumed to be proportional to the width of the mixing zone, the constant of proportionality being obtained only from experimental measurements.

Again the attempt to extend this theory to the three dimensional case failed on the account of complexity. Another drawback in applying this theory, except for rare cases, it that the pressure fluctuations to which the fluid element is subjected during its path over the distance ℓ cause the momentum to change, thus violating the major requirement.

In a manner similar to Prandtl's momentum transfer theory, Taylor developed a theory assuming that the vorticity or the conservation of the moment of momentum to be the transportable quantity. For a two-dimensional uniform flow in the x-direction with a mean velocity $<u>$, Taylor reached the expression for eddy diffusion,

$$D_T = \frac{\ell_w^2}{2} \left| \frac{d<u>}{dx_2} \right| \tag{2.35}$$

where ℓ_w is the mixing length during which vorticity is preserved. For free turbulence with the mean velocity along the x_1 -direction, Taylor's theory gives identical results to those

given by Prandtl's mixing length theory.

Reichardt (1941, 1949) found from experimental measurements in the mixing regions of free turbulence that velocity and transport distributions follow closely error functions or error integrals. He assumed that a turbulent-transport process was a statistical process similar to molecular-transport processes. Based on these experimental findings he worked out an inductive theory for free turbulent flow. Considering two-dimensional flow, neglecting the pressure term and terms containing the viscosity, the x -wise momentum of the mean flow becomes

$$\frac{\partial \langle u_1^2 \rangle}{\partial x_1} + \frac{\partial \langle u_1 u_2 \rangle}{\partial x_2} = 0 \qquad (2.36)$$

Reichardt assumed an empirical relationship for $\langle u_1 u_2 \rangle$ as

$$\langle u_1 u_2 \rangle = \Phi \frac{\partial \langle u_1^2 \rangle}{\partial x_2} \qquad (2.37)$$

where Φ is a function of x_1 only, similar to the mixing length but has no physical meaning. After substitution of (2.36), equation (2.37) reads

$$\frac{\partial \langle u_1^2 \rangle}{\partial x_1} = \Phi(x_1) \frac{\partial^2 \langle u_1^2 \rangle}{\partial x_2^2} \qquad (2.38)$$

This can be extended to the case in which heat or mass is transferred. If c denotes the concentration of the transportable quantity then for the two-dimensional axially symmetric case with negligible molecular effects and steady mean flow, the transport equation is given by

$$\frac{\partial \langle c u_1 \rangle}{\partial x_1} + \frac{\partial \langle c u_2 \rangle}{\partial x_2} = 0 \qquad (2.39)$$

By analogy with Reichardt's original hypothesis, equation (2.36),

$$\langle cu_2 \rangle = - D_T \frac{\partial \langle cu_1 \rangle}{\partial x_2} \tag{2.40}$$

Hence

$$\frac{\partial \langle cu_1 \rangle}{\partial x_1} = D_T \frac{\partial^2 \langle cu_1 \rangle}{\partial x_2} \tag{2.41}$$

This is the linear generalised heat conduction equation which yields a Gaussian solution for $\langle cu_1 \rangle$.

Again, the hypothesis (2.40) is found to be unsatisfactory as it was proved to vary under a translation at constant velocity of the coordinate system. This, of course, contradicts Newton's relativity, which states that forces on a mechanical system must be independent of the addition of a constant velocity.

More recent developments in the theory of turbulent diffusion are mostly based on the statistical theory of turbulence. As a complete knowledge of the statistical functions describing the turbulent motion are lacking then various assumptions have to be resorted to. Batchelor (1952) extended Taylor's work to three dimensions and obtained a relationship for the diffusion tensor $\langle y_i y_j \rangle$ instead of the variance $\langle y^2 \rangle$ as

for small values of the diffusion time,

$$\langle y_i(t) y_j(t) \rangle \simeq \langle y_i(o) y_j(o) \rangle + \langle v_i(t') v_j(t') \rangle t^2 \tag{2.42}$$

for large values of the diffusion time

$$\langle y_i(t) y_j(t) \rangle \simeq \langle y_i(o) y_j(o) \rangle + 2 v_i' v_j' (\tau_{ij})_L t \tag{2.43}$$

where

$$(\tau_{ij})_L = \tfrac{1}{2}\int_0^\infty ds\,\left[(R_{ij}(s)_L) + (R_{ji}(s)_L)\right] \qquad (2.44)$$

and $(R_{ij}(s))_L$ = Lagrangian correlation tensor coefficient.

Also by assuming that the field of turbulent motion is statistically homogeneous and that the probability density distributions of the three components y_i are separately, as well as jointly, Gaussian, Batchelor obtained a coefficient of diffusion D_{ij} which is a second order tensor. Thus

$$D_{ij} = \tfrac{1}{2}\frac{d}{dt}\langle y_i y_j\rangle \qquad (2.45)$$

From equations (2.41) and (2.42) then

$$\text{for small } t: \quad D_{ij} = \langle v_i(t')v_j(t')\rangle\, t \qquad (2.46)$$

$$\text{for large } t: \quad D_{ij} = v_i' v_j' (\tau_{ij})_L \qquad (2.47)$$

These generalisations to three dimensional diffusion have no practical value on account of the lack of information about the Lagrangian correlation tensor coefficient $(R_{ij}(s))_L$.

An interesting conclusion drawn by Batchelor (1949) from one-dimensional analysis is that the description of the diffusion of a marked fluid particle by a coefficient of diffusion need not be restricted to large diffusion times. It is sufficient that the probability distribution of y_2 is Gaussian. Experimental evidence for both limits confirms this condition, so one needs only to make an assumption that the distribution remains Gaussian during intermediate times.

2.5 TURBULENT DIFFUSION OF DISCRETE HEAVY PARTICLES

The 'fluid lump' approach is able to describe the transport of particles with infinitesimal sizes. As particles with larger sizes will have greater inertia they will tend to resist diffusion. Hence a certain size will be reached when the particles will move at a velocity less than that of the fluid. In this case a different approach should be used to solve the diffusion problem. This implies that a diffusion coefficient (D_p) for the particles different from that for the fluid (D_f) has to be determined.

Tchen (1947) studied the motion of a small particle suspended in a turbulent fluid. He made a number of simplifying assumptions including the condition that the particles follow Stoke's law of resistance. For a particle moving with an instantaneous velocity q' in a fluid moving with a velocity u' he obtained the following form for the conservation of particle momentum in the x_i direction.

$$\frac{\partial q_i'}{\partial t} + q_i' \frac{\partial q_j'}{\partial x_i} = \frac{1}{\tau}(u_i' - q_i') + b\left[\frac{\partial u_i'}{\partial t} + q_i' \frac{\partial u_i'}{\partial x_j} - \frac{2}{3}\frac{\partial^2 u_i'}{\partial x_j \partial x_j} + \frac{2}{3}(u_i' - q_i')\frac{\partial u_i'}{\partial x_j}\right]$$

$$+ c\int_{-\infty}^{t} \frac{dt_1}{\sqrt{t - t_1}}\left[\frac{\partial}{\partial t_1}(u_i' - q_i') + q_j \frac{\partial}{\partial x_j}(u_i' - q_i')\right] \qquad (2.48)$$

where $b = \dfrac{3\rho_f}{2\rho_p + \rho_f}$

$$c = \frac{9}{(2\rho_p + \rho_f)_r}\sqrt{\frac{\rho_f \mu}{\pi}}$$

⊛ D_p is defined in terms of the particle Lagrangian turbulence velocity and integral length scale.

$$\tau = \frac{2}{9} \frac{\rho_p a^2}{\mu}$$

μ = the dynamic viscosity of the fluid

a = particle radius

ν = the kinematic viscosity of the fluid

ρ_p and ρ_f = the densities of the particle material and the fluid.

τ represents the particle momentum relaxation time and is a measure of how quickly can a particle with density ρ_p and radius a, follow a change in the velocity of the surrounding fluid, which has a viscosity μ. A relationship between the particle diffusion coefficient D_p and the coefficient for 'fluid lump' D_f was derived as a function of the diffusion time t (Hinze 1959) as

$$\frac{D_p}{D_f} = 1 + \frac{1 - b^2}{(L_t/\tau)^2 - 1} \quad \frac{e^{-t/\tau} - e^{-t/L_t}}{1 - e^{-t/L_t}} \qquad (2.49)$$

Another recent approach was presented by Hutchinson et al (1971). In their investigation of the problem of particle deposition from turbulent gas streams, the particle was assumed to execute a random walk in the plane normal to the gas flow. This enabled the density distribution expression due to Chandrasekhar (1943) to be used. The coefficient of turbulent diffusion is given by

$$D_p = \frac{n \langle \ell^2 \rangle}{2} \qquad (2.50)$$

where $\langle \ell^2 \rangle$ is the mean square displacement distance of particles and n is the number of displacements per unit time. Equation (2.50) was related to measurable turbulent quantities and the fluid particle interaction was modelled for computations.

McComb (1974b) applied equation (2.50) to particles with infinitesimal radius, for the case of stationary homogeneous

turbulence, together with equation (2.24). Putting $n \sim L_t$ he recovered equation (2.23). This shows that for very small particles that follow closely the fluid flow the random walk approach gives the same results as Fickian diffusion. Further, McComb assumes homogeneous turbulence in which case the substitution $\langle v^2 \rangle = \langle u^2 \rangle$ is possible. With the aid of equation (2.24) and the relation $\lambda_E = \beta\lambda L$ (λ_E is the Eulerian integral length scale and $\beta \sim 1$), equation (2.23) becomes

$$D_T = \beta^1 \langle u^2 \rangle^{\frac{1}{2}} \lambda_E \qquad (2.51)$$

Again by changing equation (2.50) into Eulerian variables he obtains an Eulerian form of the Chandrasekhar diffusion coefficient similar to (2.51). This reads

$$D_c = \tfrac{1}{2} c \langle u^2 \rangle^{\frac{1}{2}} \lambda_E \qquad (2.52)$$

where c is a constant.

More recently, Davidson and McComb (1975) developed a theoretical analysis for turbulent diffusion in a round free aerosol jet. The diffusion of particles which lag the flow of the fluid is treated by a perturbation method in which the results of infinitesimal particles represent the zero order solution.

2.6 DIFFUSION OF DISCRETE HEAVY PARTICLES IN A TURBULENT JET

As this case is studied experimentally, the theoretical analysis will be presented in some detail and, as mentioned earlier, a generalisation to the case of polydisperse particles will be given.

Considering a round jet in which the mean flow is in the

x-direction, the mean quantities will depend on both axial and radial coordinates x and r, but will be independent of time. At distances greater than 8 nozzle diameters, the jet variables can be scaled to yield a similarity solution in the coordinate

$$\eta = r/x \tag{2.53}$$

Hence for a jet issuing from a nozzle with a diameter d, and exit velocity U_o, the mean and r.m.s. radial fluctuating velocities U_x and $\langle U_r^2 \rangle^{\frac{1}{2}}$ can be written as

$$U_x = AU_o \frac{d}{x} \tilde{U}_x(\eta) \tag{2.54a}$$

$$\langle U_r^2 \rangle = AU_o \frac{d}{x} \langle \tilde{U}_r^2(\eta) \rangle \tag{2.54b}$$

where $\tilde{U}_x$ and $\tilde{U}_r$ are the scaled parts of the velocities.

The incompressible fluid continuity equation for the specified jet can be written as

$$\frac{\partial U_x}{\partial x} + \frac{\partial U_r}{\partial r} + \frac{U_r}{r} = 0 \tag{2.55}$$

where U_r = mean radial velocity.

The similarity solution for U_x and U_r is of the form

$$\tilde{U}_x = \frac{1}{\eta} \frac{dF}{d\eta} \tag{2.56a}$$

$$\tilde{U}_r = \frac{dF}{d\eta} - \frac{1}{\eta} F \tag{2.56b}$$

$$\text{where } F = \int_o^\eta \eta_1 \tilde{U}_x(\eta_1) d\eta_1 \tag{2.56c}$$

The general form of the conservation of mass for the particles, for N particles moving with mean velocities Q_x and Q_r in the axial and radial directions can be written as (eg. Bird et al 1960)

$$N\left(\frac{\partial Q_x}{\partial x} + \frac{\partial Q_r}{\partial r} + \frac{Q_r}{r}\right) + Q_x \frac{\partial N}{\partial x} + Q_r \frac{\partial N}{\partial r} = \frac{1}{r} \frac{\partial}{\partial r} \left(r D_p \frac{\partial N}{\partial r}\right) \qquad (2.57)$$

Molecular and turbulent diffusion in the x-direction are neglected. The variables are separated into mean and fluctuating components according to

$$q_i' = Q_i + q_i \qquad (2.58)$$

with $\langle q_i' \rangle = Q_i$

and $\langle q_i \rangle = 0 \qquad (2.59)$

where $i = x, r.$

The relationship between the particle mean velocity and the fluid velocity is determined by equation (2.48).

Using equations (2.58) and (2.59) then the time-average of equation (2.48) neglecting the term in b as b is small, is

$$\frac{\partial Q_i}{\partial t} + Q_j \frac{\partial Q_i}{\partial x_j} + \frac{\partial}{\partial x_j} \langle q_i q_j \rangle = \frac{1}{\tau} (U_i - Q_i) + c \left[\langle I_1 \rangle + \langle I_2 \rangle\right] \qquad (2.60)$$

where $\langle I_1 \rangle = \left\langle \int_o^t \frac{dt_1}{\sqrt{t - t_1}} \left[\frac{\partial}{\partial t_1} (U_i - Q_i) + Q_j \frac{\partial}{\partial x_j} (U_i - Q_i)\right] \right\rangle \qquad (2.61a)$

$$\langle I_2 \rangle = \left\langle \int_o^t \frac{dt_1}{\sqrt{t - t_1}} \left[\frac{\partial}{\partial t_1} (u_i - q_i) + q_j \frac{\partial}{\partial x_j} (u_i - q_i)\right] \right\rangle \qquad (2.61b)$$

Assuming that the Reynolds stress term of (2.60) is balanced by part of the force resulting from the unsteady fluctuating nature of the flow then,

$$\frac{\partial}{\partial x_j} \langle q_i q_j \rangle = c \langle I_2 \rangle \qquad (2.62)$$

Substitution in equation (2.60) gives

$$\frac{\partial Q_i}{\partial t} + Q_j \frac{\partial Q_i}{\partial x_j} = \frac{1}{\tau}(U_i - Q_i) + c\langle I_1 \rangle \tag{2.63}$$

From this equation, with the assumption of steady turbulent flow the axial and radial particle conservation of momentum yields

$$Q_x \frac{\partial Q_x}{\partial x} + Q_r \frac{\partial Q_x}{\partial r} = \frac{1}{\tau}(U_x - Q_x) + c\langle I_1 \rangle_x \tag{2.64a}$$

$$Q_x \frac{\partial Q_r}{\partial x} + Q_r \frac{\partial Q_r}{\partial r} = \frac{1}{\tau}(U_r - Q_r) + c\langle I_1 \rangle_r \tag{2.64b}$$

These equations are put in a non-dimensional form by dividing distances by d and velocities by U_o.

Hence
$$\frac{U_o \tau}{d}\left[Q_x^* \frac{\partial Q_x^*}{\partial x^*} + Q_r^* \frac{\partial Q_x^*}{\partial r^*} - c\langle I_1 \rangle_x^* \right] = U_x^* - Q_x^* \tag{2.65a}$$

and
$$\frac{U_o \tau}{d}\left[Q_x^* \frac{\partial Q_r^*}{\partial x^*} + Q_r^* \frac{\partial Q_r^*}{\partial r^*} - c\langle I_1 \rangle_r^* \right] = U_r^* - Q_r^* \tag{2.65b}$$

Expanding the variables Q_x^*, Q_r^* and N^* in the non-dimensional relaxation time parameter τ (N^* is the non-dimensional form of N obtained by dividing by N_o),

$$Q_x^* = Q_x^{(0)} + \frac{U_o \tau}{d} Q_x^{(1)} + \left(\frac{U_o \tau}{d}\right)^2 Q_x^{(2)} + \cdots\cdots \tag{2.66a}$$

$$N^* = N^{(0)} + \frac{U_o \tau}{d} N^{(1)} + \left(\frac{U_o \tau}{d}\right)^2 N^{(2)} + \cdots\cdots \tag{2.66b}$$

The zero order solution represents the limit for which particles follow exactly the motion of the fluid, hence

$$Q_x^* = Q_x^{(0)} \tag{2.67a}$$

and
$$Q_x^{(0)} = U_x^* \tag{2.67b}$$

$$Q_r^{(0)} = U_r^* \tag{2.67c}$$

with the above expressions and equation (2.55), equation (2.57) in dimensionless form becomes

$$U_x^* \frac{\partial N^{(0)}}{\partial x^*} + U_r^* \frac{\partial N^{(0)}}{\partial r^*} = \frac{1}{r^*} \frac{\partial}{\partial r^*} \left(r^* \frac{D_p}{AU_o d} \frac{\partial N^{(0)}}{\partial r^*} \right) \tag{2.68}$$

A similarity solution for $N^{(0)}$ similar to (2.54) is expected, ie

$$N^{(0)} = B \frac{d}{x} \tilde{N}^{(0)}(\eta) \tag{2.69}$$

where B = constant.

Substituting the similarity solution for N and U in (2.68) the result is

$$(\tilde{U}_r - \eta \tilde{U}_x) \frac{d\tilde{N}^{(0)}}{d\eta} - \tilde{U}_x \tilde{N}^{(0)} = \frac{1}{\eta} \frac{d}{d\eta} \left(\eta \frac{D_p}{AU_o d} \frac{d\tilde{N}^{(0)}}{d\eta} \right) \tag{2.70}$$

Substituting expressions (2.56a) and (2.56b) the following ordinary differential equation is obtained

$$\frac{d(\tilde{N}^{(0)} F)}{d\eta} = - \frac{d}{d\eta} \left(\eta \frac{D_p}{AU_o d} \frac{d\tilde{N}^{(0)}}{d\eta} \right) \tag{2.71}$$

Now the particle coefficient of turbulent diffusion D_p is set equal to that of the fluid D_f. Then from equations (2.51) and (2.54b)

$$D_p = D_f = \frac{\lambda_E}{\beta} \langle \tilde{U}_r^2 \rangle^{\frac{1}{2}} AU_o \frac{d}{x} \tag{2.72}$$

For similarity requirements the Eulerian length scale is replaced by

$$\lambda_E = \gamma x \tag{2.73}$$

where γ is taken as a constant.

It follows that (2.72) can be written as

$$D_p = \frac{\gamma}{\beta} AU_o d \langle \tilde{U}_r^2 \rangle^{\frac{1}{2}} \tag{2.74}$$

Then equation (2.71) reads

$$\frac{d}{d\eta}\left(\tilde{N}^{(0)}F\right) = -\frac{d}{d\eta}\left(\eta\,\frac{\gamma}{\beta}<\tilde{U}_r^2>^{\frac{1}{2}}\,\frac{d\tilde{N}^{(0)}}{d\eta}\right) \tag{2.75}$$

Integrating equation (2.75) twice then,

$$\tilde{N}^{(0)} = \exp\left[-\int_0^{\eta}\frac{F}{\eta_1\,\gamma/\beta<\tilde{U}_r^2>^{\frac{1}{2}}}\,d\eta\right] \tag{2.76}$$

The values of the mean and r.m.s. of the velocities $\tilde{U}_x$ and $<\tilde{U}_r^2>^{\frac{1}{2}}$ are obtained from experimental measurements. The function F is then computed from equation (2.56c). For the present work, a computer program was written to obtain numerical values for $\tilde{N}^{(0)}$ for radial points η across the jet at different positions x/d downstream from the nozzle. The value of γ/β was taken as 0.0133, the same as that used by Davidson and McComb. The results are compared with experimental measurements for tracer elements and are shown in Figures (5.2), (5.7), (5.8), (5.9) and (5.10).

In order that a solution of the diffusion problem for discrete particles, which are too heavy to be represented by the above analysis, be obtained, equations (2.66) are studied to first order accuracy.

The requirement for conservation of momentum of a particle will be

$$Q_x^{(1)} = -U_x^*\frac{\partial U_x^*}{\partial x^*} - U_r^*\frac{\partial U_x^*}{\partial r^*} \tag{2.77a}$$

$$Q_r^{(1)} = -U_x^*\frac{\partial U_r^*}{\partial x^*} - U_r^*\frac{\partial U_r^*}{\partial r^*} \tag{2.77b}$$

Similarity solutions for $Q_x^{(1)}$ and $Q_r^{(1)}$ take the form

$$Q_x = A^2\,\frac{d^3}{x^3}\,\tilde{Q}_x^{(1)}(\eta) \tag{2.78}$$

Subsituting similarity solutions for $Q_x^{(1)}$, $Q_r^{(1)}$, U_x^* and U_r^*, equations

(2.76) become

$$\tilde{Q}_x^{(1)} = \tilde{U}_x^2 + (\eta\tilde{U}_x - \tilde{U}_r)\frac{d\tilde{U}_x}{d\eta} \tag{2.79a}$$

$$\tilde{Q}_r^{(1)} = \tilde{U}_x\tilde{U}_r + (\eta\tilde{U}_x - \tilde{U}_r)\frac{d\tilde{U}_r}{d\eta} \tag{2.79b}$$

or in terms of the function F from equations (2.56)

$$\tilde{Q}_x^{(1)} = \frac{1}{\eta^2}\left(\frac{d}{d\eta} - \frac{1}{\eta}\right)\left(F\frac{dF}{d\eta}\right) \tag{2.80a}$$

$$\tilde{Q}_r^{(1)} = \frac{1}{\eta}\frac{d}{d\eta}\left(F\frac{dF}{d\eta}\right) - \frac{1}{\eta^2}F\left(2\frac{d}{d\eta} - \frac{1}{\eta}\right)F \tag{2.80b}$$

Now equation (2.57) is put in dimensionless form and equations (2.66) to first order are substituted. Then with equations (2.55) and (2.68) the following form of the first order diffusion equation is obtained.

$$N^{(0)}\left(\frac{\partial Q_x^{(1)}}{\partial x^*} + \frac{\partial Q_r^{(1)}}{\partial r^*} + \frac{Q_r^{(1)}}{r^*}\right) + Q_x^{(0)}\frac{\partial N^{(1)}}{\partial x^*} + Q_x^{(1)}\frac{\partial N^{(0)}}{\partial x^*} + Q_r^{(0)}\frac{\partial N^{(1)}}{\partial r^*} + Q_r^{(1)}\frac{\partial N^{(0)}}{\partial r^*}$$

$$= \frac{1}{r^*}\frac{\partial}{\partial r^*}\left(r^*\frac{D_p}{AU_o d}\frac{\partial N^{(1)}}{\partial r^*}\right) \tag{2.81}$$

Similarity solutions for $N^{(1)}$ are of the form

$$N^{(1)} = c\frac{d^3}{x^3}\tilde{N}^{(1)}(\eta) \tag{2.82}$$

Using equations (2.82), (2.78) and (2.67) equation (2.81) after rearrangement gives

$$\frac{1}{\eta}\frac{d}{d\eta}\left(\eta\frac{D_p}{AU_o d}\frac{d\tilde{N}^{(1)}}{d\eta}\right) + (\eta\tilde{U}_x - \tilde{U}_r)\frac{d\tilde{N}^{(1)}}{d\eta} + 3\tilde{U}_x\tilde{N}^{(1)}$$

$$= \frac{AB}{C}\left[(\tilde{Q}_r^{(1)} - \eta\tilde{Q}_x^{(1)})\frac{d\tilde{N}^{(0)}}{d\eta} - 4\tilde{Q}_x^{(1)}\tilde{N}^{(0)} - \eta\tilde{N}^{(0)}\frac{d\tilde{Q}_x^{(1)}}{d\eta}\right.$$

$$\left. + \tilde{N}^{(0)}\frac{d\tilde{Q}_r^{(1)}}{d\eta} + \frac{1}{\eta}\tilde{N}^{(0)}\tilde{Q}_r^{(1)}\right] \tag{2.83}$$

Here the assumption made by Davidson and McComb is that the particle coefficient of diffusion D_p for homogeneous turbulent flow can be used in the inhomogeneous jet as the effect of inhomogenuity on D_p/D_f is expected to be slight.

Hence, equations (2.74), (2.80) reduce equation (2.83) to

$$\eta\,\gamma/\beta\langle\tilde{U}_r^2\rangle^{\frac{1}{2}}\frac{d^2\tilde{N}^{(1)}}{d\eta^2}+\left[F+\gamma/\beta\langle\tilde{U}_r^2\rangle^{\frac{1}{2}}+\eta\frac{d}{d\eta}\left(\gamma/\beta\langle\tilde{U}_r^2\rangle^{\frac{1}{2}}\right)\right]\frac{d\tilde{N}^{(1)}}{d\eta}+3\frac{dF}{d\eta}N^{(1)}$$

$$=\frac{AB}{c}\left[\frac{d\tilde{N}^{(0)}}{d\eta}\,\frac{F}{\eta}\left(\frac{F}{\eta}-\frac{dF}{d\eta}\right)-\tilde{N}^{(0)}\left(2\,\frac{F^2}{\eta^3}-\frac{5}{\eta^2}\,F\,\frac{dF}{d\eta}+\frac{3}{\eta}\left(\frac{dF}{d\eta}\right)^2\right.\right.$$

$$\left.\left.+\frac{3}{\eta}\,F\,\frac{d^2F}{d\eta^2}\right)\right] \qquad (2.84)$$

The constant $\frac{AB}{c}$ on the right-hand side of equation (2.84) is replaced by A. Using the experimental data for $\tilde{U}_x$ and $\langle\tilde{U}_r^2\rangle^{\frac{1}{2}}$, the values of F as before, and the zero order solution, the previous computer program was extended to determine the values of $\tilde{N}^{(1)}$ from equation (2.84) by a finite difference method (See Appendix 2A). The values of A, B and γ/β needed for the computations were taken from the data of Davidson and McComb as 7.02, 6.24 and 0.0133.

Then the complete solution for particle properties to first order will be

$$Q_x = AU_o\frac{d}{x}\left[\tilde{U}_x+A\left(\frac{d}{x}\right)^2\frac{U_o\tau}{d}\,\tilde{Q}_x^{(1)}\right] \qquad (2.85a)$$

$$Q_r = AU_o\frac{d}{x}\left[\tilde{U}_r+A\left(\frac{d}{x}\right)^2\frac{U_o\tau}{d}\,\tilde{Q}_r^{(1)}\right] \qquad (2.85b)$$

$$N = B\,N_o\frac{d}{x}\left[\tilde{N}^{(0)}+A\left(\frac{d}{x}\right)^2\frac{U_o\tau}{d}\,\tilde{N}^{(1)}\right] \qquad (2.85c)$$

Rewriting the expansion parameter

$$\varepsilon = A\left(\frac{d}{x}\right)^2\frac{U_o\tau}{d} \qquad (2.86)$$

$$\text{with}\quad \tilde{Q}_x = \tilde{U}_x+\varepsilon\tilde{Q}_x^{(1)} \qquad (2.87)$$

$$\text{then}\quad Q_x = AU_o\frac{d}{x}\,\tilde{Q}_x \qquad (2.88)$$

Similarly

$$\tilde{N} = \tilde{N}^{(0)} + \varepsilon \tilde{N}^{(1)} \tag{2.89}$$

and $$N = BN_o \frac{d}{x} \tilde{N} \tag{2.90}$$

The computations were made for values of ε of 0, 0.050, 0.075, 0.10, 0.20 and 0.30 and the result of the mean concentration relative to that of the jet-centre-line are presented in Figures (5.11), (5.12), (5.13), (5.14), (5.15) and (5.16).

Finally, as the above analysis is based on a monodisperse particle distribution, a crude generalisation can be given to find the effect on the treatment of a polydisperse distribution. In this case each particle size will have a separate equation of motion. This can be taken into account by generalising the perturbation solution to a concentration profile Na(r), where a, the particle radius is now to be regarded as a continuous variable. The zero order solution is expected to be unaffected by the difference in sizes as it is independent of the particle radius. The problem will then be to find out the effect to first and second order, on the particle parameters.

The perturbation solution for monodisperse particles N(r) is

$$N(r) = N^{(0)}(r) + \varepsilon N^{(1)}(r) + \varepsilon^2 N^{(2)}(r) + \ldots\ldots \tag{2.91}$$

For a concentration distribution Na(r) with probability distribution of particle size given by P(a) and characterised by a mean radius $\langle a \rangle$, then

$$\langle Na(r) \rangle = \int P(a)\, Na(r)\, da \tag{2.92}$$

where $\int P(a)da = 1.$

Now the perturbation solution of Na(r) is given to first order by

$$Na(r) = N^{(0)}(r) + \varepsilon(a)N^{(1)}(r) \tag{2.93}$$

Taking the mean value of equation (2.93) the result is

$$\langle Na(r)\rangle = N^{(0)}(r) + \langle \varepsilon(a)\rangle N^{(1)}(r) \tag{2.94}$$

Now $$\varepsilon = Ka^2 \tag{2.95}$$

where $K = \frac{2}{9} \frac{AU_o}{d} \frac{\rho_p}{\mu} (\frac{d}{x})^2$ and does not depend on 'a'.

$$\langle \varepsilon(a)\rangle = K\langle a^2\rangle \tag{2.96}$$

The variance (σ^2) of a is given by

$$\sigma^2 = \langle a^2\rangle - \langle a\rangle^2 \tag{2.97}$$

Hence $$\langle a^2\rangle = \langle a\rangle^2(1 + \frac{\sigma^2}{\langle a\rangle^2}), \tag{2.98}$$

where $\frac{\sigma^2}{\langle a\rangle^2}$ represents the error in making the replacement

$$\langle a^2\rangle = \langle a\rangle^2$$

Equation (2.94) can then be written as

$$\langle Na(r)\rangle = N^{(0)}(r) + \varepsilon(\langle a\rangle) N^{(1)}(r) \tag{2.99}$$

The standard deviation $\langle n^2\rangle^{\frac{1}{2}}$ of Na(r) will be

$$\langle n^2\rangle^{\frac{1}{2}} = \sqrt{\langle Na^2(r)\rangle - \langle Na(r)\rangle^2} \tag{2.100}$$

Now

$$\langle Na(r)\rangle^2 = (N^0(r))^2 + 2N^{(0)}(r)\varepsilon(\langle a\rangle)N^{(1)}(r) + \text{terms of } \varepsilon^2$$

$$\langle Na^2(r)\rangle = (N^0(r))^2 + 2N^{(0)}(r)\varepsilon(\langle a\rangle)N^{(1)}(r) + \text{terms of } \varepsilon^2$$

or $$\langle n^2\rangle^{\frac{1}{2}} = \sqrt{0 + \text{terms of } \varepsilon^2} \tag{2.101}$$

Hence to first order the standard deviation of the polydisperse distribution is zero provided that the mean value that characterises the size distribution is taken for 'a'.

The same procedure is followed to obtain the standard deviation of N from the mean to second order.

Thus

$$\langle Na(r)\rangle^2 = (N^{(0)}(r))^2 + \langle \varepsilon(a)\rangle^2 N^{(1)^2}(r) + 2N^{(0)}(r)\langle \varepsilon(a)\rangle N^{(1)}(r) + 2N^{(0)}(r)\langle \varepsilon^2(a)\rangle N^{(2)}(r) + \text{terms in } \varepsilon^3 \qquad (2.102)$$

$$\langle Na^2(r)\rangle = (N^{(0)}(r))^2 + \langle \varepsilon^2(a)\rangle N^{(1)^2}(r) + 2N^{(0)}(r)\langle \varepsilon(a)\rangle N^{(1)}(r) + 2N^{(0)}(r)\langle \varepsilon^2(a)\rangle N^{(2)}(r) + \text{terms in } \varepsilon^3 \qquad (2.103)$$

The standard deviation of Na(r) is then given by

$$\langle n^2\rangle^{\frac{1}{2}} = N^{(1)}\sqrt{\langle \varepsilon^2(a)\rangle - \langle \varepsilon(a)\rangle^2} \qquad (2.104)$$

This means that the standard deviation of Na(r) is the same as the standard deviation of the expansion parameter. This result is for second order solutions. The present work was taken only to first order accuracy and it can be said that using polydisperse particles and taking the mean value of particle radius will have little effect on the results, provided that the standard deviation of the radius around the mean, or $\frac{\sigma^2}{\langle a\rangle^2}$, is small compared to unity.

CHAPTER III

THEORETICAL ASPECTS OF THE OPTICAL METHOD

The Laser Doppler anemometer (LDA), as an instrument for the measurement of the velocity of a particle moving in a fluid flow field, has attracted the attention of many investigators. The method is now highly developed for scientific and engineering applications. In many instances, it is replacing the hot wire on account of its better spatial resolution and accuracy, in addition to the fact that it does not interfere with the fluid flow.

Recently it has been demonstrated that the LDA signal contains information about the dimensions of particles moving with the fluid and their number, as well as the conventional velocity relationship. In fact, in the present work, the particle number density is deduced from the LDA signal. The theoretical analysis of this deduction will be presented below in section 3.2. The remainder of this section will be devoted to a review of some of the work with the LDA. Firstly, some contributions by authors using the LDA system solely as velocimeter will be considered and then the work employing the LDA as particle sizer or counter will follow.

3.1 REVIEW OF PREVIOUS WORK ON LDA SYSTEMS

Yeh and Cummins (1964) were the first to demonstrate the use of the Doppler Shift to measure the velocity of polystyrene particles in a laminar flow of water in a 10 cm flow-tube. In their optical arrangement one of the laser beams was passed directly to the PM tube. This beam was mixed (hetrodyned) with

the light scattered by a particle illuminated by the second beam at the tube. The resulting signal which is the difference in frequency between the incident and scattered light is directly proportional to the velocity of the particle. The result obtained by these authors shows good agreement with previous measurement and theory. Forman, George and Lewis (1965) are reported to be the first to use an LDA arrangement for the measuremnnt of velocity in a gas flow. Smoke added to the air flowing through a 5 mm inside diameter glass tube, provided the scattering particles. They used a 5 mw He-Ne laser in the reference beam mode (the same as the previous arrangement) and obtained results which were in good agreement with measurement using another direct method. Goldstein and Kreid (1967) presented a theoretical analysis for the LDA and used a reference beam arrangement to measure the velocity of flow of water, marked by polystyrene particles, in a square duct. Light source was from 0.30 mw He-Ne laser, and they argued that their measurement was within 0.1% accuracy and in close agreement with the theory. Pike et al (1968) used the reference beam mode to measure the turbulent velocities in water through a 13 mm diameter glass tube. Milk was added in a small proportion to produce the scattering particles. The observed broadening in the frequency spectra of the fluctuations in turbulent velocity was attributed to the short lifetime of the Doppler shifted signal and the velocity fluctuations. The broadening due to the finite lifetimes of the Doppler signal was investigated for laminar flow. This allowed the calculations of the variance of the spectra produced by the turbulent fluctuations, and hence the fractional turbulence. The result produced is in agreement with hot-wire

measurements within 0.5% for turbulent intensity and within an accuracy of 4% for mean velocity. Adrian and Goldstein (1971) presented a theoretical analysis for an LDA arrangement in which the illuminating and reference beams intersected at the region of measurement. They derived expressions for the photocurrent and its spectrum due to a single particle in the probe volume (point of intersection of the two beams). From these expressions defining the probe volume, the spectrum bandwidth and spectrum amplitude were obtained. The work was extended for an arbitrary number of randomly positioned scattering particles. They showed that for a steady flow the r.m.s spectrum was Gaussian with the same bandwidth as the single particle spectrum. Also it was found that the amplitude of the r.m.s Doppler spectrum is proportional to the square root of the mean scattering particle concentration. Rudd (1968) presented a new model in which the two incident laser beams cross at the measuring point to produce a set of interference fringes. The output signal is interpreted in terms of a particle crossing the fringes. The observed scattered light is explained as the amount of light blocked by the particles as they cross the fringes. The result obtained for the velocity relationship is identical to that derived in terms of the Doppler shift. Rudd showed that a laser is not essential for a Dopplermeter, but is generally preferable to a conventional light source, due to its brightness and hence improved spatial coherence. Lading (1971) also showed that there is no difference in the results obtained by the interference fringe method and the Doppler shift of the light scattered from a particle. He found that the Doppler shift is independent of the

direction of detection although a large detection angle for the hetrodyning of scattered beams will lower the signal. The best signal-to-noise ratio (S/No) was given by Lading to be when the intensity of the two incident beams is the same and when the direction of detection is along the bisector of the angle between the two beams. Masumder and Wankum (1970) studied theoretically and experimentally the (S/No) and the spectral broadening of the Doppler shift. They made a comparison between the reference beam and the interference fringe modes. It was found that for a high scattered beam intensity a small solid angle subtended by the receiver area on the light scattering point can be used and the two methods will give comparable values of (S/No) and instrumental spectra broadening. For low scattered intensity the fringe method is reported to be preferred when the signal power can be appreciably increased by increasing the receiving aperture area. The reference beam arrangement is advantageous when the aperture broadening of the signal is insignificant for scattering centres located at large distance.

The use of LDA for the study of the spatial structure of turbulent flow was presented by Bourke et al (1969). They showed that the theory of the spectrum of light scattered from particles can be used to obtain the spatial distribution of velocity. The experimental results obtained for velocity distribution in a tube showed close agreement with results obtained from hot wire measurement. This agreement between spatial velocity averages by LDA and time-averaged velocities by hot wire confirms the usual assumption of equivalence of turbulent space and time averaging for flows along the axis of a tube. The Doppler spectrum was

measured and related to the mean axial velocity in the tube. This velocity is also in agreement with the theoretical prediction. Bourke et al also measured the intensity-fluctuation spectrum. This is the distribution of differences in Doppler shifts from pairs of particles within the same illuminated region thus giving the distribution of instantaneous velocity differenes between pairs of particles. Durst and Whitelaw (1971) presented a study of the optimization of the optical anemometers. They showed the difference between the interference fringe and Doppler shift anemometers and identified the best situations for the use of either arrangement. They proposed a system which is a combination of the previous two modes and is expected to enable simultaneous measurements of the instantaneous velocities in two mutually perpendicular directions. Edwards et al (1971) developed a theoretical model for the prediction of the spectrum observed with LDA. Experimental measurements of the spectra of the signal from water flow in glass tubes provided the verification of the model.

The contributions in the field of velocity measurement are too many to enumerate. Some of those are due to George and Lumley (1973) who gave a detailed theoretical analysis for the application of LDA for measurement of turbulence. Measurement of the turbulence spectrum was reported to verify the theory. Buchhave (1973) presented a collection of results for improvement of light collecting and detecting systems. Brayton et al (1973) described a two-component dual-scatter LDA utilising three laser beams. This enables the measurement of two orthogonal velocity components simultaneously. Melling and Whitelaw (1973) gave a

detailed study of the problem of seeding of gas flows for LDA. They examined the criteria which limit the particle characteristics for use in seeding. In addition they described methods of generating and sizing particles which conform to these limits. Abbiss, Chubb and Pike (1974) analysed the different configurations of LDA. They discussed the optical arrangements that would produce the best accuracy in measurements for specified situations.

Pike (1972) demonstrated the application of photon-correlation to the LDA. The train of pulses in time given by the photodetector is fed to the correlater where the frequency present is obtained by matching the signal with itself at delayed times (autocorrelation). With proper choice of the delay time this frequency is the same as the Doppler shift and is a direct measure of the velocity of flow. Birch et al (1973) applied photon-correlation spectroscopy to the measurement of turbulent flow in a round free jet. Their measurements of the mean velocity and turbulence intensity show good agreement with hot wire measurements. Abbiss (1974) used photon-correlation for measurement of supersonic velocities. He used a two-colour system from an argon laser to measure simultaneously two components of velocity in a wind tunnel. Close agreement between the results obtained and pilot-tube measurements as well as theoretical predictions is shown. She and Lucero (1973) assuming a turbulent velocity model based on Gaussian statistics, presented an expression for the photon-correlation function. This expression, which is applicable to a number of turbulent flows, amongst them free turbulence, produced close agreement with experimental data from

a free jet. These authors showed that the measured photon-correlation spectrum together with the above expression can be used effectively to find simultaneously, the mean flow velocity, the turbulent intensity and the particle concentration.

In the last few years, the LDA signal has been recognised to be applicable to the development of particle sizers and counters. Farmer and Brayton (1971) in their analysis of the atmospheric laser Doppler velocimeters showed that of the number, N, of scattering centres in the probe volume, only $\sqrt{N}$ contribute to the Doppler signal. Hence, the signal power for a large number of scatterers in the probe volume is $\sqrt{N}$ times the power from a single scattering centre. Owens (1969) presented an analysis of the feasibility of optical hetrodyne measurements of Doppler shifts as a method for remote determination of wind velocity. He showed that for this arrangement the root mean square signal amplitude due to a number of particles, N, in the probe volume is $\sqrt{N}$ times the amplitude of the signal for one particle. Later (1972) he ascertained that for the dual scatter arrangement the signal powers rather than the amplitudes vary as $\sqrt{N}$. Farmer (1972) related the ratio of signal a.c. to d.c power to the visibility or modulation. He showed that if the fringe spacing (δ), produced by the intersection of the two incident beams is of the order of magnitude of the diameter of a particle (D_p) then the visibility of the signal is directly related to the particle size through a Bessel function of the first order, if the particle is spherical in shape. However, for a cylindrical particle the relation is through a sine function. Farmer also showed that if the ratio δ/D_p is large then the visibility is

inversely proportional to the square root of the number of particles in the probe volume. The visibility was also shown to be the same as the ratio between the a.c. to d.c. powers of the signal. The theoretical analysis given by Farmer forms the basis for the method of measurement of mean concentration used in the present work and will be derived in the next section of this chapter. Farmer (1974) reported the results of experimental observation of large particles with an LDA. He found that the visibility of N particles was independent of the solid collection angle and was a function of the observation angle only when the particles are large. Farmer showed that accurate results for number density can be obtained for a size distribution when the distribution is narrow and the number of observed particles is large. He also showed that while particle sizes of the range 10 - 15 μm can be measured using the visibility method, no reason had been found for why the size range cannot be extended beyond these limits. Orloff et al (1975) used the visibility function developed by Farmer for measurement of particle sizes. They used polystyrene divinyl benzene spheres suspended in distilled water as the light scatterers. A magnetic stirrer provided the necessary fluid motion to generate the burst signal. Their results show that the experimentally obtained visibility against D_p/δ has the same trend as the theoretical prediction with a minimum visibility occuring at the value of D/δ predicted by the theory. Yet the experimental data was displaced vertically from the theoretical curve indicating an over-estimate of the particle size. However, the visibility measurement was reported to be directly from a storage oscilloscope. Orloff et al concluded that the Bessel function visibility relationship is only valid

when the critical assumptions made in the theory are met in practice by placing constraints on the optical geometry. Durst and Eliasson (1975) studied the properties of LDA signals and their use for particle size measurement. They utilised a computer program based on an exact mathematical treatment of light scattered by spherical particles taking into account the properties of the optical system and its influence on the focused Gaussian laser beam. The parameters of the LDA signal were obtained by integrating over the complete measuring volume seen by the detector. Particle sizes were measured using a laser beam in conjunction with a white light source (this method which was suggested by Durst and Umhaur (1975) was referred to in the first chapter). The result shows good aggeement with sizes obtained from electron microscope photographs. They argue that the measurement of visibility alone is insufficient to give information about the particle size and suggest that two or more properties of the LDA signal are required to quantify the particle diameter. Such properties could be the signal amplitude and the corresponding visibility. Robinson and Chu (1975) presented a theoretical analysis based on scalar diffraction theory describing the scattered field in the far-field region of the scattering centre. They considered two cases, the first for an infinite receiving aperture and the second for a finite receiving aperture. They performed a set of experiments for measurement of the visibility and showed that it depended on (1) the particle size, (2) the index of refraction, (3) the cross beam angle and (4) the collecting angle. Their experimental results are in close agreement with the theoretical predictions. It is interesting to

note that those theoretical predictions which are similar to those due to Farmer also show good agreement with Farmer's experimental results. Fristorm et al (1973) studied theoretically the conditions under which the alternating light signal generated by a particle traversing a fringe pattern falls to zero. The analysis was based on geometrical optics and particles larger than the wave-length of light. They examined the use of this with a varying fringe spacing for measurement of particle sizes. Their experiment utilised a schlieren system and the results confirm the theoretical analysis. Jones (1973) using the wave theory presented the solution for light scattering by a cylinder parallel to the system of interference fringes. The solution can be used to predict the positions of the zeros in the a.c. amplitude when the fringe spacing is varied, and the optimum angle at which scattered light may be detected. He reported that the results obtained using geometrical optics are remarkably in good agreement with the wave theory analysis even for small particles. In another paper, Jones (1974) extended his previous analysis for a sphere placed at the cross point of two incident beams. Hong and Jones (1976) used a computer program to integrate the scattered intensity obtained by Jones for a spherical particle over the angular field of view of the detector. The visibility calculated from this analysis was compared with that measured from single particles and a particle size distribution was built-up. This was compared with a distribution obtained by counting a sample under an optical microscope. For glass "ballotini" spheres the two results are in close agreement. But for titanium dioxide particles, which are irregular in shape, the scattering

method gave 0.85, the size obtained from the optical microscope counts based on the maximum dimension. They concluded that the fringe anemometer can be effectively used to measure the particle sizes and is insensitive to refractive index, simple to operate and is capable of automation.

3.2 THEORETICAL ANALYSIS OF LDA SIGNAL

Here a brief outline of the theory developed by Farmer and Brayton (1971) and Farmer (1972) will be presented. The parts of interest are those in which a relationship is developed between the signal visibility and the number of particles in the probe volume.

If only one particle is considered to be traversing a set of interference fringes then the probability that at any instant it would be on a bright fringe and hence scattering light is $\frac{1}{2}$. If, however, there are N particles, the probability that all N particles are scattering light is $(\frac{1}{2})^N$. Here all particles are assumed to be moving with the same velocity and to be randomly distributed. Some of the particles (N_d) will be on a dark fringe and the signal produced by them will tend to reduce the Doppler signal. The rest of the particles (N_b) will be on a bright fringe and their signal will add up to the total signal. Now if (N_e) is the effective number of particles whose signals actually produce the Doppler signal then

$$N_e = N_b - N_d \tag{3.1a}$$

and

$$N = N_b + N_d \tag{3.1b}$$

Naturally, all sequences have the same form of probability

ie, $(\frac{1}{2})^{N_b}$, $(\frac{1}{2})^{N_d}$.

The total number of ways N particles can be arranged to give N_e is the same as the number of ways N objects can be separated in two groups (N_b and N_d).

This is

$$\frac{N!}{N_b!\, N_d!}$$

Hence the total probability of N particles adding to give a signal is

$$P_{N_e} = \frac{N!}{N_b!\, N_d!} \left(\tfrac{1}{2}\right)^{N_b} \left(\tfrac{1}{2}\right)^{N_d} \tag{3.2a}$$

Or from (3.1b),

$$P_{N_e} = \frac{N!}{N_b!\, N_d!} \left(\tfrac{1}{2}\right)^{N} \tag{3.2b}$$

For large values of N Stirling's approximation for N! gives

$$N! \simeq (2\pi N)^{\frac{1}{2}} \left(\frac{N}{e}\right)^{N} \tag{3.3}$$

where $e = 2.71828$

With equation (3.3) and similar approximation for N_b and N_d, equation (3.2b) becomes

$$P_{N_e} \simeq \frac{(2\pi N)^{\frac{1}{2}} (N/e)^{N} (\frac{1}{2})^{N}}{(2\pi N_b)^{\frac{1}{2}} (\frac{N_b}{e})^{N_b} (2\pi N_d)^{\frac{1}{2}} (\frac{N_d}{e})^{N_d}} \tag{3.4}$$

Rearranging and using equation (3.1a) and (3.1b), equation (3.4) yields

$$P_{N_e} \simeq \frac{1}{(1 + \frac{N_e}{N})^{N_b + \frac{1}{2}} \; (1 - \frac{N_e}{N})^{N_d + \frac{1}{2}}} \left(\frac{2}{\pi N}\right)^{\frac{1}{2}} \tag{3.5}$$

Taking the natural logarithms of both sides of equation (3.5)

$$\ell n(P_{N_e}\ (\frac{\pi N}{2})^{\frac{1}{2}}) \;=\; -\ (N_b + \tfrac{1}{2})\ell n(1 + \frac{N_e}{N}) - (N_d + \tfrac{1}{2})\ell n(1 - \frac{N_e}{N}) \tag{3.6}$$

Expanding $\ell n\ (1 \pm \frac{N_e}{N})$ in a Maclauran series and taking values to second order (as $N_e << N$), then equation (3.6) can be written as

$$\ell n(P_{N_e}\ (\frac{\pi N}{2})^{\frac{1}{2}}) \;=\; -\ \frac{N_e^2}{N}\ (1 - \frac{N_e}{N}) \tag{3.7}$$

Or for $N_e << N$ then $\frac{N_e}{N} << 1$ and equation (3.7) reduces to

$$\ell n\ (P_{N_e}\ (\frac{\pi N}{2})^{\frac{1}{2}}) \;=\; -\ \frac{N_e^2}{N} \tag{3.8}$$

$$\text{or} \qquad P_{N_e} \;=\; (\frac{2}{\pi N})^{\frac{1}{2}}\ \exp\ (-\ \frac{N_e^2}{N}) \tag{3.9}$$

Now the probability of N_e being between N_e and $N_e + dN_e$ is $P_{N_e}\, dN_e$ and the mean square of N_e is given by

$$\langle N_e^2 \rangle \;=\; \int_o^\infty N_e^2\ P_{N_e}\, dN_e \tag{3.10}$$

Substituting equation (3.9) in equation (3.10) produces

$$\langle N_e^2 \rangle \;=\; \int_o^\infty (\frac{2}{N\pi})^{\frac{1}{2}} \left[\exp\ (-\ \frac{N_e^2}{2N})\right] N_e^2\ dN_e \tag{3.11}$$

After integration equation (3.11) can be written as

$$\langle N_e^2 \rangle \;=\; (\frac{2}{N\pi})^{\frac{1}{2}}\ \ \frac{\sqrt{\pi}}{4}\ (2N)^{3/2}$$

$$\text{or} \qquad \langle N_e^2 \rangle \;=\; N$$

Hence the r.m.s of N_e is given by

$$\langle N_e^2 \rangle^{\frac{1}{2}} \;=\; N^{\frac{1}{2}} \tag{3.12}$$

This means that of the N particles seen by the detector, only the

square root of N gives a velocity signal.

Now referring to figure (3.1) which represents a typical burst signal for an LDA, the visibility of the signal can be defined as

$$V = \frac{I_{max} - I_{min}}{I_{max} + I_{min}} \tag{3.13}$$

where I_{max} is the maximum scattered intensity from a birght fringe and I_{min} is the corresponding minimum scattered intensity from the next consecutive dark fringe. The signal is seen to be an a.c. modulation mounted on a d.c. pedestal. Referring to figure (3.1)

$$\text{the a.c. power} = \frac{I_{max} - I_{min}}{2} \tag{3.14}$$

and

$$\text{the d.c. power} = \frac{I_{max} + I_{min}}{2} \tag{3.15}$$

Dividing equation (3.14) by equation (3.15) then

$$\frac{\text{a.c. power}}{\text{d.c. power}} = \frac{P_{a.c.}}{P_{d.c.}} = \frac{I_{max} - I_{min}}{I_{max} + I_{min}} \tag{3.16}$$

which is identical to equation (3.13).

Hecce the visibility is the ratio between the a.c. and d.c. powers.

Now if there is only one particle in the probe volume then the visibility (V_1) will be given by

$$V_1 = \frac{P1_{a.c}}{P1_{d.c}} \tag{3.17}$$

If there are N particles then the mean a.c power from equation (3.12) is found to be

$$\langle P^{N}_{a.c} \rangle = \sqrt{N}\, P^{1}_{a.c.} \tag{3.18}$$

Each particle in the probe volume will contribute to the d.c. power. Hence

$$\langle P^{N}_{d.c} \rangle = N\, P^{1}_{d.c.} \tag{3.19}$$

The mean signal visibility $\langle V_N \rangle$ for N particles will then be

$$\langle V_N \rangle = \frac{1}{\sqrt{N}} \frac{P^{1}_{ac}}{P^{1}_{dc}} = \frac{1}{\sqrt{N}} V_1 \tag{3.20}$$

Now, V_1, the signal visibility for one particle can be interpreted as the ensemble average one particle visibility function for the size distribution of N particles. In this case, equation (3.20) can be written as

$$\langle V_N \rangle = \frac{1}{\sqrt{N}} \langle V_1 \rangle \tag{3.21}$$

For a given optical arrangement if the fringe spacing is varied (increased) until $\langle V_1 \rangle$ is constant and nearly unity, then the visibility measurement in the presence of a number of particles will be a function only of that number. When this condition is satisfied, then

$$\langle V_N \rangle \simeq \frac{1}{\sqrt{N}} \tag{3.22}$$

The above condition of having $\langle V_1 \rangle$ constant and nearly unity is easily satisfied if δ/D_p is large enough. In fact, for the first part of measurement (titanium dioxide particles) in the present work this ratio was kept above 20, while in the second part (tungsten metal powder) it was above 10.

The visibility at the centre line of the jet was used as the normalising value and was divided by subsequent values of

$\langle V_{N_i} \rangle$ radially across the jet, such that,

$$\frac{\langle V_{N_o} \rangle}{\langle V_{N_i} \rangle} = \frac{\langle N_i \rangle^{\frac{1}{2}}}{\langle N_o \rangle^{\frac{1}{2}}} \tag{3.23}$$

Hence

$$\frac{\langle N_i \rangle}{\langle N_o \rangle} = \frac{\langle V_{N_o} \rangle^2}{\langle V_{N_i} \rangle^2} \tag{3.24}$$

CHAPTER IV

DESIGN AND TESTING OF THE EXPERIMENTAL APPARATUS

4.1 DESIGN

A schematic view of the complete assembled apparatus is shown in figure (4.1) with details of the components in figures (4.2), (4.3) and (4.4).

Air was supplied by the main blower through a diffuser with a honeycomb mesh to a partially fluidized bed of solid particles. The particles were entrained by the air to pass through a nozzle (figure 4.2) with its axis vertical, mounted on the bed. The jet so produced was collected by an extraction hood (figure 4.3) and passed to an expansion chamber (figure 4.4). There, the particles were filtered to be drawn into the main blower while the excess air was extracted by an auxiliary blower.

The main objectives of the design were to produce an aerosol jet with particles flowing from the nozzle at a constant rate per unit time, or a mean rate that was constant when averaged over a short period of time. The system had to allow for the use of a range of particle sizes and provision had to be made whereby the nozzle velocity and particles number density could be varied. Effective extraction and filtering devices had to be designed so that the jet could be collected and the particles separated from the air to be recycled.

4.1.1 Design of the Fluidised Bed and the Nozzle

The aim here was to design a system that would supply a constant number of particles per unit time at entry to the nozzle. Then, by the law of conservation of mass applied between inlet and outlet of the nozzle, the number of particles leaving would be the same as the number of those entering the nozzle.

A bed of particles with air flowing through it would meet the demand if the following conditions were satisfied:

1 All particles were of the same weight.

2 The height of particles in the bed was maintained at a constant level.

3 Air was supplied at a velocity, constant with respect to time at all points over a cross-section of the bed.

4 That the air velocity was high enough to lift the particles against gravitational and other retarding forces.

To determine the velocity referred to in the last condition, it was assumed that all particles to be used

a) were spherical in shape;

b) were either of the same size (monodisperse) or could be characterised by a mean size;

c) obey Stokes' Law of Resistance.

This law could be stated in the form (Orr 1966)

$$U_s = \frac{d^2 g (\rho_p - \rho_f)}{18 \mu_f}$$

where

U_s = particle settling velocity

d = particle diameter

g = gravitational acceleration

ρ_p = particle material density

ρ_f = fluid density

μ_f = fluid dynamic viscosity

Since the fluid (air) density was small compared with the particle material density (≥ 1) in the above equation it was neglected. The velocity of a particle rising or falling in air would then be proportional to the square of the diameter of a particle multiplied by its material density (ie. $d^2\rho_p$). This was used as a basis for the choice of an upper limit of particle dimensions to be used in the apparatus. A density of 1 gm/cm^3 and a diameter of 100 x 10^{-6}m (ie. $d^2\rho_p = 10^{-4} gm/cm^1$) were selected. The settling velocity for those particles would be 3 m/s. Any other particles with $d^2\rho_p$ less than 10^{-4} would satisfy condition (4) above.

To comply with the requirement of the third condition, all obstacles that would cause a disturbance in the flow were avoided and flow-smoothing devices were introduced into the flow. This was achieved by firstly, mounting the blower with its delivery pipe vertical in order that air was supplied directly in the bed without any piping connections. Secondly, the diffuser - the only connection to the bed - was designed so that its cone angle was 5°. This is the recommended angle to give disturbance-free flow (Pankhurst 1952). Thirdly, flow-smoothing honeycomb (Aluminium, 15 cm in length, 0.3 cm hexagonal cell) was inserted in the flow.

As far as the second condition was concerned, two factors justified its validity. The first was that the time taken for a complete set of measurements was relatively short so that the

number of particles lost from the system was small. The second was that the particles were recycled and the total number remained the same except for the particles which were lost to the atmosphere or those which settled at pipe bends and inside the main blower. Occasionally, particles were added to make up for those lost.

Finally, although the first statement regarding particles to be of the same weight is not plausible, yet it was reasonable at this stage to make such an assumption. The effect of using particles different from those assumed as well as the effect of the deviation from other design parameters was tested by measuring the concentration of particles at the centre line position of the nozzle for more than the time required for one set of experimental results. The result was satisfactory in that the standard deviation of the visibility of the Laser Doppler Signal, which is a measure of the concentration, from the mean was 6% for titanium dioxide particles and 10% for tungsten metal particles. This will be given in detail in Chapter V.

To determine the size of the fluidised bed relative to the diameter of the nozzle it was necessary to make a further assumption regarding the maximum velocity of flow from the nozzle. It was assumed that the flow of air could be treated as incompressible. Hence the air velocity was restricted to a maximum value of 100 m/s, this being the accepted limit above which density variations could not be ignored.

With a maximum velocity of 3 m/s in the particles bed having to correspond to a top limit of nozzle velocity of 100 m/s, a bed diameter of 5×10^{-2}m and a nozzle diameter of 0.3×10^{-2} m were

selected. This arrangement gave a maximum velocity of 83 m/s from the nozzle and required a volume flow rate of 6 x $10^{-4}m^3/s$ (1.25 ft^3/min). A glass tube (QVF, borosilicate glass) 5 x $10^{-2}m$ diameter and 0.50 m height was used as the fluidised bed.

A Secomak blower was available and was tested for suitability as follows, (figure 4.5 shows the arrangement of equipment for this test):-

The nozzle was fitted to the outlet of the blower and a polythene tube was fitted to the outer body of the nozzle. The tube was big enough to contain the nozzle and it had provision for a small tube connection to measure the total pressure drop relative to the atmosphere. The large tube was connected to a dry gas meter. The blower was driven at the maximum speed and was found to deliver 6 x $10^{-4}m^3/s$ (1.25 ft^3/min). The total head was 0.48 m H_2O indicating a pressure drop of 0.05 m H_2O in overcoming friction in the pipe and in the nozzle.

This part of the apparatus was assembled by bolting the blower to a 1.2 x 1.8 x 0.02 m steel plate and mounting it with its delivery pipe vertical. Power was supplied to the blower through a variac that allowed the variation of the blower speed and hence the nozzle velocity. The honeycomb was placed in the diffuser which was connected between the blower and the fluidised bed, with the nozzle at the top. Three lengths of angle-section, sheet metal were used to tie the assembled part of the equipment to the steel plate to prevent lateral movement (figure 4.1). The combination was balanced, using a spirit level, until the nozzle axis was vertical.

4.1.2 Design of Extraction Hood

In order to design the hood it was necessary to know the spread of the jet as well as the distance above the nozzle where the hood was to be placed.

According to Pai (1954) the diameter of the circle of fluid for which the ratio of the mean velocity to that of the nozzle velocity is 10%, lies on a cone of semi-angle 9.2^{o} with apex at the centre of the jet exit. This was used to obtain an estimate of the jet diameter at entry to the hood.

The distance between the hood and the nozzle was kept at 0.70 m. This provided adequate measuring space for nozzles with diameters larger than 3×10^{-3} m, to be used. The jet spread at that position was of the order of 0.25 m.

A schematic diagram of the hood is shown in figure (4.3). It was made of sheet metal drawn into a conical section with the bottom and top circles having diameters of 0.40 m and 0.06 m respectively. The height of the tapered part was 0.45 m. It was mounted with its axis coinciding with the nozzle axis and the top end had a 0.05 m length of piping to allow for connection to the expansion chamber. This was made by a 1.2 m long, 0.06 m diameter polythene tube. The flow had to reverse direction when entering the expansion chamber. The polythene tube was bent in a semi-circle to accomplish this.

4.1.3 Design of the Expansion Chamber

The purpose of the expansion chamber was to filter the particles collected by the extraction hood and extract the air entrained by the jet through an auxiliary blower.

The chamber had to be designed so that it would expand the air/particle mixture and ensure that the mixture reached the filter with a velocity of the order of magnitude of the settling velocity of the particles. Thus separation would take place with the minimum of the particles penetrating the filter. The design of the filter was to be based on the velocity of the smallest particles to be used.

The pressure drop due to pipe friction, bends in the pipe connecting the hood to the expansion chamber, and across the filter had to be determined. These, together with the volume of air to be removed from the chamber were obtained and formed the criteria for the choice of the auxiliary blower.

To find the velocity of air at entry to the expansion chamber, the velocity of flow in the extraction hood had to be obtained. This was determined from the mean velocity and the cross-sectional area of the jet at the point where it met the hood wall (0.80 m from the nozzle).

The centre line mean velocity, U_1, at an axial distance x downstream from the nozzle could be determined from a relation of the form (Pai 1954).

$$\tilde{U}_1 = 6.5\, U_o \frac{d}{x},$$

where U_o = nozzle velocity

and d = nozzle diameter

At a distance of 0.80 m (position 2) from the nozzle the jet centre-line mean velocity for a nozzle velocity of 83 m/s was 2 m/s.

By conservation of momentum between the nozzle exit (position 1) and position 2

$$A_1 U_o^2 = A_2 U_2^2,$$

where A_1 and A_2 are the cross-sectional areas of the jet at the two points considered.

Substituting the values of A_1, U_o and U_2 the value of A_2 was found to be $1.2 \times 10^{-2} m^2$ giving a volume flow rate at position 2 of $2.4 \times 10^{-2} m^3/s$. Thus the velocity at exit from the extraction hood (6×10^{-2}m diameter pipe) was 8.5 m/s.

As mentioned earlier, the size of the filter was designed such that the particles would approach the filter with a velocity near the particle settling velocity, to avoid penetration of the particles into the filter. Taking the smallest particles to be used in the system to be of 10 micron diameter and 1 gm/cm^3 density the settling velocity (from Stokes' law) would be 0.3×10^{-2}m/s. With a volume flow rate of $2.4 \times 10^{-2} m^3/s$ the filtering area required would be 8 m^2. This would have been too large to make from a practical point of view. However, a smaller size of 0.80 x 0.80 m was chosen in this case. This would filter effectively particles of 20 micron diameter and unit density if the nozzle flow was at half the maximum velocity.

The filter consisted of a sheet of foam rubber covered on the front face by a sheet of tissue paper. It was placed in a wooden box 0.80 x 0.80 x 0.50 m with the filter dividing the box

into two halves (figure 4.4). An auxiliary blower was installed at the back face of the box and would extract the air entrained by the jet. After filtration the particles were collected at a funnel-shaped container. This was made to have no horizontal surface so that no particles would deposit on it. It was mounted on the lower frontal part of the wooden box ending at a 6×10^{-2}m diameter pipe. The box with the filter, the funnel-shaped container and the auxiliary blower constituted the expansion chamber. It was connected through the 6×10^{-2}m pipe to the inlet of the main blower by a polythene pipe.

To determine the characteristics required by the auxiliary blower, the volume flow rate of the air to be extracted had to be known. Also the pressure drop across the piping connections between the hood and the expansion chamber as well as that across the filter ought to be known.

The volume flow rate of air was the volume rate of the jet delivered at the hood less the main blower intake volume rate. This worked out to be 2.3×10^{-2}m^3/s (50 ft^3/min).

The pressure drop across piping connections consisted of two components. Friction loss in pipe connecting the extraction hood to the expansion chamber and loss due to $2 \times 90^{\circ}$ bends in the same pipe. (The polythene pipe curved into a semi-circle changing the direction of flow by 180° or $2 \times 90^{\circ}$). These two components were computed while the pressure drop across the filter was found by experiment.

Pipe friction loss was estimated from charts (Spiers 1955),

assuming that the relative roughness of polythene piping was of the same order of magnitude as drawn tubing. The pressure drop thus obtained was 0.45 of the dynamic head.

The head loss in pipe bends was calculated by assuming that each of the 90^{o} bends would consume 20% of the dynamic head (Duncan, Thom and Young 1960). Hence the pressure drop in the two bends was 0.40 of the dynamic head.

The arrangement for the experiment to determine the pressure drop across the filter is shown in figure (4.6) and the experiment was carried out as follows.

A circular sample of the filter, 3.5×10^{-2}m in diameter, was carefully cut and fitted onto a plastic stopper with a hole 3.0×10^{-2}m diameter. The filter was arranged to cover the hole. The stopper was plugged on either side into the ends of two polythese tubes. One of the free ends of the tubes was connected to the outlet of a blower and the other end to a dry gas meter. Provision was made to obtain the pressure drop between two points immediately upstream and downstream of the filter. The speed of the blower was varied until a volume flow rate, as measured by the gas meter, that would give the same velocity across the filter as that in the expansion chamber under optimum conditions (3×10^{-2} m/s), was maintained. The pressure drop was measured by a water manometer and found to be 2.20×10^{-2}m H_2O.

The total pressure drop on the auxiliary blower added up to 2.6×10^{-2}m H_2O ($\sim$ 1 in. H_2O). Hence the auxiliary blower should be capable of delivering $2.30 \times 10^{-2}m^3/s$ (50 cu.ft/min).of air against a head of 2.6×10^{-2}m H_2O ($\sim$ 1 in H_2O).

The blower used was an Airflow Development make, size 45CT delivering 50 cu.ft/min of air at a head of 1.1 in. H_2O - the same characteristics required by the expansion chamber.

Finally, it was found necessary, at a later stage, to use two other nozzles of diameters 0.5 x 10^{-2}m and 1 x 10^{-2}m, with the apparatus. The effect of those two nozzles on the design parameters was to allow particles of larger sizes to be used if the apparatus were to be operated at the maximum velocity. It was found that if the apparatus was working at a nozzle velocity of 30 m/s with 0.5 x 10^{-2}m diameter nozzle, then the velocity in the fluidised bed (3 m/s), the volume of air delivered by the nozzle (6 x $10^{-4}m^3/s$) and the area of the jet where it met the hood (1.2 x $10^{-2}m^3$) were the same as those for the 0.30 x 10^{-2}m diameter nozzle.

The mean velocity of flow on the jet centre line at intersection with the hood was 1.2 m/s giving a volume flow rate across the filter of 1.44 x $10^{-2}m^3/s$ (less than that for the 0.30 x 10^{-2}m diameter nozzle). This meant that the velocity of flow across the filter was lower and hence an improved filtration process. The highest velocity used with the 0.50 x 10^{-2}m diameter nozzle was 50 m/s. This gave a velocity of flow across the filter of the same order of magnitude as that for the 0.30 x 10^{-2}m diameter nozzle.

As a whole, the use of the other two larger nozzles did not affect the design parameters of the apparatus, especially when the system was operated at velocities less than the maximum nozzle velocity.

4.2 TESTING OF APPARATUS

Before any particles were introduced in the system, the nozzles were tested for symmetry by measuring mean velocity profiles at different sections in the axial direction by a pitot tube and a hot wire anemometer. Also r.m.s values of the fluctuating velocities in the axial direction were measured by the hot wire anemometer.

The results thus obtained were compared with each other and with previous experimental results.

4.2.1 Pitot Tube Measurements

The pressure drop h m H_2O obtained by placing a pitot tube in a stream of air flowing at a velocity v m/s is proportional to the square of that velocity, or

$$v = \sqrt{2gh}$$

where g = gravitational acceleration.

The pitot tube used in this experiment had a main tube diameter of 0.635 x 10^{-2}m with the sensor inside diameter of 0.8 x 10^{-3}m. The pitot tube was mounted on a traversing mechanism which would allow motion of the tube along any of the three principal axes.

Each time a set of readings was to be taken the pitot tube was positioned at the required height from the nozzle with the sensor axis coinciding with the nozzle axis. The tube was then moved to one side of the jet and traversed in small steps to the other side. At each point the pressure drop was measured and the velocity calculated.

The tube output was measured by a Furness Controls Limited Type MDC, electric micromanometer, the output of which was displayed by a Solartron Type TM 1440.2, digital voltmeter. For each measuring point at least ten readings were taken and averaged. Then the mean velocities calculated from the above equation.

The results were then normalised by dividing all velocities by the mean centre-line velocity at the corresponding section, and all radial distances by the distance of the measuring plane from the geometrical origin of the jet. Those results were plotted and are shown in Figures (4.7), (4.8) and (4.9) as compared with previous experimental data (Wygnanski and Fiedler 1969).

4.2.2 Hot Wire Anemometers

A hot wire anemometer probe consists of a very fine short metal wire, which is heated by an electric current. When the wire is placed in the flow it will be cooled causing the temperature, and consequently the electric resistance, to drop. This heat transfer is a measure of the flow velocity if the metal and fluid physical properties, as well as the difference in temperature between the wire and the fluid are known.

Generally, heat is considered to be transferred in cooling the wire by conduction to the wire supports and by forced convection only, other modes having negligible effects. Hinze (1959) and Bradshaw (1971) quote the result of Kramers who found satisfactory agreement with the empirical relation for heat transfer from a cylinder of diameter d:

$$Nu = 0.42\ Pr^{0.20} + 0.57\ Pr^{0.33}Re^{0.50} \qquad (4.1)$$

where Nu = Nusselt number = $\frac{\alpha d}{Kg}$

Pr = Prandtl number = $\frac{Cp\mu g}{kg}$

Re = Reynolds number = $\frac{\rho g U d}{\mu g}$

with α = heat transfer coefficient

Kg = heat conductivity of gas at temperature θg

μg = absolute viscosity of gas at temperature θg

Cp = specific heat of gas at constant pressure

ρg = density of gas at temperature θg

$\Delta\theta$ = temperature difference between wire and gas

U = velocity of gas

d = diameter of cylinder (wire)

The above equation was shown to be valid for air in the range $0.01 < Re < 10000$

Now for thermal equilibrium the heat transferred by the wire is equal to the heat generated by the electric current I. Setting this equilibrium equation:

$$I^2R_w = e\pi K_f \ell(\theta_w - \theta_g)\left[0.42\ (Pr)_f^{0.20} + 0.57(Pr)_f^{0.33}(Re)_f^{0.50}\right] \qquad (4.2)$$

where R_w = total electric resistance of the wire

e = conversion factor = 4.3

ℓ = length of wire

θ_w = wire temperature

θ_g = gas temperature

Subscript 'f' denotes that the values of the gas properties were evaluated at the film temperature θ_f given by

$$\theta_f = \frac{\theta_w + \theta_g}{2} = \theta_g + \frac{\Delta\theta}{2} \qquad (4.3)$$

The electric resistance of the wire is a function of temperature and the relation can be stated as:

$$R_w = R_o(1 + \beta(\theta_w - \theta_o) + \beta_1(\theta_w - \theta_o)^2 + ...) \qquad (4.4)$$

where R_o = resistance at reference temperature θ_o

β, β_1 = temperature coefficients of electric resistivity of the wire.

Neglecting the quadratic term in equation (4.4) as β_1 is much smaller than β, then $\theta_w - \theta_g$ can be expressed in terms of resistances as follows:

$$\theta_w - \theta_g = \frac{R_w - R_g}{\beta R_o} \qquad (4.5)$$

where R_g = electric resistance of the wire at gas temperature θ_g. Equation (4.2) can then be replaced by

$$I^2R_w = \frac{e\pi K_f \ell}{\beta} \frac{R_w - R_g}{R_o} \left[0.42Pr^{0.20} + 0.57\ Pr^{0.33}Re^{0.5}\right] \qquad (4.6)$$

This equation can be expressed in a form suitable for hot wire anemometry as:-

$$\frac{I^2R_w}{R_w - R_g} = A_1 + B_1\sqrt{U} \qquad (4.7)$$

with $A_1 = 0.42 \frac{e\pi K_f \ell}{\beta R_o} (Pr)^{0.20}$

and $B_1 = 0.57 \frac{e\pi K_f \ell}{\beta R_o} (Pr)^{0.33} \left(\frac{\rho_f d}{\mu_f}\right)^{0.50}$

For a constant temperature anemometer the wire temperature is kept constant and so is its resistance. Equation (4.7) can be rewritten in terms of potential difference E (where $E = IR_w$) as:

$$E^2 = A + B\sqrt{U} \qquad (4.8)$$

with A = constant x A_1

and B = constant x B_1

The wire can be calibrated by noting the voltage produced by a certain velocity and this repeated for a number of points and a calibration curve plotted. Any other velocity can then be obtained from this curve if the voltage produced by the wire at this velocity was known.

As the relationship between E and U is not linear, it would be desirable to have a relationship of the form:

$$E = K\,U \qquad (4.9)$$

where K = constant.

Equation (4.8) can be rearranged to give

$$U = \left(\frac{E^2 - A}{B}\right)^2 \qquad (4.10)$$

Substituting (4.10) in (4.9) then

$$E_1 = \frac{K}{B^2}(E^2 - A)^2 \qquad (4.11)$$

or $$E_1 = K_1(E^2 - A)^2 \qquad (4.11)$$

Equation (4.11) can be put in a more general form

$$E_1 = K_1(E^2 - A)^m \qquad (4.12)$$

Equation (4.12) is identical to the transfer function of a

linearizer with

E_1 = linearizer output voltage

E = CTA bridge voltage output

m, A, K_1 = constants.

In principle, the constant temperature anemometer consists of a wheatstone bridge with the probe as one of its component resistances. When the bridge is in balance no voltage difference exists between the end points of the bridge diagonals. When the wire is placed in the flow then it will be heated or cooled, its resistance will change and a voltage difference will now exist between the bridge end points. This voltage is fed back to the bridge input through a servo-amplifier after necessary phase alterations such that the original probe temperature will be restored by increasing or decreasing the bridge operating voltage.

The wire used in this experiment was Disa 55P01, platinum-plated tungsten sensor. The signal was analysed by a system composed of a 55M01 Disa Main unit with a 55M05 Power Pack and a 55M10 Standard Bridge. The signal was linearized by a Disa 55D10 Linearizer.

The probe cable (5m) was connected to the probe socket of the main unit and the free end of the cable was connected to the probe support which was plugged in a mounting tube. The tube was held on the same traverse mechanism used with the pitot tube measurements.

Before any readings were taken the standard bridge was calibrated by: 1) Compensating for wire leads resistance,
2) Finding out the working resistance of the wire and setting the

main unit decade resistance to that value, and 3) Aligning the bridge for high frequencies. (Details of the calibration procedure for the measuring system are in Appendix 4A).

The bridge output voltage was fed to the 55D10 linearizer. This was calibrated making use of a small wind tunnel available in the laboratory. The velocity for calibration purposes was measured by a pitot tube with output fed to the electric micromanometer and digital voltmeter referred to previously. The pitot tube and the wire were placed side by side at two points on a cross-section of the tunnel exit pipe. The velocity distribution across any section of that exit pipe was known to be constant.

The linearizer was set to give an output voltage directly proportional to the velocity (details of linearizer calibration procedure are in Appendix 4B).

The probe was traversed across the jet at different sections, in the axial direction. At each point, the linearizer output was fed to a Solartron Type TM 1440.2 D.C digital voltmeter and at least 10 values of the D.C output were recorded and then averaged. The signal was next connected to a B and K Type 2425 RMS voltmeter with an external time constant. The D.C. output of the RMS voltmeter was fed to the digital voltmeter and again at least 10 readings were recorded for each point and then averaged.

The D.C. output of the linearizer represented the mean velocity of the flow. Normalisation by dividing all velocities by

corresponding centre-line mean velocities and radial distances (r) by the distance of the measuring plane from the geometric origin of the jet (x), then took place. Mean velocities of flow at different sections are plotted against the similarity parameter $\eta(= r/x)$. The results are compared with previous experimental results by Wygnanski and Fiedler (1969) in Figures (4.10), (4.11) and (4.12).

The A.C. output of the signal represented the r.m.s. of the fluctuating velocity. Normalisation, in the same manner as before, was followed by plotting r.m.s. of the fluctuations against η. The results are shown in comparison to those measured by Wygnanski and Fiedler in Figures (4.13), (4.14) and (4.15).

CHAPTER V

EXPERIMENTAL PROCEDURE

5.1 INTRODUCTION

In this chapter the methods used for determination of particle size and number density in a turbulent aerosol jet flow will be described in some detail. Firstly, the optical arrangement, which was common to all cases, will be presented while minor changes for different aspects of measurement will be given later at the relevant points. Secondly, the experimental procedure for measurement with titanium dioxide particles will be described. Thirdly, the slightly different procedure for measurement with tungsten metal particles will be given. For the case of titanium dioxide, measurement was made using two methods. In the first method, the LDA signal was displayed on and stored by a storage oscilloscope and the visibility was measured directly from the oscilloscope trace. In the second method, the signal was processed electronically and the parameters leading to the visibility were obtained using an r.m.s voltmeter. The first method will be described first, next an assessment of this method will be given and then the second method will be introduced.

It was shown in Chapter II that the expansion parameter, ε, which is dependent on the particle diameter (D_p), is a measure of how closely a particle follows the fluid flow. The smaller the value of ε, the nearer is the behaviour of a particle to that of a tracer-element. It was also shown that the value of

ε depends on the nozzle velocity (U_o) and the distance of the plane of measurement from the nozzle (x). For titanium dioxide particles ($D_p \simeq 2 \times 10^{-6}$ m, density 4.26 gm/cc) the value of ε as calculated from equation (2.86) was in the range 0.002 to 0.004. This low value of ε justified considering titanium dioxide particles to diffuse in a manner similar to heat or tracer-element. The result was compared with that of measurement using tracer-gas and with the zero order solution of the theory. In the case of tungsten metal particles where the particles were larger ($D_p \simeq 6 \times 10^{-6}$m) and heavier (density 19.3 gm/cc) larger values of ε (as calculated from equation (2.86)), could be obtained. The measurements were taken with the experimental apparatus arranged to give the calculated values of ε. The values taken in the present work for ε were 0.05, 0.075, 0.10, 0.20 and 0.30 to compare with the theoretical calculations for these values. Theoretical and experimental results are compared and discussed in Chapter VI.

5.1.1 Optical Arrangement

As was mentioned earlier, the experimental apparatus was assembled with the nozzle axis vertical. The optical arrangement which is shown in Figure (5.1), was mounted on a steel plate (1.7 x 0.15 x 0.01 m) that was bolted to a heavy bench. The optical bench, on which all the optics were mounted, rested on the steel plate and could be traversed over short distances in the horizontal direction. The steel plate could be moved vertically in discrete steps, thus permitting measurements to be

taken at different positions downstream from the nozzle.

A 15 mw He-Ne laser (Spectra Physics, type 124A Stabilite) produced the source of light and its beam was split (in a vertical plane) into two beams of equal intensity, by a beam splitter (Precision Devices). The two beams were then focused by a lens (f = 600 mm) to form an interference-fringe pattern at their point of intersection (probe volume). The light scattered from the probe volume was collected by a photo-multiplier (Disa 55L10) placed at an angle of 25^{o} to the bisector of the two beams, and the signal produced was displayed by a storage oscilloscope (Hewlett-Packard 141A).

5.2 MEASUREMENT WITH TITANIUM DIOXIDE PARTICLES:

5.2.1 Direct Measurement from Oscilloscope Trace

Before any experiment was performed, the experimental apparatus was tested to find out the variation of the signal visibility with respect to time at the centre-line of the jet. The above optical arrangement was set such that the probe volume coincided with the jet centre-line at a distance of 45 nozzle diameters from the nozzle. To produce the maximum contrast in the fringe pattern, the two laser beams were adjusted to give equal intensities of 7.0 ± 0.1 mw as measured by a power meter (Spectra Physics, type 401C). The fringe spacing, δ, was increased by reducing the beam separation to 8 mm. This last step was taken to satisfy the condition that for the visibility to be a measure of the number density, then δ must be much larger than the particle diameter (Farmer 1972).

The fringe-spacing was calculated using the beam separation, the focal length of the lens and the vacuum wave number of the laser light (6328 Å), to be 47.5 x 10^{-6} m. This value was more than 20 times D_p which was known to be of the order of 2 micron (Melling and Whitelaw 1973).

The LDA trace was stored on the screen of the storage oscilloscope and the values of I_{max} and I_{min} (I_{max} and I_{min} were defined in Chapter III) measured by a travelling telescope with a vernier scale and the value of the visibility was obtained from equation (3.13). Values from three or four signals were taken every five minutes and averaged, for one hour. The mean centre-line visibility and the standard deviation from the mean were then obtained. The test was repeated for different nozzle velocities and it was found that the standard deviation was 17% of the mean for a nozzle velocity of 60 m/s, 14% for a nozzle velocity of 40 m/s and 12% for a velocity of 30 m/s. This showed that the concentration at the centre-line was fluctuating around a mean value and implied that the smaller the nozzle velocity the smaller were the fluctuations. For high nozzle velocities a large number of signals should be taken to average out these fluctuations. Most of the measurements by this method were done at low nozzle velocities.

5.2.1a Particle Size Measurement

Two methods were used to obtain the mean particle diameter of a titanium dioxide particle. Firstly, a sample was taken from the jet and two photomicrographs of the sample were obtained at magnifications of 16,800 and 8,400. From each photograph

fifty particles were measured and the mean and the standard deviation from the mean was obtained. The values of the mean particle diameter, based on the average between the maximum dimension and that at right angles to it, from the two photomicrographs were found to be 2.2 ± 0.3 and 2.3 ± 0.4 micron.

The second method used for particle sizing utilised the laser-Doppler arrangement referred to above. It was shown by Farmer (1972) that the signal visibility (V) is related to the particle diameter by

$$V = \frac{2\left|J_1\left(\frac{\pi D_p}{\delta}\right)\right|}{\pi D_p / \delta}$$

where J_1 = Bessel function of first order.

This relationship was obtained assuming that,

1) the intensities of the two incident beams were equal;

2) the fringe spacing was of the order of magnitude of the particle diameter;

3) the particle was spherical;

and

4) the particles are transparent.

Assumptions (1) and (2) were easily satisfied by adjusting the two beams to have equal intensity of 7.0 ± 0.1 mw (within 1.4 %) and increasing the angle between the two beams. This was done by increasing the beam separation and using a lens with a shorter focal length (f = 300 mm). Assumptions (3) and (4) could not be met, but it was shown by Hong and Jones (1976) that the method could be made fairly independent of refractive index by using a small finite aperture. They also suggested

that the use of irregular particles would not involve a serious error.

The probe volume was adjusted to coincide with a point away from the direction of the main flow and the velocity of the nozzle reduced to a very low value to increase the chance that the LDA signal was from one particle. Five values of beam separation were taken and each time ten signal visibilities were measured and averaged. The particle diameter was obtained from the above relationship and the mean and the standard deviation from the mean for the five readings was determined. The method gave a mean particle diameter of 2.8 ± 0.2 micron.

5.2.1b Relative Concentration Measurement

The laser beam separation was reduced to 8 mm to give a fringe spacing of 47.5×10^{-6} m. The probe volume was made to coincide with the jet axis at the required distance from the nozzle. The nozzle velocity was set to a known value and the mean signal visibility was obtained by direct measurement from the storage oscilloscope trace. The probe volume was then traversed a small distance, the scattered light from the new position focused on the photomultiplier pin-hole and the mean visibility obtained as before. Each time at least five values of the visibility were measured and averaged. Only signals with intensity higher than the preset oscilloscope triggering level and free from distortion were selected. (This last point will be discussed in more detail in the next chapter.) The mean centre-line visibility was divided by the mean visibility at each radial position across the jet and the result squared to

give the relative concentration. This procedure was repeated for different nozzle velocities and measurements were obtained at different positions downstream from the nozzle. The results were plotted against the normalised radial distance (η) [η = r/x, where r is the radial distance from the jet centre-line]. These results are shown in Figure (5.2).

5.2.2 Electronic Signal Processing

Although the above method gave satisfactory results, yet some points of uncertainty could be raised. These will be stated briefly here and discussed in more detail in the next chapter. The main points are

1) At least three factors influence the fluctuation of the LDA signal and the number of signals averaged at each measuring point were too few to give a mean value that characterizes the concentration. These factors are:

   a) the indication from the measurement of the centre-line visibility that the fluidised bed was producing a number of particles which were fluctuating with respect to time;

   b) the effect of turbulence; and

   c) the fluctuations in the LDA signal which are known to exist even in the case of laminar flow due to the fact that the photomultiplier signal is the sum of the signals produced by particles of different sizes and at different positions in the probe volume.

2) It was found that if the centre-line visibility was arranged to be relatively high to make measurement easier and reduce the reading error, then unreliable results would be obtained at positions near the edge of the jet. This can be explained in the following manner: Assuming that the centre-line visibility was 0.50, then the particle number density will be proportional to $(\frac{1}{0.50})^2$. At points close to the edge of the jet the visibility will increase and approach the maximum value of unity. Hence the concentration profile will tend to be assymptotic to the η axis as its value tends to $(0.5)^2$ and no concentration less than this value can be measured. This effect is shown in Figure (5.3).

In addition to the uncertainty this method is laborious and time consuming even if only few signals are taken and averaged.

To resolve the uncertainty in the measurement produced by these points, an electronic method for processing the signal was developed. It was shown in Chapter III that the signal visibility is the ratio between the a.c and d.c power components of the signal (equation 3.16). The d.c. power in this respect is the modulated pedestal on which the velocity signal is mounted. The method employed in the present work relies upon proper separation of the a.c. and d.c power components in the signal spectrum and the obvious way for this is by high-pass and low-pass filtering. Attempts to do that, however, showed that the cut-off points for the filtering were not well defined and

suggested that the a.c. and d.c. peaks in the spectrum were overlapping. This point was investigated as follows.

The optics arrangement described above was set such that the probe volume was at the jet centre-line. The photo-multiplier output was fed to a spectrum analyser (Marconi, TF 2330, resolution 50 KHz) which was used to scan the signal from a few hertz to 50 KHz. The output from the spectrum analyser was measured by an r.m.s voltmeter with an external time-constant (B and K type 2425). The result showed that, indeed, the a.c and d.c components of the signal overlapped and this suggested the use of a frequency shifter.

It is well established that the Doppler frequency can be increased or decreased by a certain selected frequency if the incident two laser beams can be arranged to have their frequency changed with respect to the original beams by that selected frequency. In the present work a frequency modulator (Disa, type 55L02, Flow Direction Adapter) was used and replaced the beam splitter in the optics arrangement. The modulator was adjusted such that the selected frequency was added to the signal. The above test to obtain the signal spectrum was repeated with and without frequency shifting. The measurements were taken at a distance of 50 nozzle diameters and for two nozzle velocities (Re_j = 10,000 and 4,000 where Re_j is the Reynold's Number based on the nozzle velocity) with the Doppler Signal upshifted by 75 and 25 KHz respectively. The effect of frequency shifting is indicated by Figures (5.4) and (5.5) and from these figures it is clear that the filtering process can

be achieved by frequency shifting.

The only difficulty with using the frequency modulator was that it had a constant beam separation of 50 mm. This produced a fringe spacing which was only about three times the titanium dioxide particle diameter. The beam separation was reduced by the use of two parallel mirrors to deflect the bottom laser beam towards the top one, thus giving the desired value of beam separation of 8 mm. As the mirrors were not perfect reflectors, then the lower beam would be reduced in intensity relative to the upper. The intensity of this beam was reduced to compensate and the reading of the power meter for the two beams was 1.50 ± 0.05 mw.

The optics arrangement was the same as that of figure (5.1) except that the beam splitter was replaced by the Flow Direction Adapter. The two laser beams emerging from this were frequency shifted by 250 KHz and this value was used throughout the present work. The scattered light was collected by the photo-multiplier and the output passed through a high-pass, low-pass filter (Disa, Signal Conditioner, type 55D26) and was amplified by a factor of ten. The filter was jointly connected to the r.m.s voltmeter (with external time constant) and an oscilloscope (Solartron, type DC 1014.2). The signal processing electronics are shown as a block diagram in Figure (5.6). The filter was found to have a maximum high-pass frequency of 100 KHz and its cut-off was not sharp in that if it was set to high-pass 100 KHz, frequencies as low as 40 KHz would still pass. Hence the method adopted in the present work was to measure the mean powers of the

unfiltered signal and that of the low-pass filtered part of it. This last component was obtained by reducing the low-pass filter frequency from the maximum value (1,000 KHz) in steps until the Doppler signal was removed as observed from the oscilloscope trace, and only the pedestal on which that signal was mounted remained. This was checked by moving the filter frequency one step up and another one down while noting the voltmeter reading for each case. When no change in the voltmeter reading was observed for the three cases then this would imply that the selected cut-off frequency was in the proper position between the d.c and a.c components of the signal. The readings of the r.m.s voltmeter for the unfiltered signal and the low-pass filtered part of it are proportional to the mean signal powers corresponding to the two cases. The d.c. power was subtracted from the unfiltered power to give the a.c power. Finally, it is known that one of the troubles of the LDA signal is the inherent noise level produced by background light in addition to the dark count of the photomultiplier. In the present case, the whole experimental apparatus was surrounded by a darkened enclosure and the residual noise level was measured at the beginning of each experiment. This was assumed to be shot noise and hence constant throughout the time of the experiment and was subtracted from the measured intensities before any analysis was made.

As a check on the previous measurements to test the experimental apparatus, the above electronic method was used. The centre-line visibility at 40 nozzle diameters and a velocity of

30 m/s was measured over a period of three hours. Readings were taken every ten minutes of the unfiltered and the low-pass filtered mean powers. The visibility was calculated in each case by dividing the a.c. power by the d.c. power. The mean value over the period of the test and the standard deviation were obtained. This test shows that the standard deviation of the visibility from the mean value is only 6% (the result is shown in table 5.1). The average visibility in each case was obtained over a comparatively long period (voltmeter time constants of 3 and 10s). This implies that a large number of signals had been averaged rather than three or four signals and this indicates that the last result is more reliable than the previous one.

It is worth noting that the electronic signal processing method was not used for particle size measurement. The probe volume was away from the main flow of the jet and the nozzle velocity was very low to increase the chance that the LDA signal was due to a single particle. This arrangement produced too few burst signals to be averaged by the voltmeter even at the greatest time constant of 100s.

5.2.3 Reltative Concentration Measurement

The above optical arrangement was set with the beams intersection point lying on the jet centre-line at a certain position downstream from the nozzle. The unfiltered signal and the d.c mean powers were measured as before. The shot noise was subtracted and the a.c mean power was obtained from the difference between the two readings. The centre-line visibility was obtained by

dividing the a.c by d.c powers. The optical set-up was traversed a small distance in the horizontal direction and the visibility obtained in the same manner. This was repeated for different positions radially across the jet. The centre-line visibility was divided by that at each point and the quotient squared. The result which represents the relative concentration was plotted against the normalised radial distance (η). The procedure was repeated for different nozzle velocities and at different positions downstream from the nozzle and for nozzle diameters of 10 and 5 mm. The results are shown in Figures (5.7), (5.8), (5.9) and (5.10) and will be discussed in the next chapter.

5.3 MEASUREMENT WITH TUNGSTEN METAL PARTICLES

All the measurements with the exception of particle sizing in this case were made using the electronic signal processing method. The procedure was essentially the same as before for testing the apparatus with tungsten metal particles. It was found that the fluctuations of the r.m.s voltmeter were greater than the case of titanium dioxide particles and larger voltmeter time constants (30 and 100s) had to be employed. The result, which is presented in table (5.2), shows that the standard deviation of the centre-line visibility, over the period of three hours, is 10% of the mean value.

5.3.1 Particle Size Measurement

Two photomicrographs of a sample were taken at a magnification of 455. Fifty particles from one photograph and fourty

from the other were measured and the mean and the standard deviation for each case were obtained. The result showed that the mean particle diameter, based on the average between the largest dimension and that at right angles to it was 5.7 ± 1.9 micron for one photograph and 5.7 ± 1.4 for the other.

The optical method was the same as that used for titanium dioxide, but the fringe spacing was kept at a higher value as the tungsten metal particles were known to be larger. A 130 mm focal length lens was used to focus the laser beams and five beam separations were taken. For each beam separation at least ten signals were measured from the storage oscilloscope trace and averaged. The same Bessel function relationship mentioned above was used to calculate the ratio $\frac{D_p}{\delta}$ and with the known value of δ, D_p was obtained. The mean value of the resulting five particle diameters and the standard deviation from the mean were obtained. The result shows that the mean tungsten metal particle diameter is 5.6 ± 0.6 micron.

5.3.2 Relative Concentration Measurement

The same optical arrangement described for the measurement with titanium dioxide was used in this case. The minor differences in the procedure were:

1) The beam separation and the 600 mm focal length lens produced a probe volume which was 0.4 x 0.4 x 6,5 mm. The larger dimension was in the direction of the beams. Only 1.9 mm of that dimension was viewed by the photomultiplier as it was placed at 25° to the bisector of the two beams

(Brayton et al 1973). The traversing distance had to be of the order of magnitude of this dimension of the probe volume. To obtain values of ε of 0.20 and 0.30, measurements had to be taken at shorter distances from the nozzle and hence implied that very small traverses had to be made. In these cases, each experiment was carried out twice. Firstly, measurements were taken in comparatively large steps and then the whole experiment was repeated for measurements at intermediate positions.

2) Due to larger fluctuations of the r.m.s voltmeter, it was necessary to use a larger time constant (30 and 100 s).

3) Measurements were obtained with nozzle diameters of 5 and 3 mm.

The concentration profiles against normalised radial positions (η) are shown in figures (5.11), (5.12), (5.13), (5.14), (5.15) and (5.16). These are compared with the theoretical results and will be discussed in the next chapter.

TABLE (5.1)

TESTING THE APPARATUS

WITH TITANIUM DIOXIDE PARTICLES

$\frac{x}{d}$ = 40 d = 5 mm Re = 10 x 10^3 centre-line position

Time Hours	Unfiltered Signal Power Volts	D.C. Power Volts	A.C. Power Volts	Corrected D.C. Power Volts	$\langle V \rangle = \frac{A.C.}{D.C.}$
0.00	0.325	0.275	0.050	0.250	0.200
0.10	0.318	0.268	0.050	0.243	0.206
0.20	0.317	0.267	0.050	0.242	0.207
0.30	0.315	0.260	0.055	0.235	0.234
0.40	0.310	0.260	0.050	0.235	0.213
0.50	0.305	0.255	0.050	0.230	0.217
1.00	0.305	0.255	0.050	0.230	0.217
1.10	0.305	0.250	0.055	0.225	0.244
1.20	0.300	0.250	0.050	0.225	0.222
1.30	0.298	0.248	0.050	0.223	0.224
1.40	0.295	0.250	0.045	0.225	0.200
1.50	0.295	0.245	0.050	0.220	0.227
2.00	0.290	0.240	0.050	0.215	0.2325
2.10	0.285	0.238	0.047	0.213	0.220
2.20	0.275	0.230	0.045	0.205	0.220
2.30	0.273	0.228	0.045	0.203	0.222
2.40	0.272	0.225	0.047	0.200	0.235
2.50	0.272	0.225	0.047	0.200	0.235
3.00	0.272	0.225	0.047	0.200	0.235
				Mean Visibility $\langle V \rangle_m$	0.22
				Standard deviation σ	0.013
				$\frac{\sigma}{\langle V \rangle_m}$ %	6%

TABLE (5.2)

TESTING THE APPARATUS

WITH TUNGSTEN METAL PARTICLES

$\frac{x}{d}$ = 20 d = 5 mm Re = 10 x 10^3 centre-line position

Time Hours	Unfiltered Signal Power Volts	D.C. Power Volts	A.C. Power Volts	Corrected D.C. Power Volts	$\langle V \rangle = \frac{\text{A.C.}}{\text{D.C.}}$
0.00	0.370	0.355	0.015	0.330	0.0454
0.10	0.320	0.305	0.015	0.280	0.0536
0.20	0.300	0.287	0.013	0.262	0.0496
0.30	0.290	0.277	0.013	0.252	0.0516
0.40	0.267	0.255	0.012	0.230	0.0522
0.50	0.255	0.243	0.012	0.218	0.0551
1.00	0.250	0.238	0.012	0.213	0.0563
1.10	0.246	0.233	0.013	0.208	0.0625
1.20	0.245	0.232	0.013	0.207	0.0628
1.30	0.232	0.220	0.012	0.195	0.0615
1.40	0.226	0.214	0.012	0.189	0.0635
1.50	0.225	0.214	0.011	0.189	0.0582
2.00	0.225	0.213	0.012	0.188	0.0638
2.10	0.225	0.213	0.012	0.188	0.0638
2.20	0.210	0.200	0.010	0.175	0.0571
2.30	0.190	0.180	0.010	0.155	0.0645
2.40	0.180	0.172	0.008	0.147	0.0544
2.50	0.180	0.172	0.008	0.147	0.0544
3.00	0.173	0.166	0.007	0.141	0.0497

Mean Visibility $\langle V \rangle_m$	0.057
Standard deviation σ	0.0056
$\frac{\sigma}{\langle V \rangle_m}$ %	10%

CHAPTER VI

DISCUSSION OF RESULTS

6.1 TESTING THE EXPERIMENTAL APPARATUS

6.1.1 Pitot Tube Measurement

The mean velocity profiles obtained from pitot tube measurement for three nozzles of diameters 3, 5 and 10 mm are shown in Figures (4.7), (4.8) and (4.9) respectively. The solid line represents the measurement by Wygnanski and Fiedler (1969) using hot wire anemometers. The measurement in the present work shows that the three nozzles are axisymmetric and that the mean velocity profiles are similar for values of $\frac{x}{d} > 10$. These results are also in good agreement with that of Wygnanski and Fiedler. The scatter in the results is within ± 10% and this is expected from pitot tube measurement due to its comparatively low sensitivity to pressure drop. Figure (4.8) shows that for large values of $\frac{x}{d}$ (50 and 100) measurement was possible up to about 75% of the jet width. This was due to the fact that beyond that region the velocity was too low to be sensed by a pitot tube.

6.1.2 Hot Wire Anemometer Measurements

Mean velocity measurements with hot wire anemometers are shown in Figures (4.10), (4.11) and (4.12). From these figures the agreement with measurements by Wygnanski and Fiedler is good and within the estimated error of ± 5%. The velocity profiles are symmetrical about the jet axis and similarity is

obtainable at values of $\frac{x}{d}$ larger than 10.

The r.m.s values of the fluctuating velocities are shown in Figures (4.13), (4.14) and (4.15) for the three nozzles used. Similarity of the fluctuating velocities is obtainable at values of $\frac{x}{d}$ greater than 20. Figures (4.13) and (4.14) show that for a value of $\frac{x}{d}$ of 20 the r.m.s fluctuating velocities measured in the present work are about 10% lower than those obtained by Wygnanski and Fiedler. For values of $\frac{x}{d}$ of 30 the disagreement is by about 7% and for values of $\frac{x}{d}$ greater than 30 the agreement is within the estimated experimental error of 5%. Wygnanski and Fiedler reported a discrepancy of 25% in the r.m.s fluctuating velocities, at $\frac{x}{d} = 20$, from the results used for comparison with the present work. These were for $\frac{x}{d} > 40$.

6.2 PARTICLE SIZING

The titanium dioxide particle diameter obtained from the LDA signal analysis was about 20% larger than that obtained from photomicrography. A possible explanation of this is that some of the signals measured might have been produced by more than a single particle. It is believed that the result obtained from photomicrography is more accurate and is in good agreement with value of 'about' 2 micron obtained by Melling and Whitelaw (1973).

Tungsten metal particle diameters by photomicrography show that the size distribution has some 30% scatter around the mean value. The LDA result, however, shows a smaller scatter of 10%. Again, the result obtained from photomicrography is considered to be more realistic as the LDA result was obtained from signals

whose intensity was higher than the oscilloscope triggering level. This means that larger particles were taken as those scatter light with intensity higher than small particles.

6.3 RELATIVE CONCENTRATION MEASUREMENT

6.3.1 Direct Measurement from Oscilloscope Trace

The results obtained from direct measurement are shown in Figure (5.2). The agreement with previous measurement of tracer-gas concentration by Hinze and van der Hegge Zijnen (1949) is fair and is well within the estimated experimental error of 12%, indicated by the error bars for one set of readings. In Chapter V it was mentioned that the number of signals averaged at each measuring point were too few to average out the expected fluctuations in the concentration. It was also mentioned that only certain signals, namely those with intensity higher than the oscilloscope triggering level and free from distortion, were selected. This selection is justified by the fact that signals from the centre-most part of the probe volume will have higher intensity and be free from distortion (Durst and Eliasson 1975).

To find out the ratio of the type of selected signals to the total number of signals in a certain period of time, a film was taken for all the signals occuring, at the jet centre-line, in the film duration of 700 ms. The total number of signals in that period was counted and divided into three categories: (1) signals with too low an intensity to trigger the oscilloscope - 25% of the total number of signals were of this type. (2) Signals distorted due to being produced by particles positioned at a point off the centre of the probe volume - 35% of the signals

were of this kind. (3) The remaining 40% of the signals were of the type selected. However, the film condition was different from the actual measuring case in that the total number of particles in the system was increased appreciably and so was the nozzle velocity (Re_j = 20,000). This was done to increase the number of burst signals so that as many of them as possible could be filmed during the short period of filming. The effect of increasing the number of particles and the nozzle velocity was expected to increase the number of the distorted signals as particles failing to be collected by the extraction hood would fall at positions within the probe volume and thus produce a distorted signal or distort the signals produced by particles at the centre of the probe volume.

6.3.2 Electronic Signal Processing

6.3.2.1 Titanium Dioxide Particles

The results obtained for titanium dioxide particles are shown in Figures (5.7), (5.8) and (5.9) for the 5 mm diameter nozzle and Figure (5.10) for the 10 mm diameter nozzle. Agreement with the experimental result obtained by Hinze and van der Hegge Zijnen (1949) is good and is well within the estimated experimental error as indicated for one set of results by the bars in Figure (6.1). The measurements cover values of $\frac{x}{d}$ from 20 to 60 and the results indicate that similarity of the concentration profiles of particles with infinitesimal sizes that follow closely the air flow is obtainable for values of $\frac{x}{d} > 20$.

6.3.2.2 Tungsten Metal Particles

The results for tungsten metal particles are shown, for the values of ϵ of 0.05, 0.075, 0.10, 0.20 and 0.30, in Figures (5.11), (5.12), (5.13), (5.14) and (5.15). respectively. These results are compared with theoretical predictions utilising the theory developed by Davidson and McComb (1975). For each plot the theoretical result for ϵ = 0.0 is drawn for comparison. Figure (5.16) shows the theoretical curves for ϵ = 0, 0.10, 0.20 and 0.30 and one experimental set of data for each of these values. This figure indicates the trend with increasing ϵ and shows that each experimental set of data is more closely related to the corresponding theoretical prediction than to the others. The agreement between the experimental result and the theory is good and is within the estimated experimental error. This may be seen where some representative results are plotted with error bars in Figures (5.11), (5.12), (6.2), (6.3) and (6.4). The scatter in the experimental result is probably to be attributed mainly to the variation in the particle size distribution evidenced from the photomicrograph particle size result.

6.4 ERROR ANALYSIS

It was shown in Chapter III that the mean LDA signal visibility $\langle v \rangle$ is inversely proportional to the square root of the mean particle concentration, $\sqrt{\langle N \rangle}$

or $$\langle v \rangle = \frac{1}{\sqrt{\langle N \rangle}} \qquad (6.1)$$

If the mean visibility is changed by an amount $\mp dv$ the mean concentration will change by an amount of $\pm dN$.

Substituting in equation (6.1) and squaring gives,

$$(\langle v\rangle \mp dv)^2 = \frac{1}{\langle N\rangle \pm dN} \tag{6.2}$$

Substituting for the value of $\langle N\rangle$ from (6.1) and rearranging yields

$$(\langle v\rangle \mp dv)^2 \left(\frac{1}{\langle v\rangle^2} \pm dN\right) = 1 \tag{6.3}$$

$$\text{or} \quad \mp \frac{2dv}{\langle v\rangle} \mp \left(\frac{dv}{\langle v\rangle}\right)^2 \pm dN\ (\langle v\rangle \mp dv)^2 = 0 \tag{6.4}$$

$$\text{or} \quad \frac{2dv}{\langle v\rangle} \pm \left(\frac{dv}{\langle v\rangle}\right)^2 = dN\ (\langle v\rangle \pm dv)^2 \tag{6.5}$$

$$\text{and} \quad dN = \frac{\frac{dv}{\langle v\rangle}\left(2 \pm \frac{dv}{\langle v\rangle}\right)}{\langle v\rangle^2 \left(1 \pm \frac{dv}{v}\right)^2} \tag{6.6}$$

Now substituting for $\langle v\rangle^2$ from equation (6.1) the result is

$$\frac{dN}{\langle N\rangle} = \frac{\frac{dv}{\langle v\rangle}\left(2 \pm \frac{dv}{\langle v\rangle}\right)}{\left(1 \pm \frac{dv}{\langle v\rangle}\right)^2} \tag{6.7}$$

for small values of $\frac{dv}{\langle v\rangle}$ then

$$\frac{dN}{\langle N\rangle} \simeq \pm 2\,\frac{dv}{\langle v\rangle} \tag{6.8}$$

In the present work the experimental error was estimated and then the effect of that error on the signal visibility was determined. This was used in equation (6.8) to obtain the error in the concentration measurement.

For the measurements of the visibility directly from the storage oscilloscope trace the reading error from the telescope vernier scale was estimated to be within ±1% producing a maximum

concentration variation of 12%. The experimental error bars shown in Figure (5.2) are based on the above analysis. The error bars for the other experimental results of Figure (5.2) are expected to be the same as for those presented.

In the electronic signal processing methods readings were obtained from the r.m.s voltmeter for the components of the visibility. The voltmeter accuracy was estimated to be within ±0.1%. The error analysis was based on the worst case in which the error was added to the a.c. component of the signal and subtracted from the corresponding d.c. component. This was found to give the maximum variation in the visibility close to 5% and hence a maximum variation of 10% in the concentration measurement. The experimental error bars shown in Figures (5.11), (5.12), (6.1), (6.2), (6.3) and (6.4) are based on the above analysis.

6.5 MEASUREMENT OF VELOCITY PROFILE FOR TUNGSTEN METAL PARTICLES

It was intended for this work to measure velocity profiles at different values of ε corresponding to those at which the concentration profiles were obtained, and hence the mass flow rate could be determined. A frequency tracker was tried with the LDA arrangement described in Chapter V to obtain the velocity but this did not work especially at radial positions away from the jet centre-line as the burst signals were too few to give a continuous signal for frequency tracking. However, a Disa type 55L90 counter with Disa type 55L94 mean velocity computer was available for a few hours and one velocity profile across the

jet was measured for a value of ε of 0.20. The result is shown in Figure (6.5) and is compared with the prediction based on the theory developed by Davidson and McComb (1975). The dotted curve is for the air velocity and the figure shows that the heavy tungsten metal particles are lagging behind the clean air flow. The figure also indicates good agreement between theory and experiment.

CHAPTER VII

CONCLUSION

The design of the experimental apparatus to produce a turbulent aerosol jet with a number of particles fairly constant per unit time, has been described in detail. The methods for testing the apparatus for axisymmetry and similarity of the velocity profiles are given, as are the methods for testing the apparatus with particles. It was found that the jet was axisymmetric and mean velocity profiles became similar at distances of 10 nozzle diameters downstream of the nozzle. It was also found that the fluctuations in the number of particles delivered by the nozzle were quite small and could be averaged out over comparatively short periods of time. The particles used for the measurement were sized by photomicrography and by an optical method. The two results were in close agreement with each other. Relative concentration profiles for titanium dioxide particles were measured by an optical method and were compared with the classical results obtained using heat or tracer-elements. The two profiles were found to agree quite well. It was also found that the concentration profiles of infinitesimal size titanium dioxide particles became similar at distances greater than 20 nozzle diameters downstream of the nozzle. The signal produced by the optical arrangement was originally measured directly from a storage oscilloscope trace, but later an electronic signal processing method was developed.

Relative concentration profiles for tungsten metal particles, which were known to be heavy and expected to lag the fluid flow, were measured. The result was found to be in good agreement with the

predicted values. The theoretical solution of the diffusion problem was obtained from the theory developed by Davidson and McComb. This theory, which was developed for monodisperse particles, was derived in detail and a crude generalisation to the case of polydisperse particles was given. A computer program was then written to obtain numerical values for the particle velocities and concentrations for comparison with experimental results.

One velocity profile for heavy particles was measured and this shows that these particles do lag the flow and by values in close agreement with the predicted values.

It has been shown that the laser Doppler anemometer is an accurate intrument for measurement of particle sizes and number density. The optical arrangement is fairly easy to set up and the requirements for its use as a particle sizer and/or counter are easily met.

It is suggested that as an improvement to the experimental apparatus to give a constant number of particles per unit time, the particles be fluidised in a separate chamber and the required amount tapped off and injected at the entry to the nozzle. This arrangement is reported to give fairly constant mass flow rate and for the desired period of time (Albright, Holden, Simons and Schmidt 1949). It is also suggested that the LDA signal be processed by a computer. This has the advantage of reducing the experimental error as the method is found to be very sensitive to the error. This can be done by either feeding the signal, after digitization, directly to the computer if a terminal is available, or alternatively by having it recorded on a tape recorder with a high frequency range.

A possible extension of this problem would be to measure the concentration of particles issuing from the nozzle in a pressurised confinement and find out the effect of diffusion in that case. This problem can be treated analytically as an extension of the available theory. Another possibility of extension of the problem would be to find the effect of diffusion of liquid particles injected in a pressurised container. This would be a similar problem and could give a better understanding of the problem of combustion in the cylinders of a compression ignition engine.

APPENDIX 2A

COMPUTER PROGRAM

```
C       COMPLETE PROGRAM TO FIRST ORDER ACCURACY
        INTEGER E
        DIMENSION X(2500),Y(2500),B(2500),C(2500),D(2500),YC(2500)
        DIMENSION YCC(2500),F(2500),Z(2500),DN(2500),P(2500)
        DIMENSION Q(2500),QC(2500),DDN(2500),W(2500),YN(2500)
        DIMENSION ZN(2500),DF(2500),DFF(2500),DUR(2500),DNO(2500)
        DIMENSION QX(2500),QR(2500),QMX(2500),QMR(2500),QTX(2500)
        DIMENSION DMN(2500),DTN(2500),U(2500),DS(2500),R(10)
        DIMENSION A(6,6),T(6,6),S(10,10)
        READ,E,N
        DO 10 I=1,N
   10   READ,X(I),Y(I),Q(I)
        DO 13 I=1,E
        DO 13 J=1,E
        A(I,J) =0
        DO 13 K=1,N
        IF(I+J-2)12,11,12
   11   B(K) =1
        GO TO 70
   12   B(K) =X(K)**(I+J-2)
   70   A(I,J) =A(I,J)+B(K)
   13    T(I,J)=A(I,J)
        M=E+4
        DO 14 I=1,M
        DO 14 J=1,M
        S(I,J)=0
        DO 14 K=1,N
        IF(I+J-2)61,60,61
   60   B(K) =1
        GO TO 62
   61   B(K) =X(K)**(I+J-2)
   62   S(I,J) =S(I,J)+B(K)
   14   CONTINUE
        DO 17 I=1,M
        R(I) =0
        DO 17 K=1,N
        IF(I-1)16,15,16
   15   C(K)=Y(K)
        GO TO 17
   16   C(K)=Y(K)*(X(K)**(I-1))
   17   R(I)=R(I)+C(K)
        CALL GELB(R,A,E,1,(E-1),(E-1),10**(-7),1)
        DO 18 I=1,E
   18   P(I)=R(I)
        DO 21 I=1,M
        R(I)=0
        DO 21 K=1,N
         IF(I-1)20,19,20
   19   C(K)=Q(K)
        GO TO 21
```

```
20 C(K)=Q(K)*(X(K)**(I-1))
21 R(I)=R(I)+C(K)
   CALL GELB(R,S,M,1,(M-1),(M-1),10**(-7),1)
   L=1+(20*N)
   H=0.21000000/(L-1)
   DO 22 I=2,L
22 X(I)=X(I-1)+H
   DO 23 I=1,L
   QC(I)=R(1)
   DO 23 J=2,M
23 QC(I)=QC(I)+R(J)*(X(I)**(J-1))
   DO 65 I=1,L
   YC(I) =P(1)
   DO 65 J=2,E
65 YC(I) =YC(I)+P(J)*(X(I)**(J-1))
   E=L-20
   DO 25 I=1,E,20
   K=I+20
   DO 24 J=1,K
24 YCC(J)=YC(J)*X(J)
25 CALL QSF(H,YCC,Z,K)
   DO 26 I=1,L
26 F(I)=Z(I)
   G=0.0133000
   D(1)=0
   DO 28 I=1,E,20
   K=I+20
   DO 27 J=2,K
27 D(J)=F(J)/(X(J)*G*QC(J))
28 CALL QSF(H,D,Z,K)
   J=0
   DO 29 I=1,L,20
   J=J+1
   DN(I)=EXP(-Z(I))
   DN(J)=DN(I)
29 U(J)=X(I)
   N=N+1
   M=M-4
   DO 32 I=1,M
   R(I)=0
   DO 32 J=1,N
   IF(I-1)31,30,31
30 C(J)=DN(J)
   GO TO 32
31 C(J)=DN(J)*(U(J)**(I-1))
32 R(I)=R(I)+C(J)
   CALL GELB(R,T,M,1,(M-1),(M-1),10**(-7),1)
   DO 33 I=1,L
   DN(I)=R(1)
```

```
      DO 33 J=2,M
   33 DN(I)=DN(I)+R(J)*(X(I)**(J-1))
      P(1)=0
      Q(1)=0
      QX(1)=1
      QR(1)=0
      L=L-20
      DO 34 I=2,L
      B(I) = 1/(X(I)*G*QC(I))
      DUR(I)=(QC(I+1)-QC(I-1))/(H*2)
      DF(I) =(F(I+1)-F(I-1))/(H*2)
      DNO(I)=(DN(I+1)-DN(I-1))/(H*2)
      DFF(I)=(F(I+1)-(2*F(I))+F(I-1))/(H**2)
      W(I)=B(I)*(F(I)+(G*QC(I))+(X(I)*G*DUR(I)))
      C(I) =W(I)
      W(I) =1-(C(I)*H/2)
      D(I) =1+(C(I)*H/2)
      YN(I)=2-((3*B(I)*DF(I))*(H**2))
      U(I) =(F(I)/X(I))*((F(I)/X(I))-DF(I))*DNO(I)
      Z(I) =2*(F(I)**2)/(X(I)**3)
      Z(I)=Z(I)-(5*F(I)*DF(I)/(X(I)**2))
      Z(I)=Z(I)+(3*(DF(I)**2)/X(I))
      Z(I)=DN(I)*(Z(I)+(3*F(I)*DFF(I)/X(I)))
      ZN(I)=B(I)*(U(I)-Z(I))*(H**2)
      QX(I)=(DF(I)**2)/(X(I)**2)
      QX(I)=QX(I)+(F(I)*DFF(I)/(X(I)**2))
      QX(I)=QX(I)-(F(I)*DF(I)/(X(I)**3))
      QR(I)=((DF(I)**2)/X(I))+(F(I)*DFF(I)/X(I))
      QR(I)=QR(I)-(2*F(I)*DF(I)/(X(I)**2))
      QR(I)=QR(I)+((F(I)**2)/(X(I)**3))
      P(I)=(DF(I)**2)/X(I)
   34 Q(I)=DN(I)*DF(I)
      DDN(1)=1
      DDN(2)=1
      K=L-1
      DO 35 I=2,K
   35 DDN(I+1)=(ZN(I)+(YN(I)*DDN(I))-(W(I)*DDN(I-1)))/D(I)
      K=L-40
      CALL QSF(H,P,Z,K)
      AA =SQRT(1/(Z(K)*8))
      CALL QSF(H,Q,Z,K)
      BB =(1/(Z(K)*AA*8))
      WRITE(6,53)
   53 FORMAT(///10X,'ETA',10X,'M.VEL.',10X,'RMS V.'//)
      DO 54 I=1,L,20
   54 WRITE(6,55)X(I),YC(I),QC(I)
   55 FORMAT(5X,F10.5,2(5X,F12.8))
      WRITE(6,36)
   36 FORMAT(//10X,'ETA',10X,'M.QX1',13X,'M.QR1'/)
      DO 37 I=1,L,20
```

```
 37 WRITE(6,38)X(I),QX(I),QR(I)
 38 FORMAT(5X,F10.5,2(5X,F12.8))
    WRITE(6,39)
 39 FORMAT(//10X,'ETA ',10X,'M.NO. ',13X,'M.N1 '/)
    DO 40 I=1,L,20
 40 WRITE(6,41)X(I),DN(I),DDN(I)
 41 FORMAT(5X,F10.5,2(5X,F12.8))
    V=0
    DO 51 K=1,3
100 QMR(1)=0
    QMX(1)=1+V
    DO 42 I=2,L
    QMX(I)=(DF(I)/X(I))+(V*QX(I))
 42 QMR(I)=(DF(I)-(F(I)/X(I))+(V*QR(I)))
    NM=1000
    UU=3000
    DM=0.50000
    XL=25
    DO 43 I=1,L
    QTX(I)=AA*UU*DM*QMX(I)/XL
    DMN(I)=DN(I)+(V*DDN(I))
    DTN(I)=BB*NM*DM*DMN(I)/XL
 43 DS(I)=DTN(I)*QTX(I)/(DTN(1)*QTX(1))
    WRITE(6,44)V
 44 FORMAT(//5X,'RESULTS FUR EPS. =',1X,F6.3)
    WRITE(6,45)
 45 FORMAT(//10X,'ETA ',10X,'M.AX.VEL ',10X,'M.RD.VEL '/)
    DO 46 I=1,L,20
 46 WRITE(6,47)X(I),QMX(I),QMR(I)
 47 FORMAT(5X,F10.5,2(5X,F12.8))
    WRITE(6,48)
 48 FORMAT(//10X,'ETA ',10X,'M.NU.DE ',10X,'M.MASS F. '/)
    DO 49 I=1,L,20
 49 WRITE(6,50)X(I),DMN(I),DS(I)
 50 FORMAT(5X,F10.5,2(5X,F12.8))
    IF(V-0.100)101,102,103
101 V=V+0.02500
    GO TO 100
102 V=0.2000
    GO TO 100
103 CONTINUE
 51 V = V+0.10000000
    WRITE(6,52)AA,BB
 52 FORMAT(//10X,'A =  ',10X,F6.4/10X,'B =  ',10X,F6.4)
```

APPENDIX 4A

CALIBRATION OF THE STANDARD BRIDGE FOR HOT WIRE ANEMOMETRY

The measuring equipment was initially set as follows:

SQUARE WAVE	:	OFF
H F FILTER	:	1
VOLTS	:	1
FUNCTION	:	STD. BY
PROBE TYPE	:	WIRE
GAIN	:	1
DECADE RESIST.	:	0.00

The probe cable was connected to the probe socket and the free end of the cable was connected to the probe support.

Using the shorting probe, the support was short circuited, then the measurement of the probe resistance and the compensation for the leads resistance was carried out as follows:

1) FUNCTION switch was set to Res. Meas.

2) The ZERO OHMS was adjusted until the meter deflected to red scale mark.

3) The shorting probe was removed and the probe connected.

4) The DECADE was set so that the meter deflected to the red scale mark.

5) The DECADE setting was reduced by the lead resistance stated on the probe test card.

The DECADE setting then indicated the sensor resistance R_o.

As it was not possible to compensate for all, the lead, support, cable and sensor resistances, a modified procedure was followed. This allowed part of these resistances to be compensated for. The procedure was as follows:

1) The free end of the probe cable was short circuited.

2) The ZERO OHMS was adjusted so that the meter deflected to the red mark.

3) The short circuit was removed and replaced by probe support and probe.

4) The DECADE was set so that the meter deflected to red mark.

5) The probe resistance R_o was subtracted from the Decade reading. The result was the leads, probe support and additional cable resistances. DECADE was set to this result.

6) The sensor hot resistance was calculated from the formula on the probe test card and the result was added to the DECADE setting.

7) FUNCTION was then set to operate.

Next the bridge was aligned for high frequencies.

An oscilloscope was connected to one of the OUT sockets and:

1) The probe was placed in the flow.

2) The SQUARE WAVE was switched on.

3) The GAIN and H F FILTER were stepwise increased to higher values adjusting CABLE COMPENSATION Q and L until any tendency to

oscillation in the system was eliminated.

4) Highest setting at which adequate stability was obtained represented optimum alignment.

5) The SQUARE WAVE generator was switched off.

The system was then ready for operation.

This procedure was carried out every time a new probe was used.

APPENDIX 4B

CALIBRATION OF THE LINEARIZER

1) The probe operating resistance was noted down (R_w).

2) The anemometer output voltage at zero flow (V_o) was also noted.

3) 1) V_o^1 was calculated from $V_o^1 = 0.925\ V_o$.

   2) Calibration equipment was arranged to give a known velocity U_1 and the corresponding anemometer voltage V_1 recorded.

   3) Calibration equipment was then arranged to give a velocity $U_2 = 2U_1$ and anemometer voltage V_2 obtained.

   4) The following values were calculated:

$$Y_1 = \left(\frac{V_1}{V_o}\right)^2 - 1$$

$$Y_2 = \left(\frac{V_2}{V_o}\right)^2 - 1$$

   5) $Y = \frac{Y_2}{Y_1}$ and $X = \frac{U_2}{U_1} = 2$

$$m = \frac{\text{LOG } X}{\text{LOG } Y}$$

4) The value of m was selected by the two EXPONENT controls.

5) The MODE SELECTOR was set to 2 and RANGE switch to 4.

6) The Decade resistance was reduced until anemometer output voltage reading reached the value V_o^1.

7) With the ZERO push-button depressed, the two zero adjustment controls were set to give approximately zero linearizer output. voltage. The push-button was then released and DECADE set to original value (R_w).

8) With the TEMPERATURE COMP. button depressed, the temperature compensation control was adjusted to give approximately zero linearizer output. The button was released.

9) With the input to the linearizer disconnected, and X1/X10 push-button depressed, the LEVEL control was adjusted to give zero linearizer output.

10) Calibration equipment was adjusted to give a velocity U_2 and both GAIN controls were set so that a simple relationship existed between linearizer output and velocity, (eg. 5 volts at 50 m/s). Linearizer maximum output voltage was 10 volts.

11) Calibration equipment was adjusted to give a velocity $U_1 = \frac{1}{2}U_2$, when linearizer output voltage $V_1 = \frac{1}{2}V_2$, the linearizer was properly calibrated. When $V_1 > \frac{1}{2}V_2$ the value of m was increased only slightly and steps 6 to 11 were repeated until a satisfactory value of m that gave the best linearization was reached. When $V_1 < \frac{1}{2}V_2$ the value of m was reduced slightly and the rest of the procedure carried out

This calibration was repeated each time a new probe was used. Frequent checks were made by placing the probe in a flow of known velocity and noting the linearizer voltage.

REFERENCES

ABBISS, J.B., CHUBB, T.W. and PIKE, E.R. (1974)

Optics and Laser Tech. (249).

ABBISS, J.B. (1974)

Electro-Optics Inter. Conf. Brighton, UK. March (19-21).

ADRIAN, R.J. and GOLDSTEIN, R.J. (1971)

J. of Phys. E. (sc. intr.), Vol. 4, (505).

ALBRIGHT, C.W., HOLDEN, J.H., SIMONS, H.P. and SCHMIDT, L.D. (1949)

Chem. Engng., Vol. 56, (108).

ALEXANDER, L.G., ARNOLD KIVNICK, COMINGS, E.W. and HENZE, E.D. (1955)

A.I.CH.E.J., 1, (55).

ALEXANDER, L.G.,and GOLDERN, C.L. (1951)

Ind. Engng. Chem., 43, (1325).

BALESCU, R. and SENATORSKI, A. (1970)

Ann. Phys., NY 58, (587).

BARON, T. (1949)

Paper presented at A.I.CH.E., Tulsa, Okla., May (8-12).

BARON, TH. and ALEXANDER, L.G. (1951)

Chem. Engng. Prog., Vol. 47, (181).

BATCHELOR, G.K. (1949)

Aust. J. Sci. Res., A, 2, (437).

BATCHELOR, G.K. (1950)

Quart. J. R. Met. Soc., 76, (133).

BATCHELOR, G.K. (1952)

Proc. Camb. Phil. Soc., 48, (345).

BATCHELOR, G.K. (1959)

J. Fluid Mech., 5, (113) and (134).

BATCHELOR, G.K. (1976)

J. Fluid Mech., 74, (1).

BECKER, A.H., HOTTEL, H.C. and WILLIAMS, G.C. (1965a)

J. Fluid Mech., 30, (259).

BECKER, A.H., HOTTEL, H.C. and WILLIAMS, G.C. (1965b)

J. Fluid Mech., 30, (285).

BIRCH, A.D., BROWN, D.R., THOMAS, J.R. and PIKE, E.R. (1973)

J. of Phys. D. App. Phys., 6, (L 71).

BIRD, R.B., STEWART, W.E. and LIGHTFOOT, E.N. (1960)

"Transport Phenomenon", Wiley, New York.

BOURKE, P.T. et al (1969)

J. of Phys. A, Gen. Phys., Vol. 3, (216).

BOUSSINESQ, J. (1877)

Mem. pres par div. savants a l'ocal. sci., Paris, 23 (46).

BRADSHAW, P. (1971)

"An Introduction to Turbulence and its Measurements".

Pergamon Press.

BRAGG, G.M. and BEDNARIK, H.V. (1974)

Intr. J. Heat Mass Transfer, Vol. 18 (443).

BRAYTON, D.B., KALB, H.T. and CROSSWY, F.L. (1973)

App. Optics, 12 (1145).

BUCHHAVE, P. (1973)

Disa Inform., No. 15, (15).

BUSH, N.E. (1965)

Riso Report No 99.

CHANDRASEKHAR, S. (1943)

Rev. Mod. Phys., 15 (1).

COMTE-BELLOT and CORRSIN, S. (1971)

J. Fluid Mech., 48, (278).

CORRSIN, S. (1943)

Nat. Adv. Comm. Aeronaut. Wartime Rep. No. 94.

CORRSIN, S. (1949)

Nat. Adv. Comm. Aeronaut. Tech. Note, No. 1865.

CORRSIN, S. (1952)

J. of App. Phys., Vol. 23, No. 1, (113).

CORRSIN, S. (1972)

Phys. of Fluids, Vol. 15, No. 6, (986).

COUSINS, L.B., DENTON, W.H. and HEWITT, G.F. (1965).

Proc. Symp. on Two-Phase Flow, Exeter, England, 2, C401.

COUSINS, L.B. and HEWITT, G.F. (1968)

U.K.A.E.A. Rep. No. R-5657, Harwell.

DAVIDSON, G.A. and McCOMB, W.D. (1975)

J. of Aerosol Sci., Vol.,6, (227).

DUNCAN, W.J., THOM, A.S. and YOUNG, A.D. (1960)

"An Elem. Treatise on the Mech. of Fluids."

Edward Arnold (Pub.) Ltd, London.

DURST, F. and WHITELAW, J.H. (1971)

Proc. Roy. Soc. London A, 324, (157).

DURST, F. and ELLIASON, B. (1975)

LDA Symp., Copenhagen, August.

DURST, F. and UMHAUER, H. (1975)

LDA Symp., Copenhagen, August.

DURST, F. and ZARE, M. (1975)

SFB 80/TM/63. Univ. of Karlsruhe.

EDWARDS, S.F. (1964)

J. Fluid Mech., 18, (239).

EDWARDS, S.F. and McCOMB, W.D. (1969)

J. Phys. A, Gen. Phys., 2, (157).

EDWARDS, S.F. and McCOMB, W.D. (1971)

Proc. Roy. Soc. A, 325, (313).

EDWARDS, S.F. and McCOMB, W.D. (1972)

Proc. Roy. Soc. A, 330, (495).

EDWARDS, R.V., ANGUS, J.C., FRENCH, M.J. and DUNNING JR, J.W. (1971)

J. of App. Phys., Vol. 42, (837).

ELIAS, F. (1929)

Z. Agnew. Math. u. Mech., 9, (434).

ERTEL, H. (1942)

Z. Meteorol., 59, (277).

FARMER, W.M. and BRAYTON, D.B. (1971)

App. Optics, Vol. 10, (2319).

FARMER, W.M. (1972)

App. Optics, Vol. 11, (2603).

FARMER, W.M. (1974)

App. Optics, Vol. 13, (610).

FLINT, D.L., KADA, J and HANRATTY, T.J. (1960)

A.I.CH.E.J., Vol. 6, (325).

FORMAN, J.N., GEORGE, E.W. and LEWIS, R.L. (1965)

App. Phys. Lett., Vol. 7, (77).

FORSTALL, W. and GAYLORD, E.W. (1955)

J. App. Mech., 22, (161)

FRENKIEL, F.N. (1953)

Adv. in App. Mech. Academic Press, N.Y. Vol. III, (61)

FRIEDLANDER, S.K. (1957)

A.I.CH.E.J., Vol. 3, No. 3, (381).

FRIEDLANDER, S.K. and JOHNSTONE, H.F. (1957)

Ind. Engng. Chem., 49, (1151).

FRISTORM, R.M., JONES, A.R., SCHWAR, M.J.R. and WEINBERG, F.J. (1973)

Faraday Symp. of Chem. Soc., No. 7, (183).

GEORGE, W.K. and LUMLEY, J.L. (1973)

J. Fluid Mech., 60, Part 2, (321).

GOLDSCHMIDT, V.W. (1965)

J. of Colloid. Sci., 20, (617).

GOLDSCHMIDT, V.W. and ESKINAZI, S. (1966)

J. of App. Mech., Trans. ASME, (735).

GOLDSTEIN, R.J. and KRIED, D.K. (1967)

J. of App. Mech., 34, (814).

GORTLER, H. (1942)

ZAMM, Vol. 22, (244).

HERRING, J.R. (1965)

Phys. Fluids, 8, (2219).

HINKLE, D.L., ORR, C. and DALLAVALLE, J.M. (1955)

J. Colloid, Sci., 9, (70).

HINZE, J.O. and VAN DER HEGGE ZIJNEN, B.J. (1949)

App. Sci. Res., 1A, (435)

HINZE, J.O. (1959)

"Turbulence". McGraw-Hill, New York.

HONG, N.S. and JONES, A.R. (1976)

J. Phys. D., App. Phys., Vol. 9, (1839).

HUTCHINSON, P., HEWITT, G.F. and DUKLER, A.E. (1971)

Chem. Engng. Sci., 26, (419).

JONES, A.R. (1973)

J. Phys. D., App. Phys., Vol. 6, (417).

JONES, A.R. (1974)

J. Phys. D., App. Phys., Vol. 7, (1369).

KARMAN, TH. VON. (1930)

Nachr. Akad. Wiss. Gottingen Matt-Phy. Kl., (58).

KAMPÉ DE FERIET. (1939)

Ann. Soc. Sci. Bruxelles, 59, (145).

KOFOED-HANSEN, O. and WANDEL, C.F. (1967)

Riso Report No. 50.

KRAICHNAN, R.H. (1959)

J. Fluid Mech., 5, (497).

KRAICHNAN, R.H. (1968)

Phys. Fluids, 11, (945).

KRAICHNAN, R.H. (1972)

J. Fluid Mech., 56, (287).

LADING, L. (1971)

App. Optics, Vol. 10, (1943).

LESLIE, D.C. (1973)

"Development in the Theory of Turbulence". Clarendon Press.

LEWIS, C.H., PETERSON, E.E., ACRIVOS, A. and TAO, S.C. (1961)

Paper presented at ACS Symposium.

LUMLEY, J.L. (1957)

"Some Problems Connected with the Motion of Small Particles in Turbulent Fluid." PhD Thesis. Johns Hopkins Univ.

LUMLEY, J.L. and PANOFSKY, H.A. (1964)

Interscience Publ., New York.

LUMLEY, J.L. (1976)

J. Fluid Mech., 74, (433).

MASUMDER, M.K. and WANKUM, D.L. (1970)

App. Optics, Vol. 9, (633).

McCARTER, R.J., STUTZMAN, L.F. and KOCH, H.A. (1949).

Ind. Engng. Chem., 41, (1290).

McCOMB, W.D. (1974a)

J. Phys. A., Math., Nucl. Gen., Vol. 7, (632).

McCOMB, W.D. (1974b)

J. Phys. A., 7, (L 164).

McCOMB, W.D. (1976)

J. Phys. A, Math., Nucl. Gen., Vol. 9, (179).

MELLING, A. and WHITELAW, J.H. (1973)

Disa Information No. 15, (5).

MICHELSON, W.R. (1955)

Nat. Adv. Comm. Aeronaut. Tech. Note No. 3570.

NEILSON, J.H. and GILCHRIST, A. (1968)

J. Fluid Mech., 33, (131).

NUNNER, W. (1956)

VDI-Forschungsheft No 455.

ORLOFF, K.L., MYER, F.C., MIKASA, M.F. and PHILLIPS, J.R. (1975)

Minnesota Symp. on Laser Anemom., Univ. of Minnesota, October (22-24).

ORR, C. JR. (1966)

"Particulate Technology". Macmillan, N.Y.

OWENS, J.C. (1969)

Proc. of I.E.E.E., Vol. 57, (530).

OWENS, J.C. (1972)

App. Optics, Vol. 11, (2977).

PAI, S.I. (1954)

"Fluid Dynamics of Jets". Van Nostrand.

PANKHURST, R.C. and HOLDER, D.W. (1952)

"Wind Tunnel Technique". Pitman.

PESKIN, R.L. (1959)

"Some Effects of Particle-Particle and Particle-Fluid Interactions in Two-Phase Flow Systems".

PhD Thesis, Princeton Univ., N.J.

PESKIN, R.L. (1962)

Paper presented at the Nat. Meeting, A.I.CH.E., Baltimore.

PIKE, E.R., JACKSON, D.A., BOURKE, P.J. and PAGE, D.I. (1968)

J. of Phys. E. (Sci. Instr.), Vol. 1, (727).

PIKE, E.R. (1972)

J. of Phys. D., App. Phys., 5, (L 23).

PRANDTL, L. (1925)

Z. angew. Math. u. Mech., 5, (136).

PRANDTL, L. (1942)

Z. angew. Math. u. Mech., 22, (241).

RAUDKIVI, A.J. and CALLANDER, R.A. (1975)

"Advanced Fluid Mechanics". Edward Arnold (Pub.)Ltd.

REICHARDT, H. (1941)

Z. angew. Math. u. Mech., 21, (257)

REICHARDT, H. (1949)

Oudart, A. : Publ. Sci. et tech. ministere air No. 234.

RICHARDSON, L.F. (1926)

Proc. Roy. Soc. London, 110 A, (709).

ROBINSON, D.M. and CHU, W.P. (1975)

App. Optics, Vol. 14, (2177)

ROSENWEIG, R.E., HOTTEL, H.C. and WILLIAMS, G.C. (1961)

Chem. Engng. Sci., 15, (111).

RUDD, M.J. (1968)

J. of Phys. E. (Sci. Instr.), Vol. 2, (55).

RUDEN, P. (1933)

Naturwissenschaften, 21, 375.

SAFFMAN, P.G. and TUNNER, J.S. (1956)

J. Fluid Mech., Vol. 1, (16).

SHE, C.Y. and LUCERO, J.A. (1973)

Optics Comm., Vol. 9, No. 3, (300).

SHLIEN, D.J. and CORRSIN, S. (1974)

J. Fluid Mech., 62 (225).

SOO, S.L. and PESKIN, R.L. (1958)

Project SQUID Tech. Report. PR-80-R (ONR).

Princeton Univ., N.J.

SOO, S.L. (1967)

"Fluid Dynamics of Multi-Phase Systems". Blaisdell Pub.Co.

SPIERS, H.M. (1955)

"Tech. Data on Fluids". Pub. by B.N.C. World Power Conf.

TAYLOR, G.I. (1915)

Phil. Trans. Roy. Soc., London, 215 A, (1).

TAYLOR, G.I. (1921)

Proc. London Math. Soc., 20, (196).

TAYLOR, G.I. (1932)

Proc. Roy. Soc., London, 135 A, (685).

TAYLOR, J.F., GREMMETT, H.L. and COMINGS, E.W. (1951)

Chem. Engng. Prog., Vol. 47, 175.

TCHEN, C.M. (1947)

"Mean Value and Correlation problems Connected with the Motion of Small Particles suspended in a Turbulent Field". PhD Thesis, Delft.

TOWLE, W.L. and SHERWOOD, T.K. (1939)

Ind. Engng. Chem., 31, 457.

TOWNSEND, A.A. (1947)

Proc. Roy. Soc., London, 190 A, (551).

TOWNSEND, A.A. (1948)

Austr. J. Res., 1A, (161).

TOWNSEND, A.A. (1949)

Austr. J. Res., 2A, (451).

UBEROI, M.S. and CORRSIN, S. (1953)

N.A.C.A. Tech. Rep. No. 1142.

WOERTZ, B.B. and SHERWOOD, R.K. (1939)

Trans. A.I.CH.E., 35, (517).

WYGNANSKI, I. and FIEDLER, H. (1969)

J. Fluid Mech., 38, (577).

WYLD, H.W. (1961)

Ann. Phys., N.Y. 14 (143).

YEH, Y. and CUMMINS, H.Z. (1964)

App. Phys. Lett., Vol. 4, (176).

FIGURE CAPTIONS

LDA BURST SIGNAL

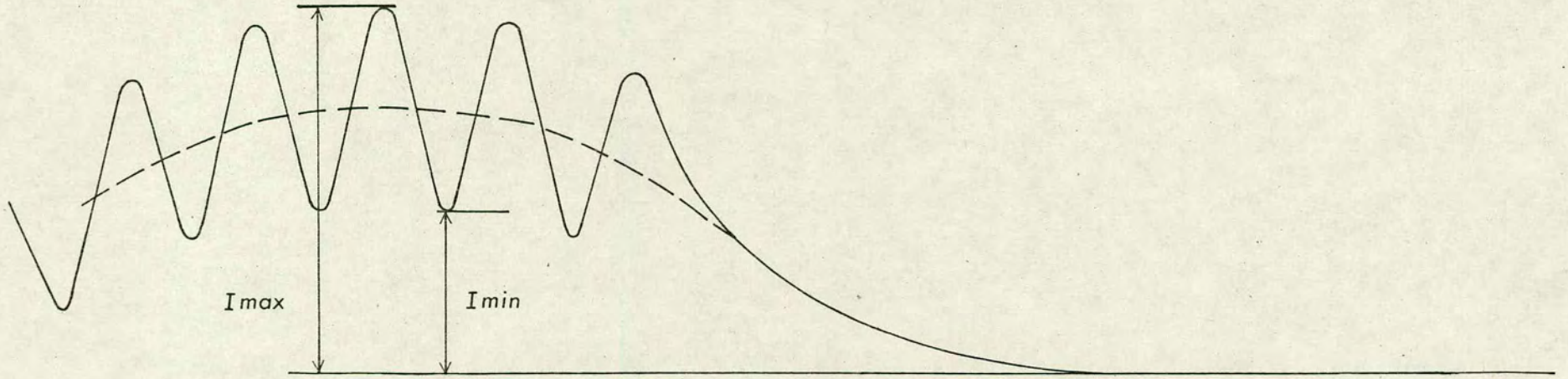

Figure 3.1

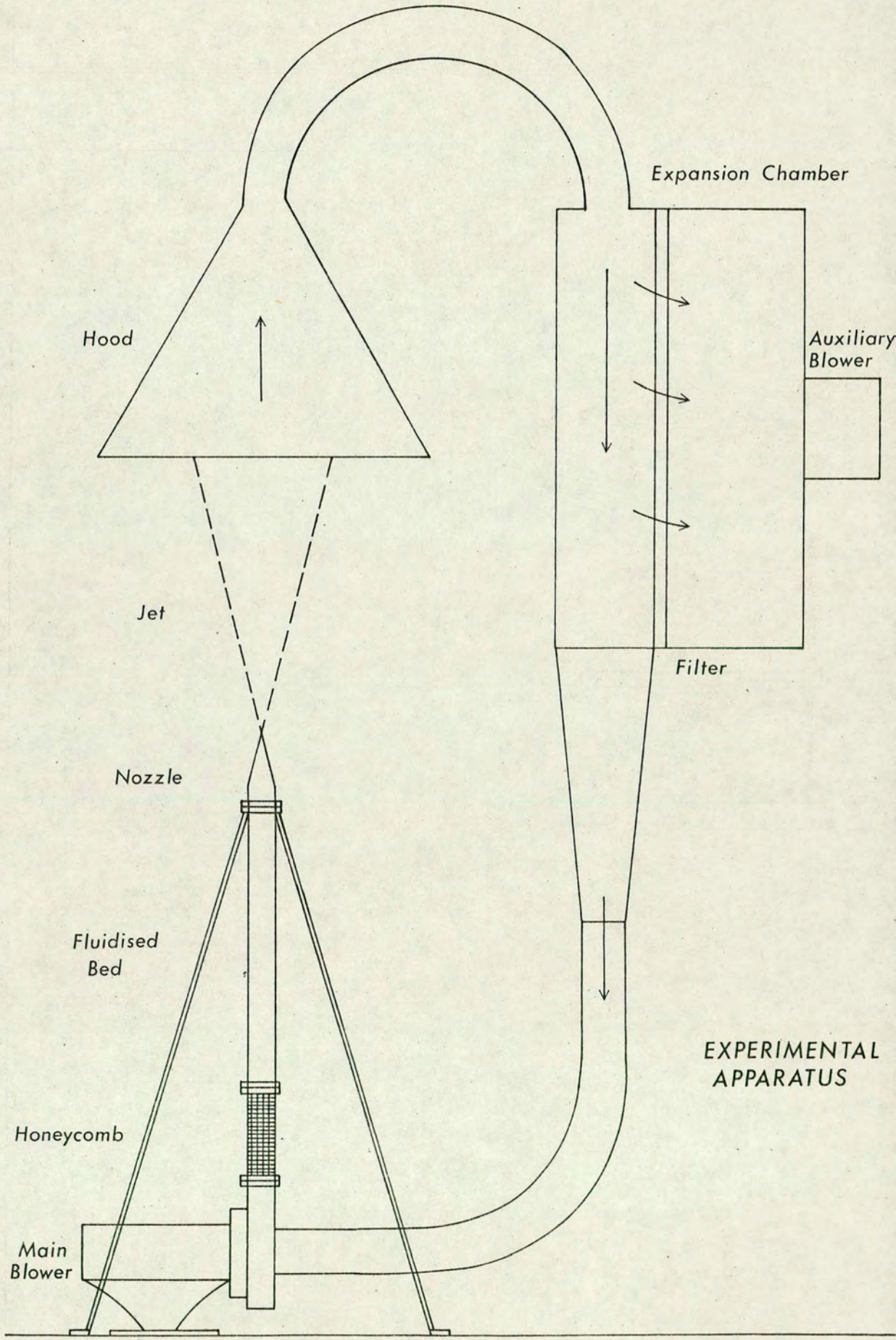
Expansion Chamber
Hood
Auxiliary Blower
Jet
Filter
Nozzle
Fluidised Bed
EXPERIMENTAL APPARATUS
Honeycomb
Main Blower

Figure 4.1

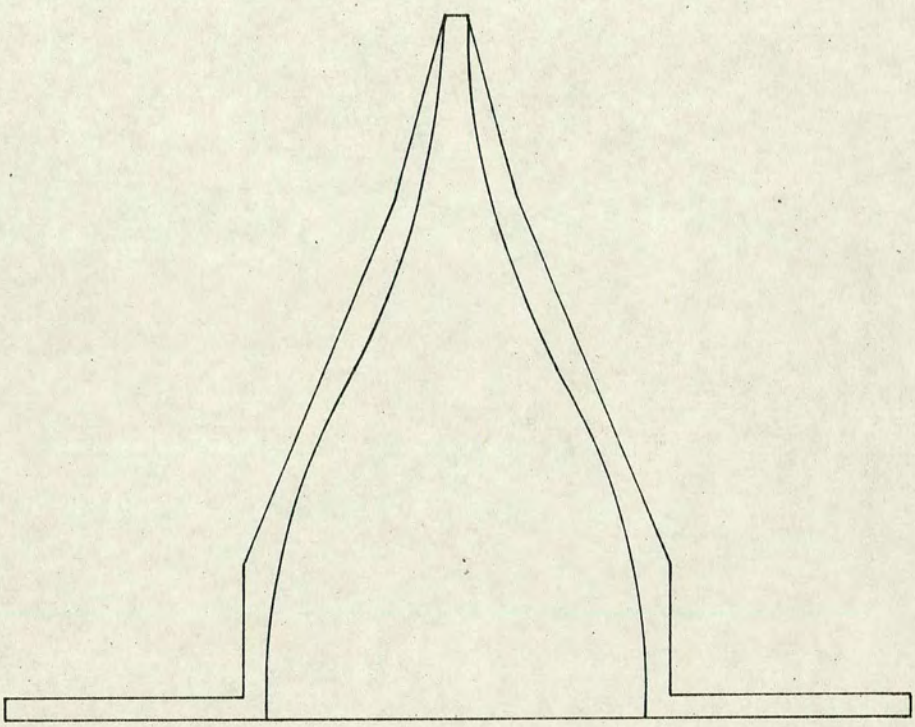

NOZZLE

Figure 4.2

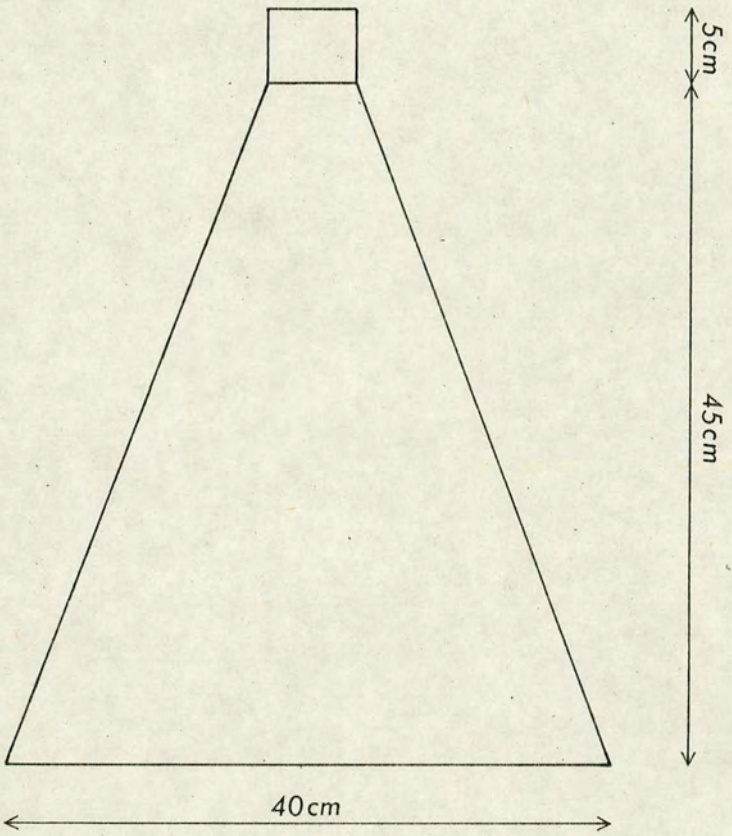

EXTRACTION HOOD

Figure 4.3

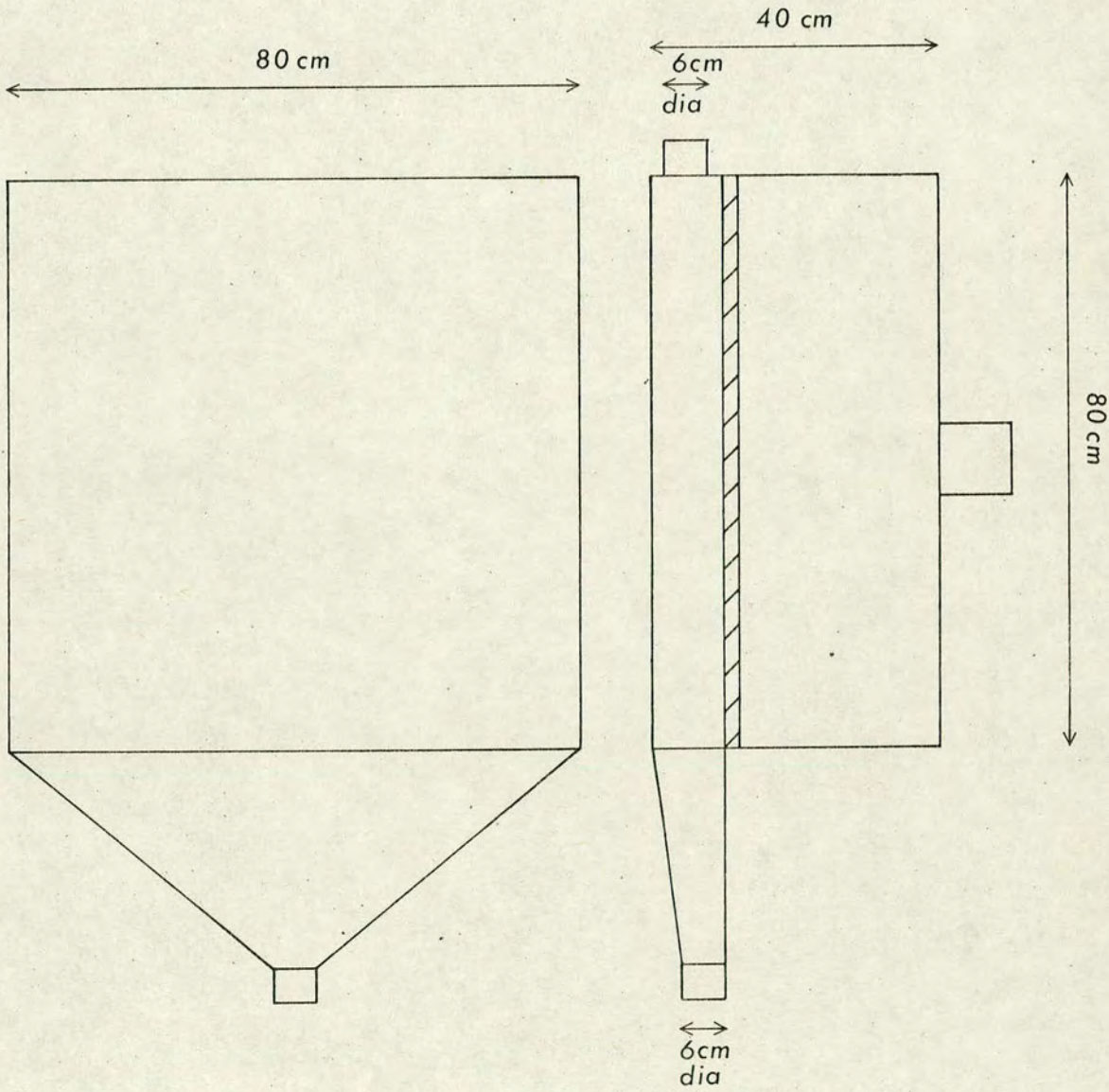

EXPANSION CHAMBER

Figure 4.4

BLOWER SUITABILITY TEST

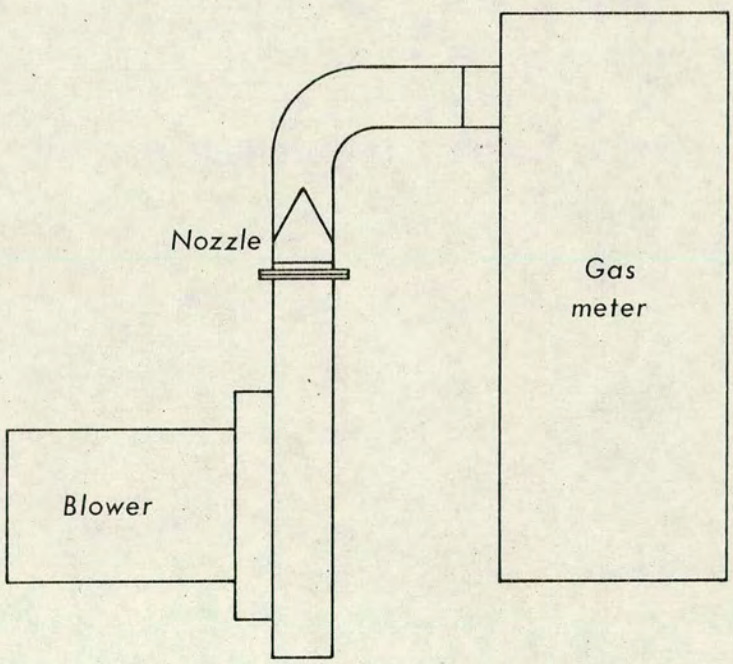

Figure 4.5

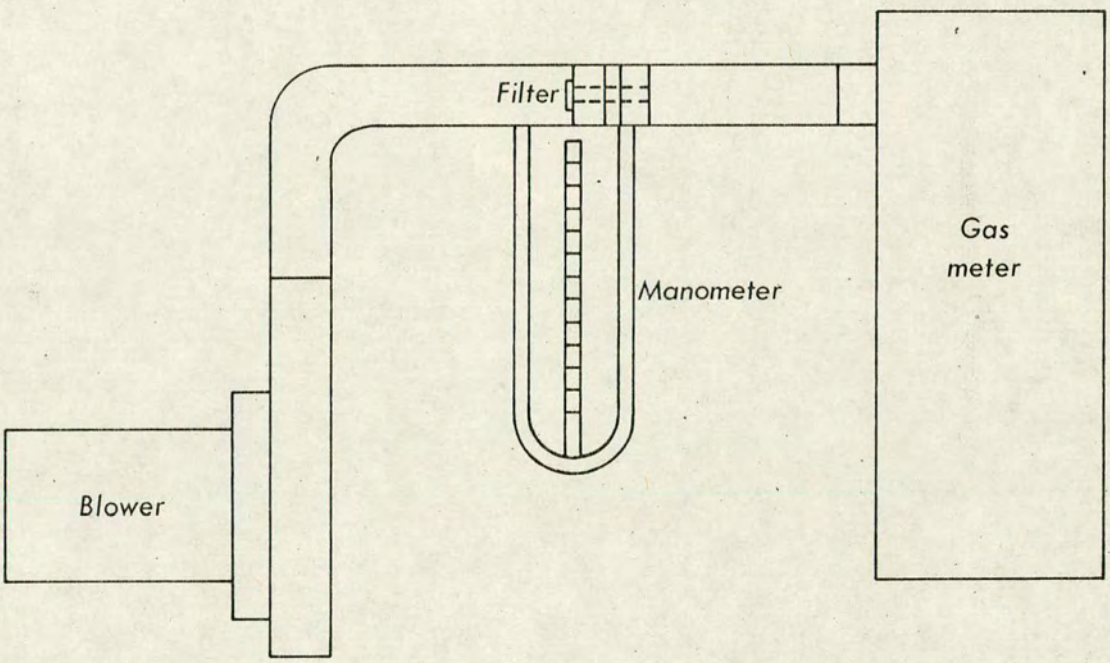

PRESSURE DROP ACROSS FILTER

Figure 4.6

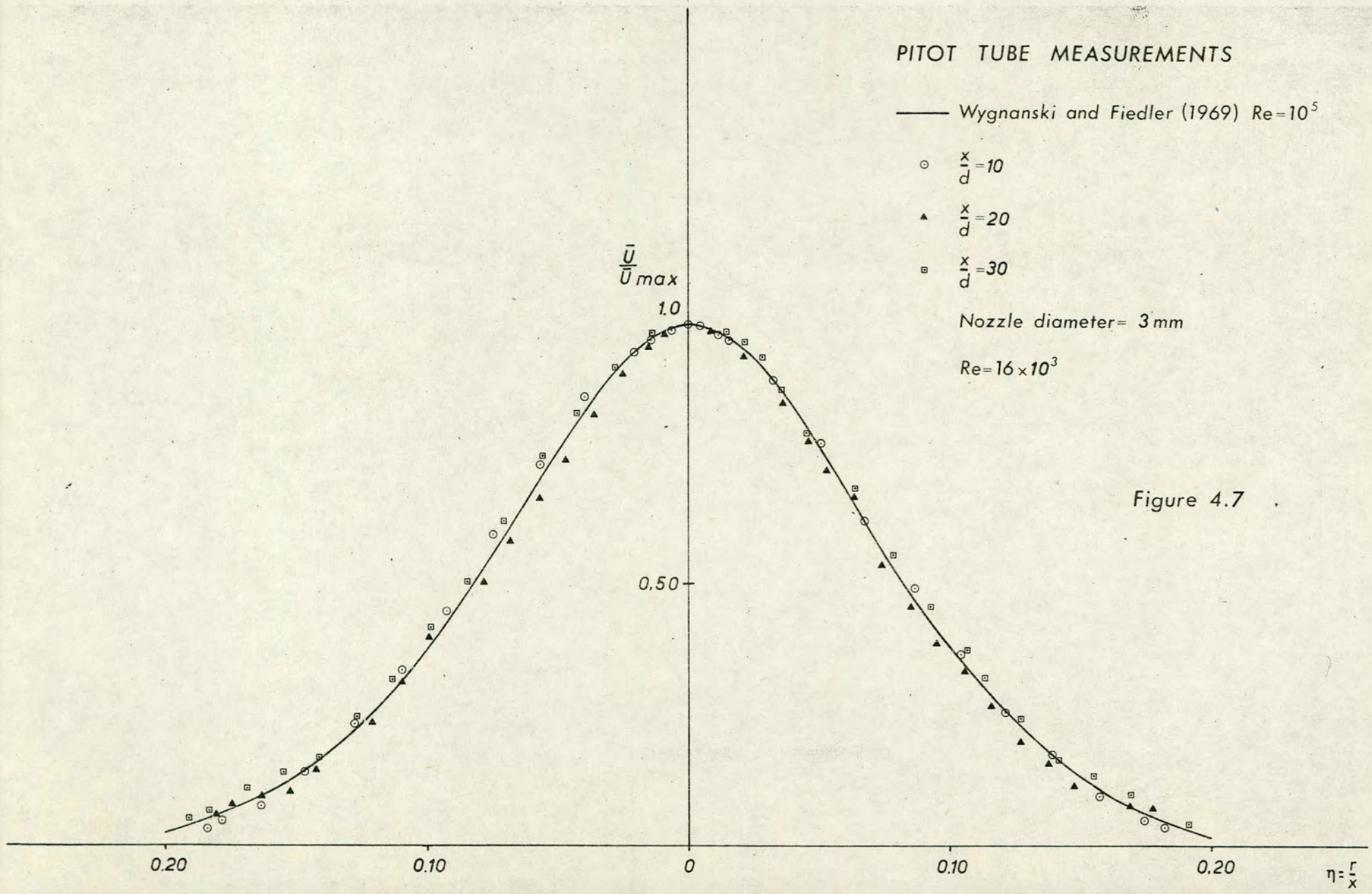
PITOT TUBE MEASUREMENTS
Wygnanski and Fiedler (1969) Re=10^5
x/d=10
x/d=20
x/d=30
Nozzle diameter= 3 mm
Re=16×10^3
Ū/Ū max
1.0
0.50
0.20
0.10
0
0.10
0.20
η=r/x

Figure 4.7

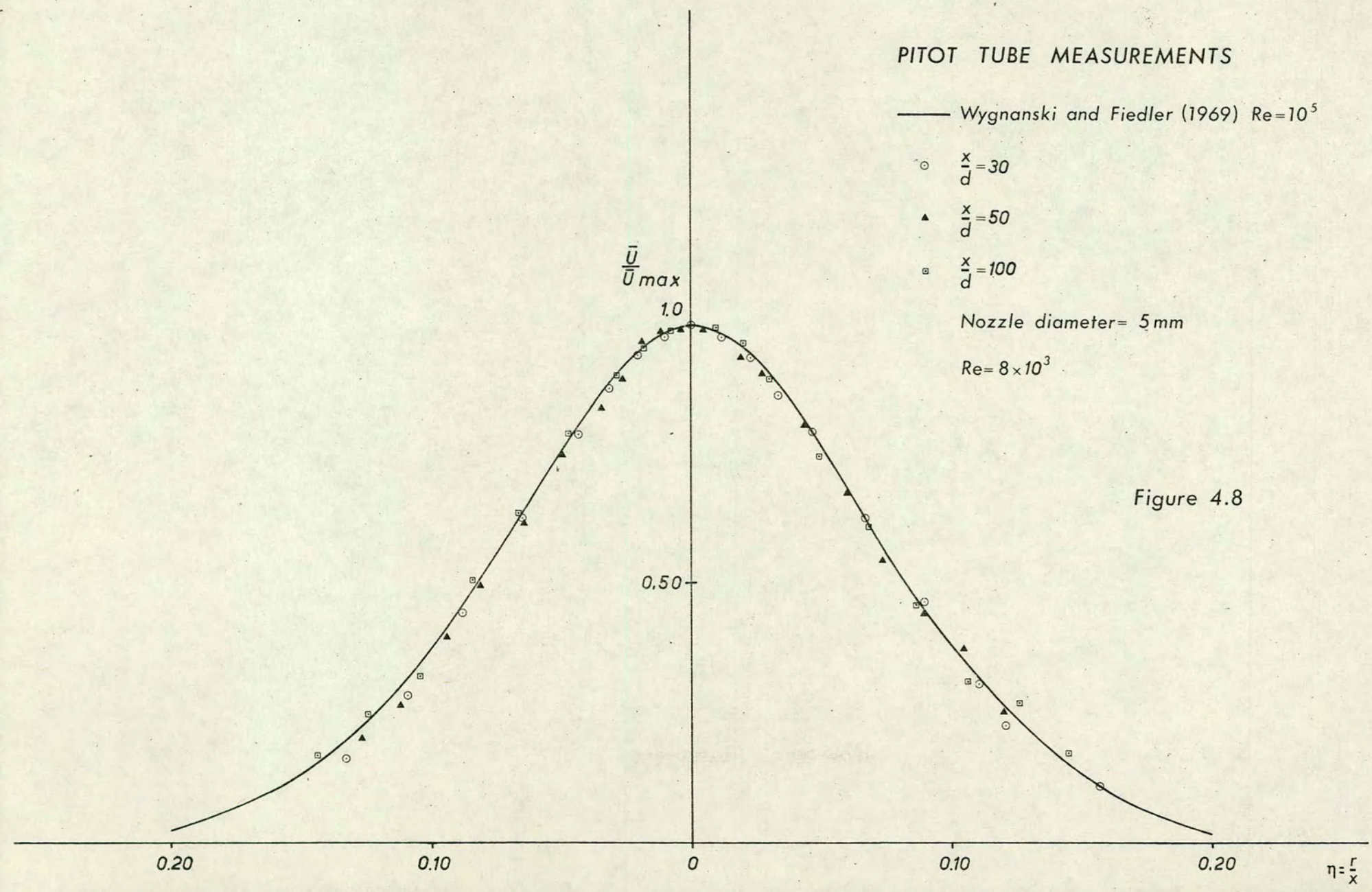
PITOT TUBE MEASUREMENTS
Wygnanski and Fiedler (1969) Re=10^5
x/d=30
x/d=50
x/d=100
Nozzle diameter= 5mm
Re= 8×10^3
Ū/Ū max
1.0
0,50
0.20
0.10
0
0.10
0.20
η=r/x

Figure 4.8

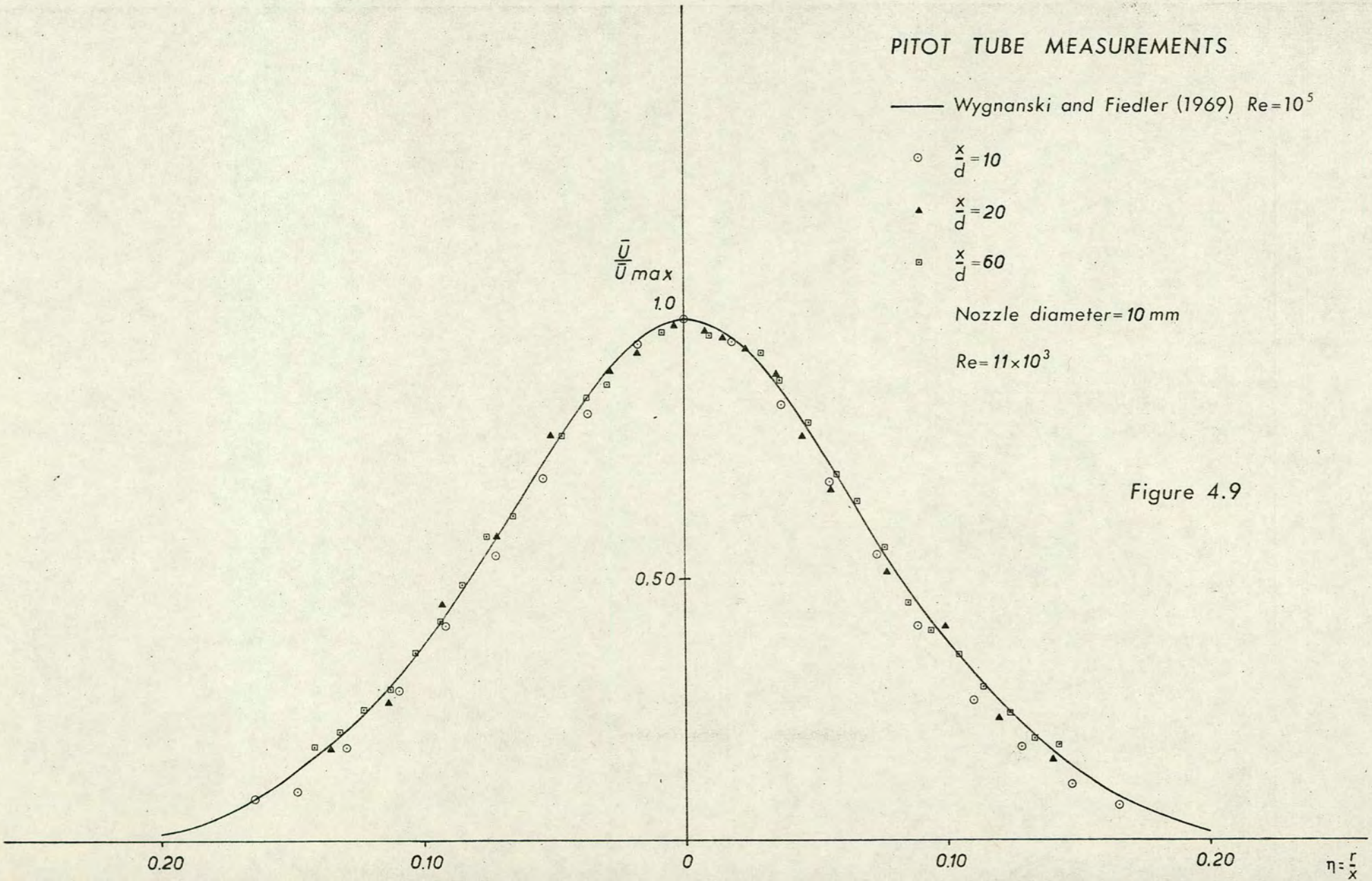
PITOT TUBE MEASUREMENTS
Wygnanski and Fiedler (1969) Re=10^5
x/d=10
x/d=20
x/d=60
Nozzle diameter=10 mm
Re=11×10^3
Ū/Ū max
1.0
0.50
0.20
0.10
0
0.10
0.20
η=r/x

Figure 4.9

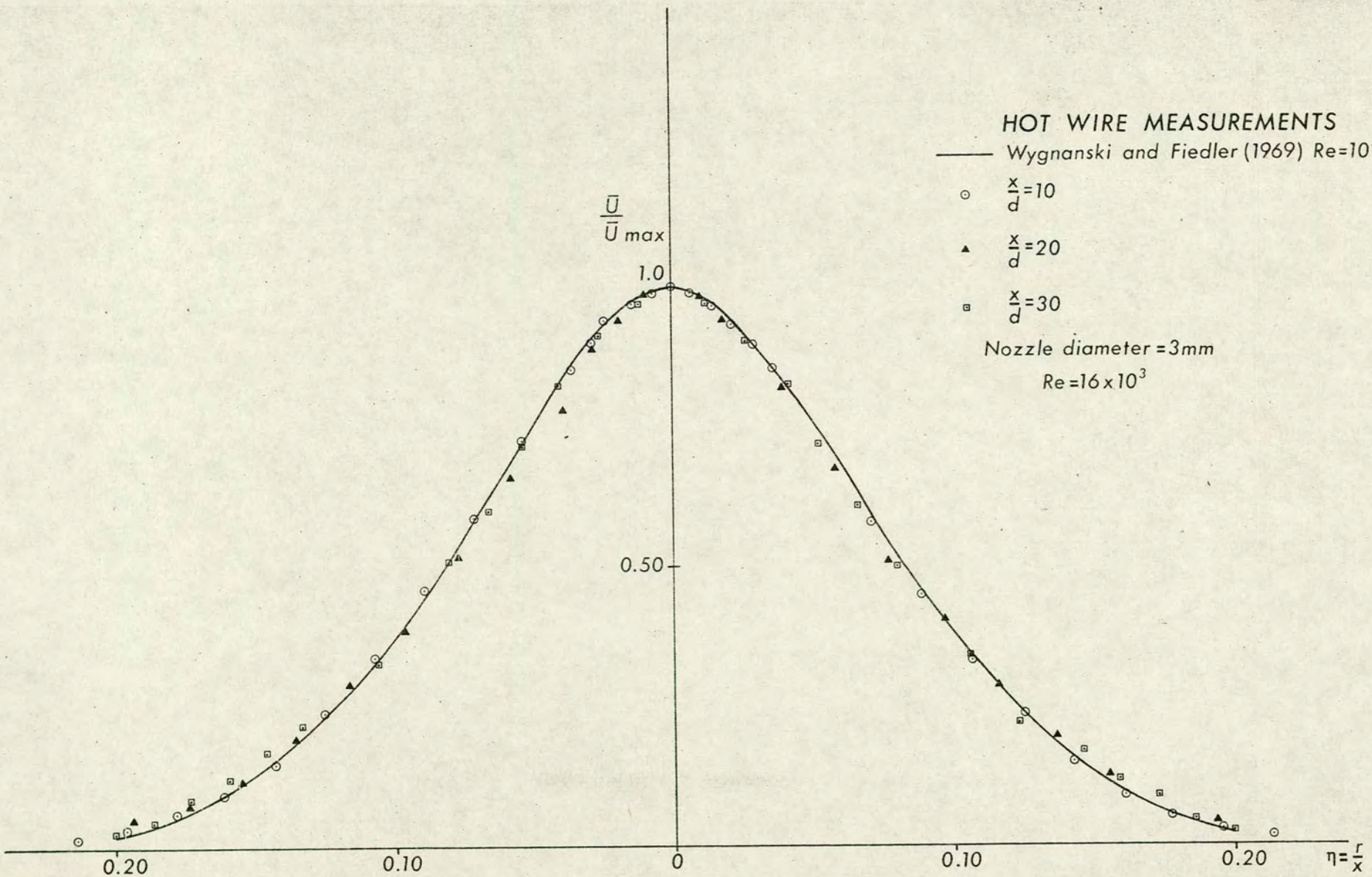
HOT WIRE MEASUREMENTS
Wygnanski and Fiedler (1969) Re=10^5
x/d=10
x/d=20
x/d=30
Nozzle diameter =3mm
Re =16 x 10^3
Ū/Ū max
1.0
0.50
0.20
0.10
0
0.10
0.20
η= r/x

Figure 4.10

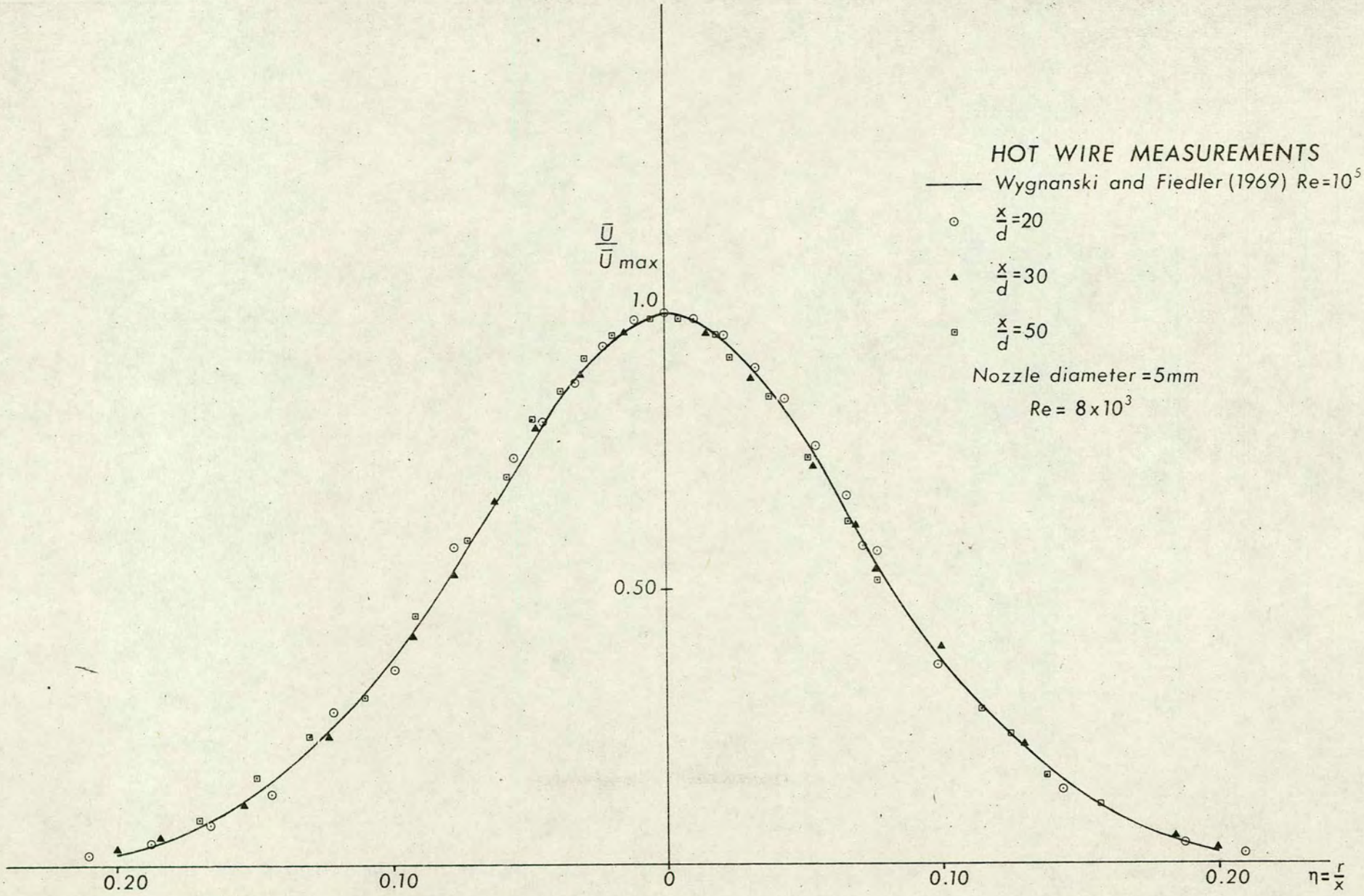
HOT WIRE MEASUREMENTS
Wygnanski and Fiedler (1969) Re=10^5
x/d=20
x/d=30
x/d=50
Nozzle diameter =5mm
Re = 8x10^3
Ū/Ū max
1.0
0.50
0.20
0.10
0
0.10
0.20
η=r/x

Figure 4.11

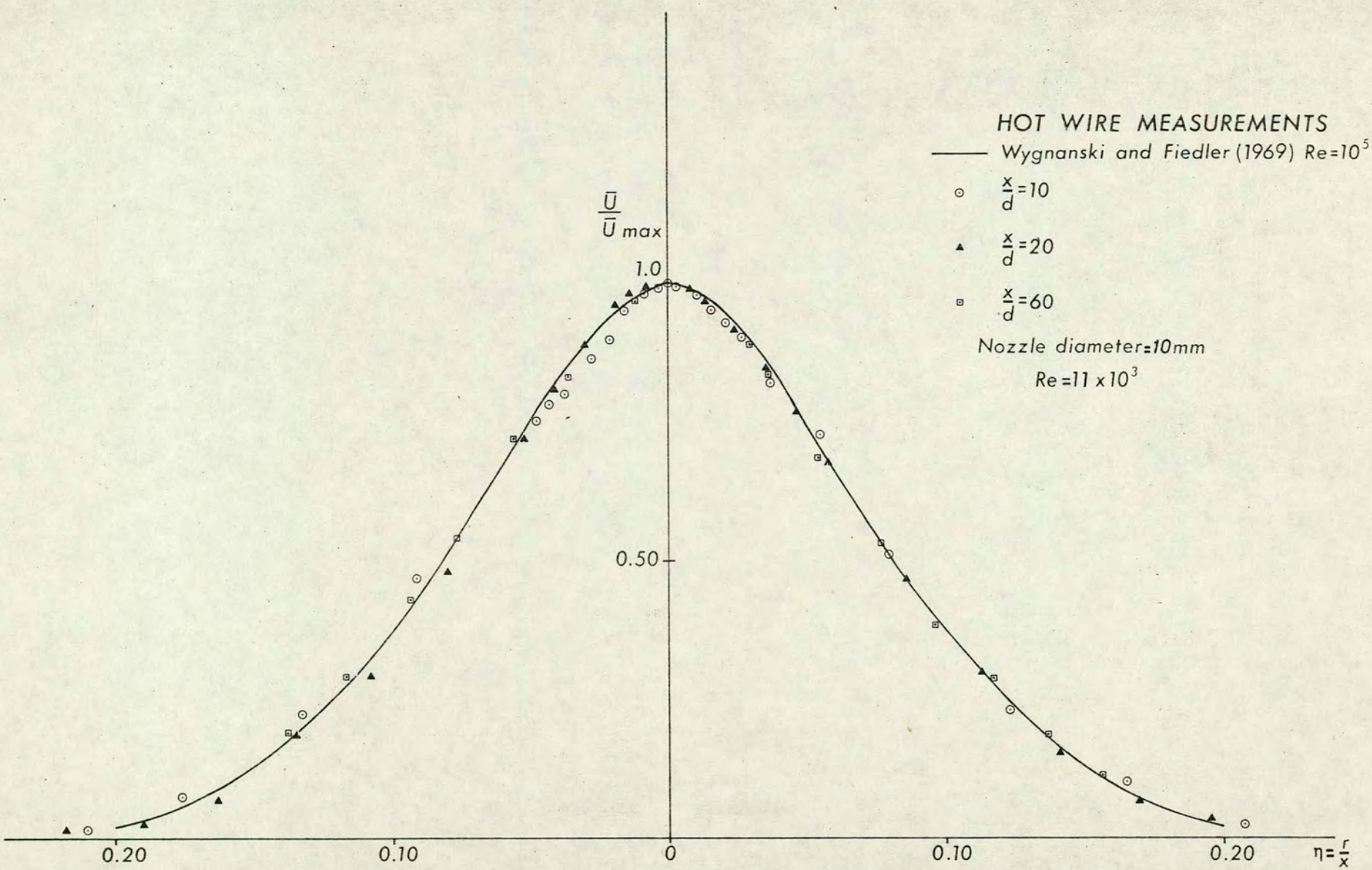
HOT WIRE MEASUREMENTS
Wygnanski and Fiedler (1969) Re=10^5
x/d=10
x/d=20
x/d=60
Nozzle diameter=10mm
Re=11 x 10^3
U/U max
1.0
0.50
0.20
0.10
0
0.10
0.20
η=r/x

Figure 4.12

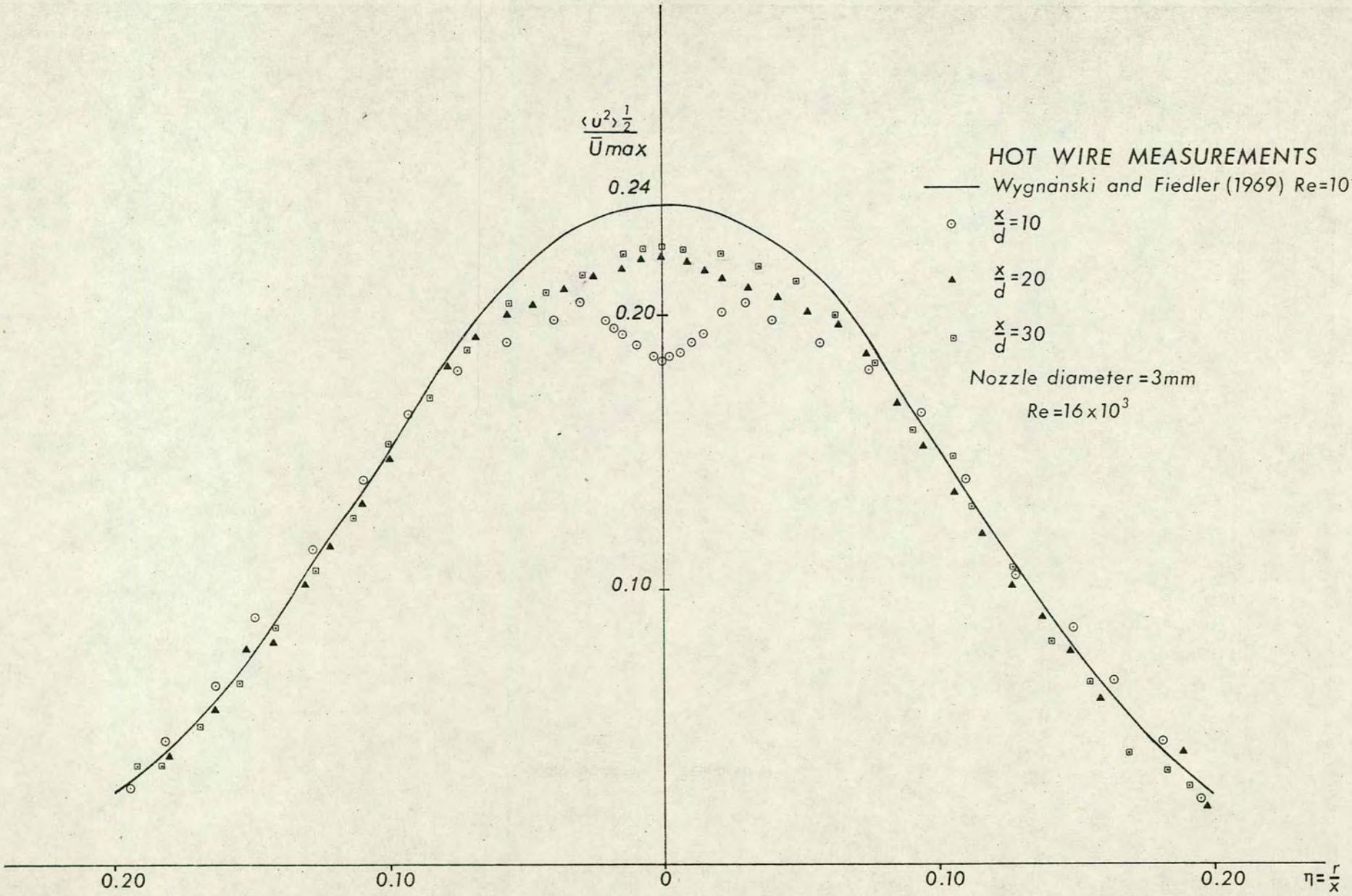
$\frac{\langle u^2 \rangle^{\frac{1}{2}}}{\bar{U}max}$
0.24
0.20
0.10
HOT WIRE MEASUREMENTS
Wygnanski and Fiedler (1969) $Re=10^5$
$\frac{x}{d}=10$
$\frac{x}{d}=20$
$\frac{x}{d}=30$
Nozzle diameter = 3mm
$Re=16\times10^3$
0.20
0.10
0
0.10
0.20
$\eta=\frac{r}{x}$

Figure 4.13

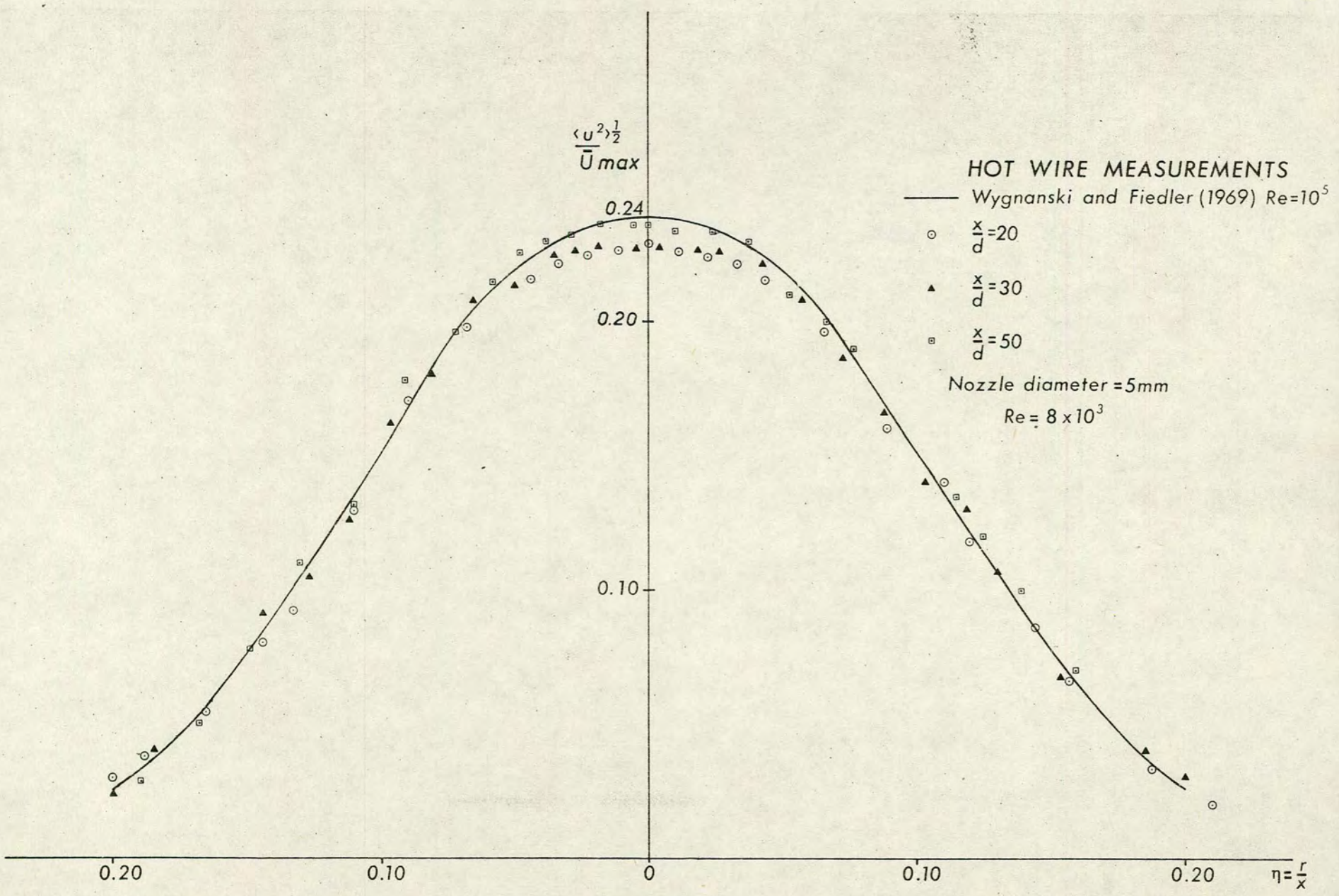
$\frac{\langle u^2 \rangle^{\frac{1}{2}}}{\bar{U}\,max}$
0.24
0.20
0.10
0.20
0.10
0
0.10
0.20
$\eta = \frac{r}{x}$
HOT WIRE MEASUREMENTS
Wygnanski and Fiedler (1969) Re=10^5
$\frac{x}{d}$=20
$\frac{x}{d}$=30
$\frac{x}{d}$=50
Nozzle diameter = 5mm
Re = 8×10^3

Figure 4.14

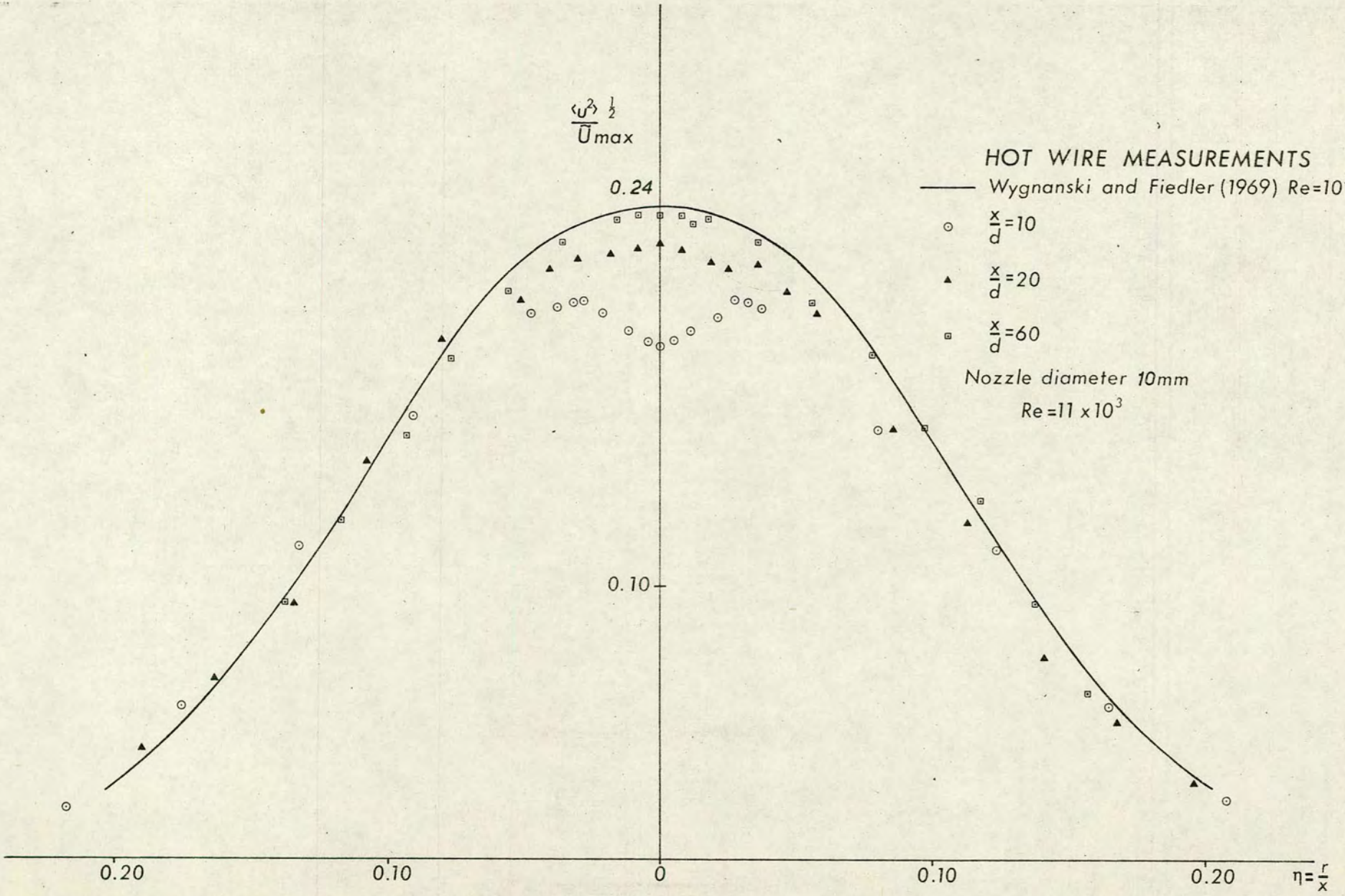
$\frac{\langle u^2 \rangle^{\frac{1}{2}}}{U_{max}}$
0.24
0.10
HOT WIRE MEASUREMENTS
Wygnanski and Fiedler (1969) Re=10^5
x/d=10
x/d=20
x/d=60
Nozzle diameter 10mm
Re=11 x 10^3
0.20
0.10
0
0.10
0.20
η=r/x

Figure 4.15

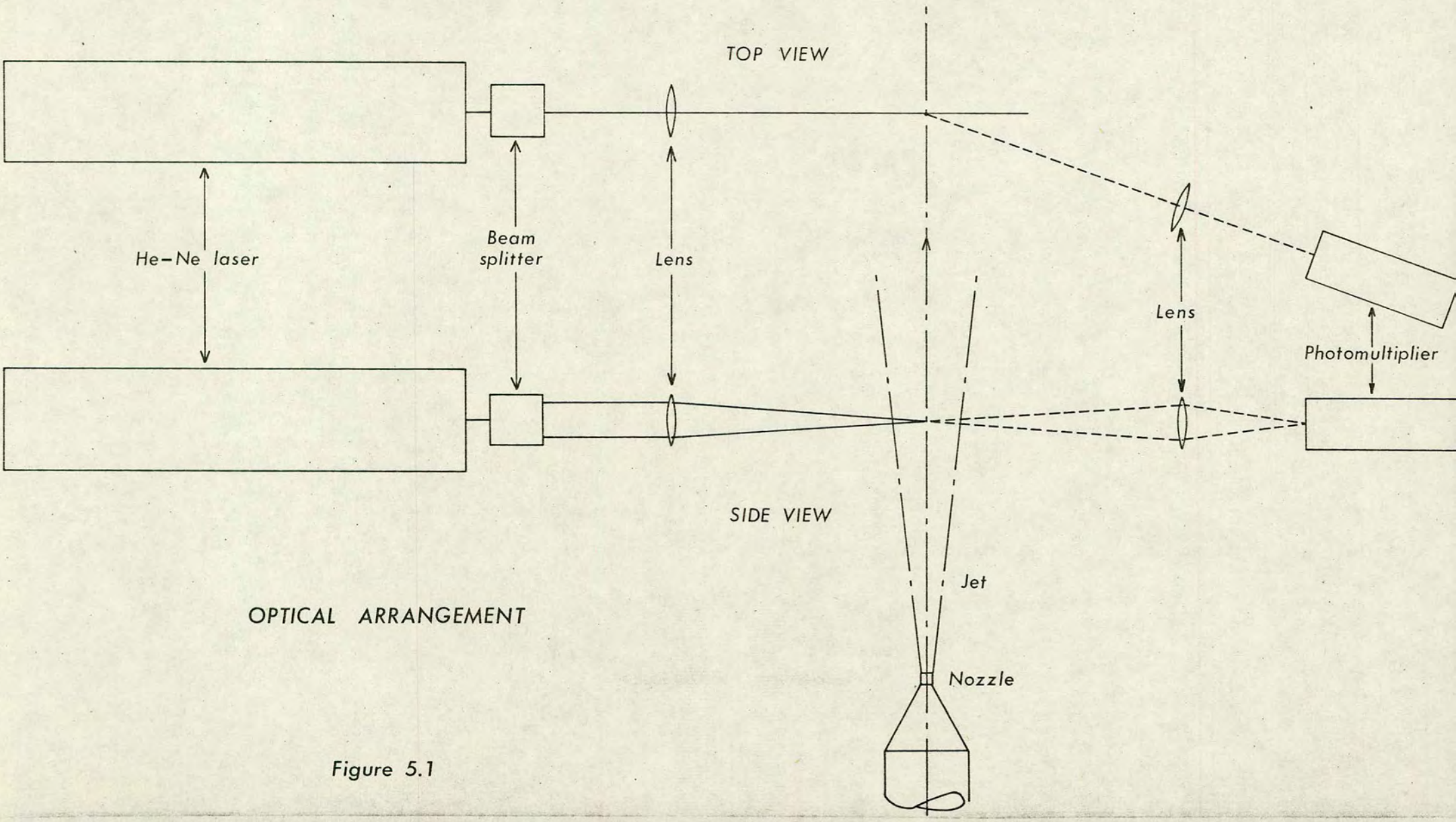

OPTICAL ARRANGEMENT

Figure 5.1

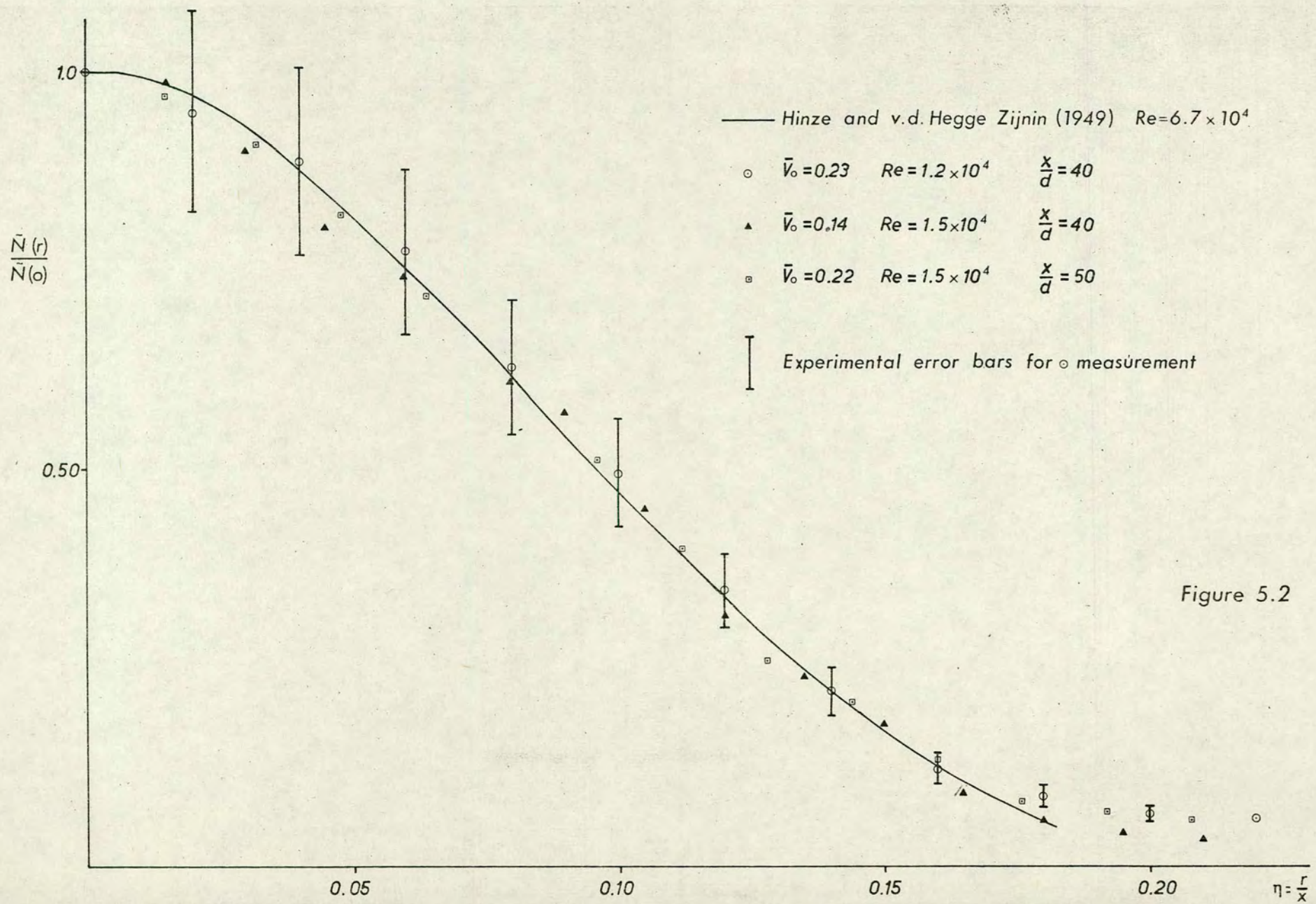
1.0
0.50
$\frac{\bar{N}(r)}{\bar{N}(o)}$
0.05
0.10
0.15
0.20
$\eta = \frac{r}{x}$
Hinze and v.d. Hegge Zijnin (1949) Re=6.7 × 10⁴
$\bar{V}_o$ =0.23 Re = 1.2 ×10⁴ $\frac{x}{d}$ =40
$\bar{V}_o$ =0.14 Re = 1.5×10⁴ $\frac{x}{d}$ =40
$\bar{V}_o$ =0.22 Re = 1.5 × 10⁴ $\frac{x}{d}$ = 50
Experimental error bars for ⊙ measurement

Figure 5.2

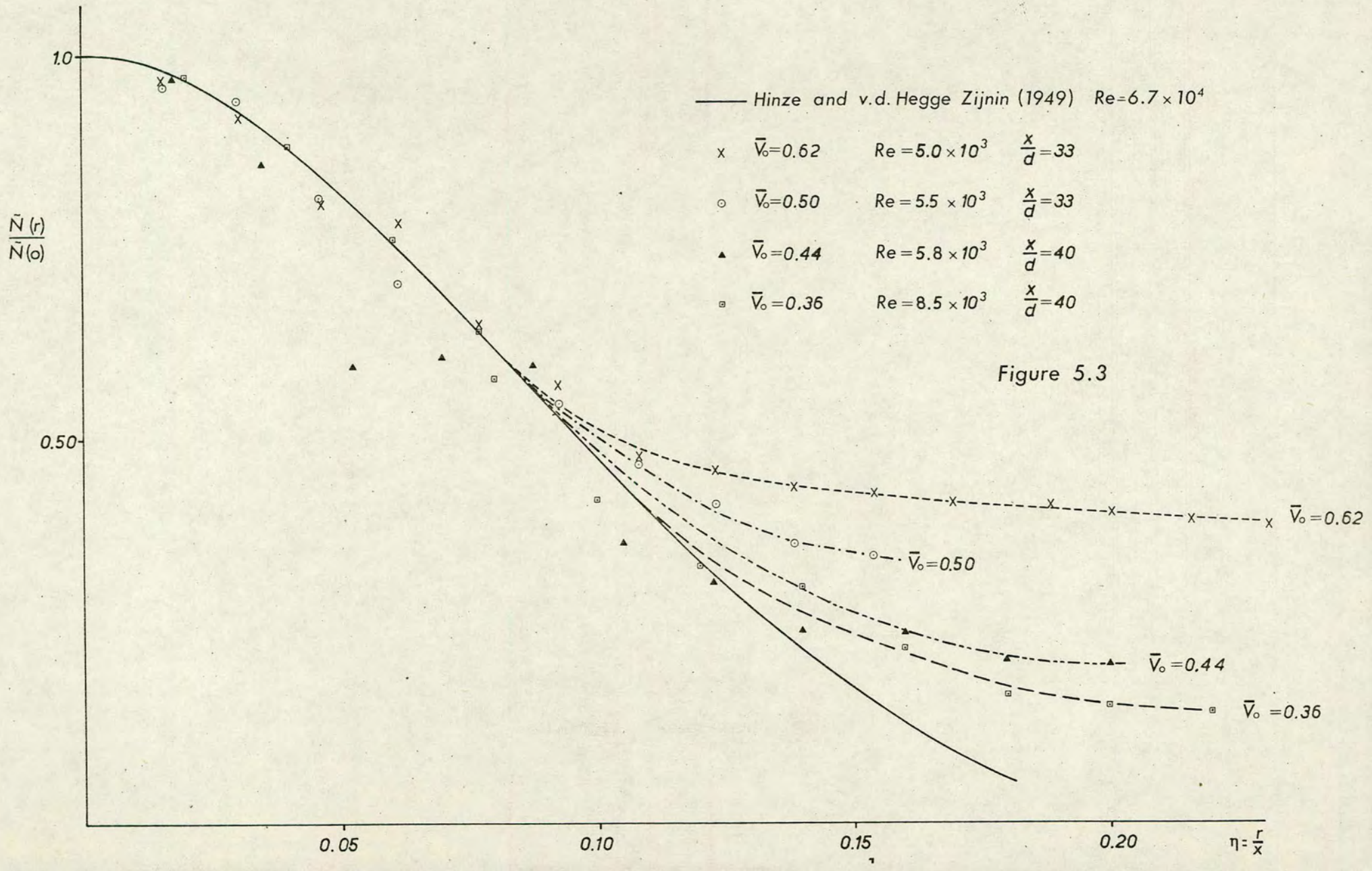
1.0
0.50
$\frac{\tilde{N}(r)}{\tilde{N}(o)}$
0.05
0.10
0.15
0.20
$\eta = \frac{r}{x}$
Hinze and v.d. Hegge Zijnin (1949) Re=6.7 × 10⁴
$\bar{V}_o$=0.62 Re = 5.0 × 10³ $\frac{x}{d}$=33
$\bar{V}_o$=0.50 Re = 5.5 × 10³ $\frac{x}{d}$=33
$\bar{V}_o$=0.44 Re = 5.8 × 10³ $\frac{x}{d}$=40
$\bar{V}_o$=0.36 Re = 8.5 × 10³ $\frac{x}{d}$=40
$\bar{V}_o$=0.62
$\bar{V}_o$=0.50
$\bar{V}_o$=0.44
$\bar{V}_o$=0.36

Figure 5.3

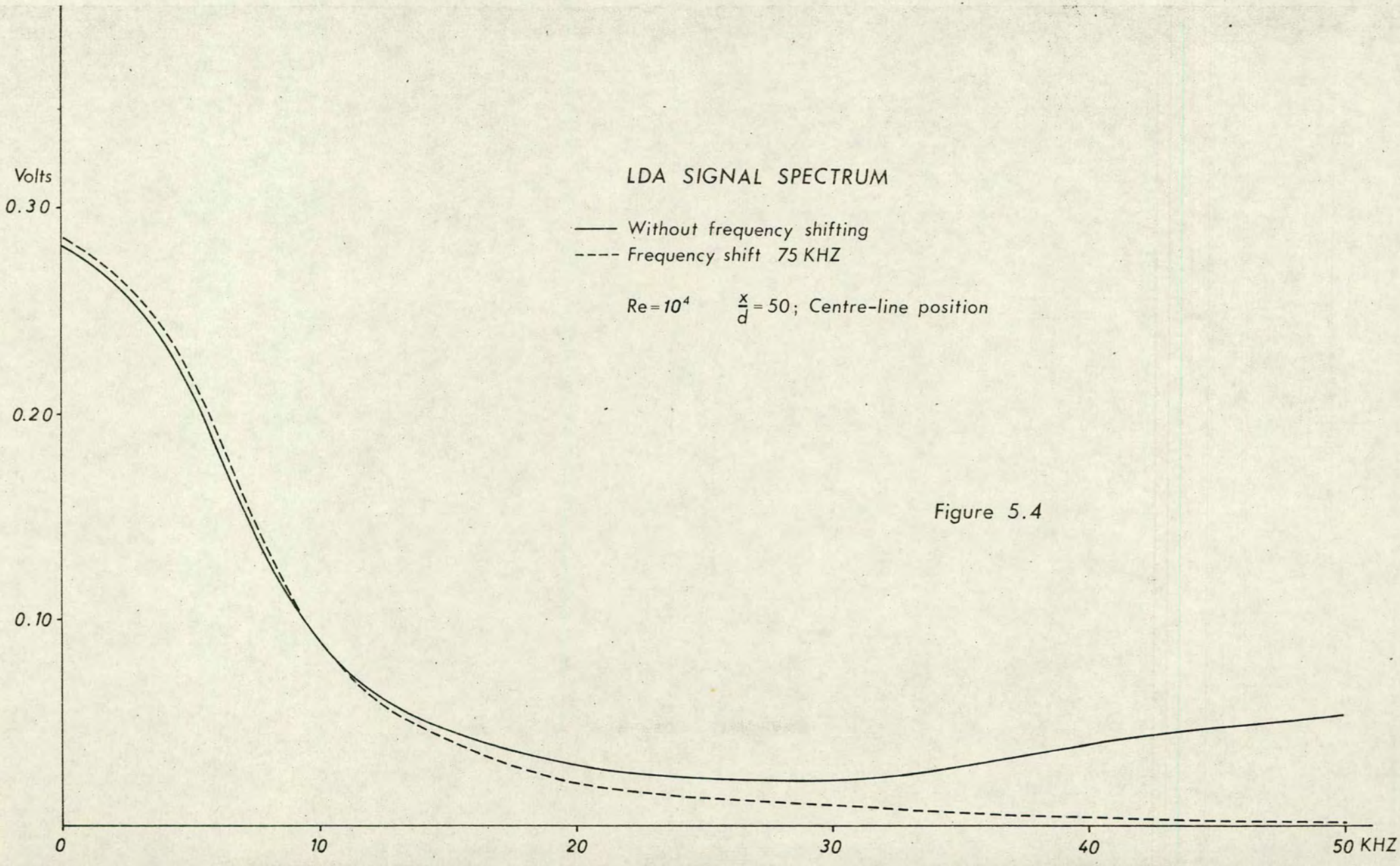
LDA SIGNAL SPECTRUM
Without frequency shifting
Frequency shift 75 KHZ
Re = 10⁴ x/d = 50; Centre-line position
Volts
0.30
0.20
0.10
0
10
20
30
40
50 KHZ

Figure 5.4

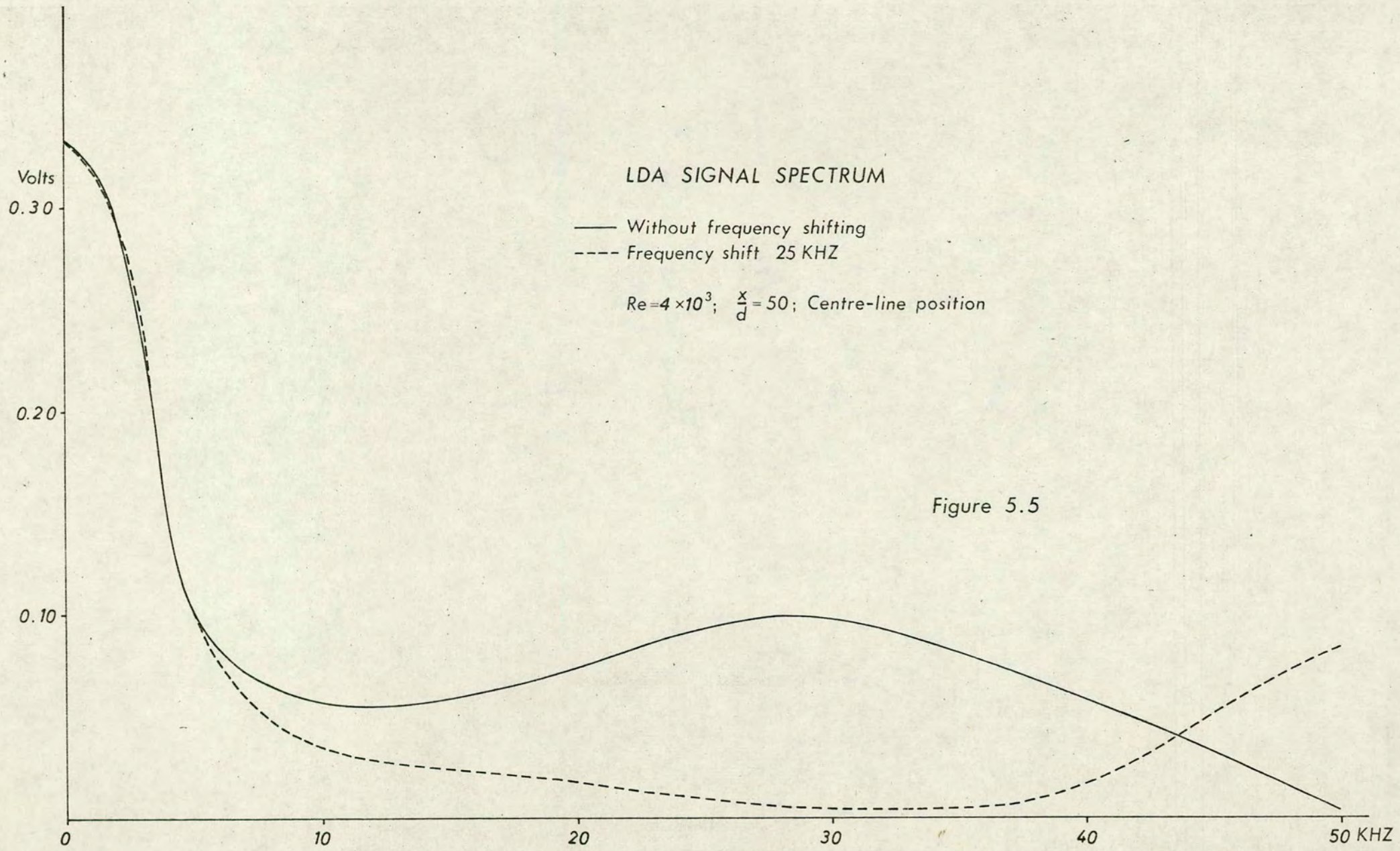
LDA SIGNAL SPECTRUM
Without frequency shifting
Frequency shift 25 KHZ
Re = 4 ×10³; x/d = 50; Centre-line position
Volts
0.30
0.20
0.10
0
10
20
30
40
50 KHZ

Figure 5.5

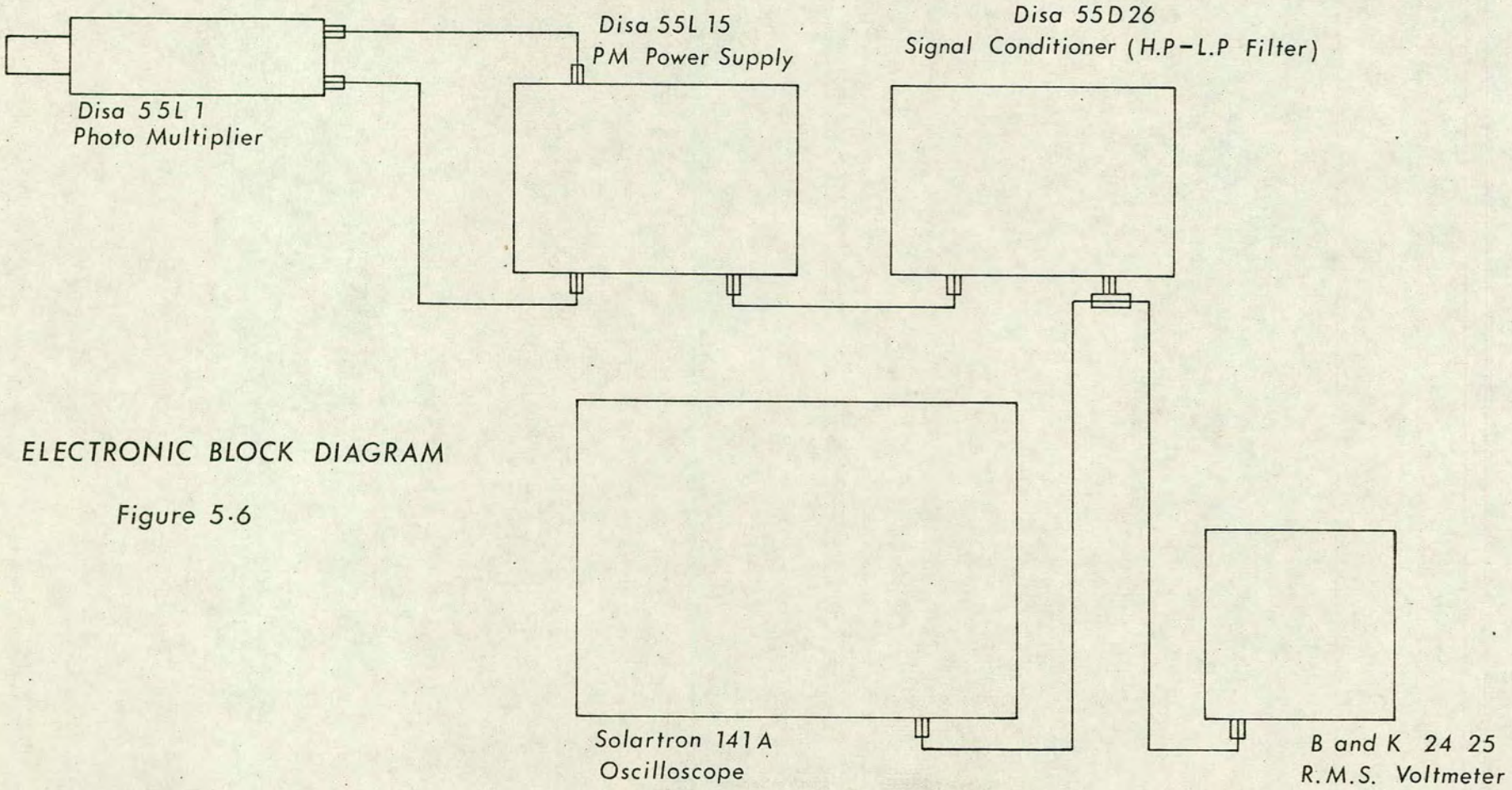

ELECTRONIC BLOCK DIAGRAM

Figure 5.6

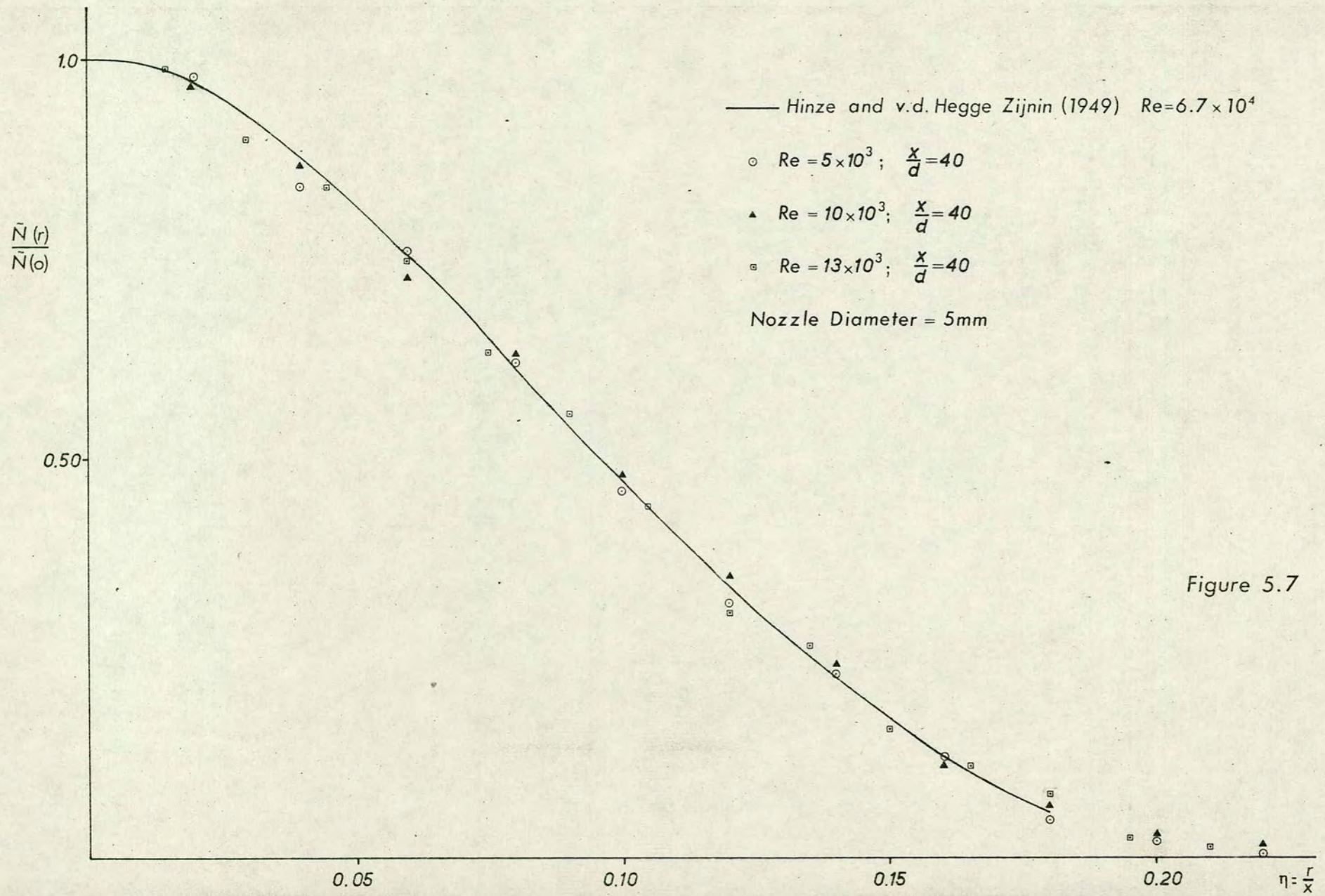
1.0
0.50
$\frac{\bar{N}(r)}{\bar{N}(o)}$
0.05
0.10
0.15
0.20
$\eta = \frac{r}{x}$
Hinze and v.d. Hegge Zijnin (1949) Re=6.7 × 10⁴
Re = 5 × 10³ ; $\frac{x}{d}$ = 40
Re = 10 × 10³; $\frac{x}{d}$ = 40
Re = 13 × 10³; $\frac{x}{d}$ = 40
Nozzle Diameter = 5mm

Figure 5.7

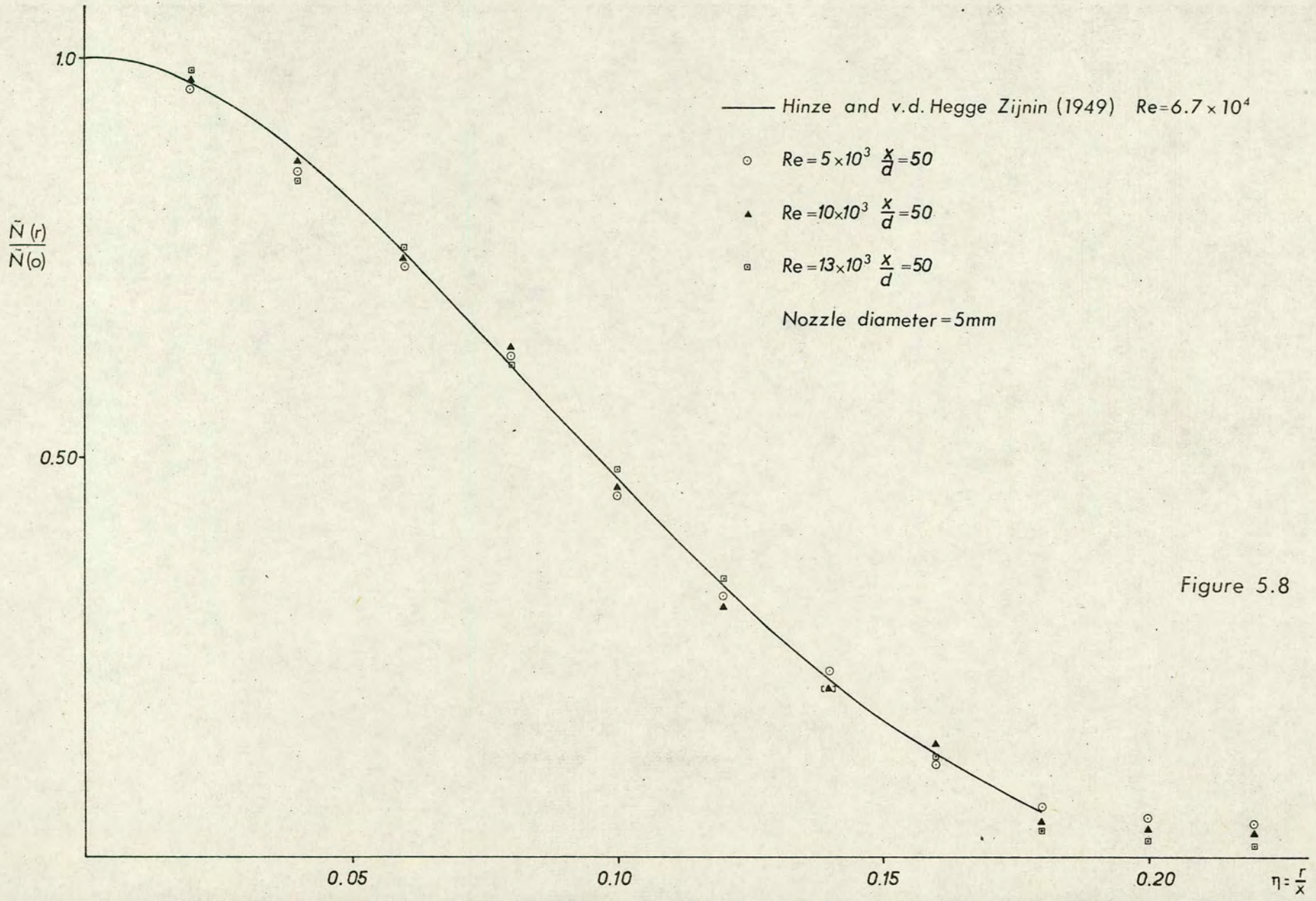
1.0
0.50
$\frac{\tilde{N}(r)}{\tilde{N}(o)}$
0.05
0.10
0.15
0.20
$\eta = \frac{r}{x}$
Hinze and v.d. Hegge Zijnin (1949) Re=6.7 × 10⁴
Re=5×10³ $\frac{x}{d}$=50
Re=10×10³ $\frac{x}{d}$=50
Re=13×10³ $\frac{x}{d}$=50
Nozzle diameter=5mm

Figure 5.8

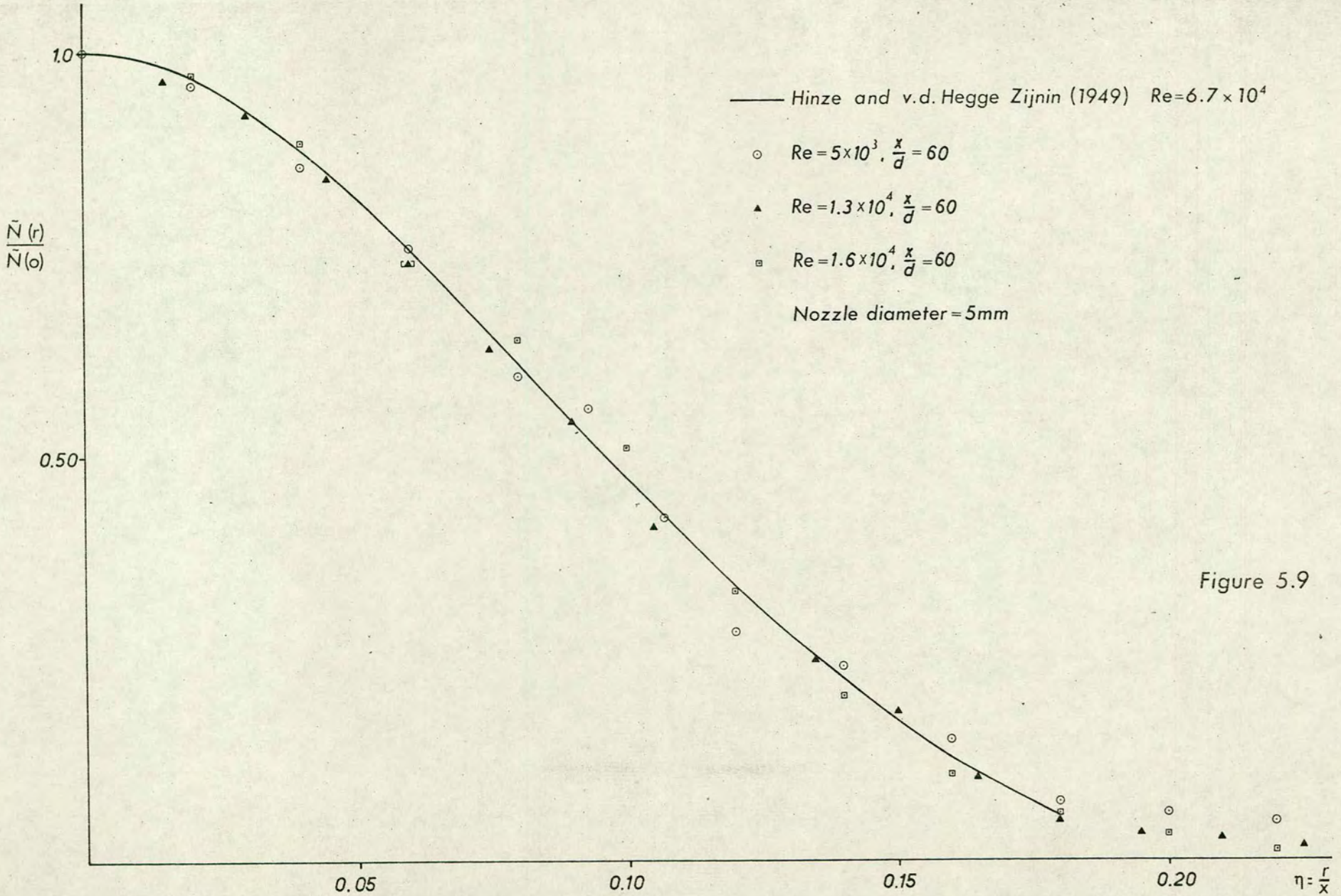
1.0
0.50
$\frac{\tilde{N}(r)}{\tilde{N}(o)}$
0.05
0.10
0.15
0.20
$\eta = \frac{r}{x}$
Hinze and v.d. Hegge Zijnin (1949) Re=6.7 × 10⁴
Re = 5×10³, x/d = 60
Re = 1.3×10⁴, x/d = 60
Re = 1.6×10⁴, x/d = 60
Nozzle diameter = 5mm

Figure 5.9

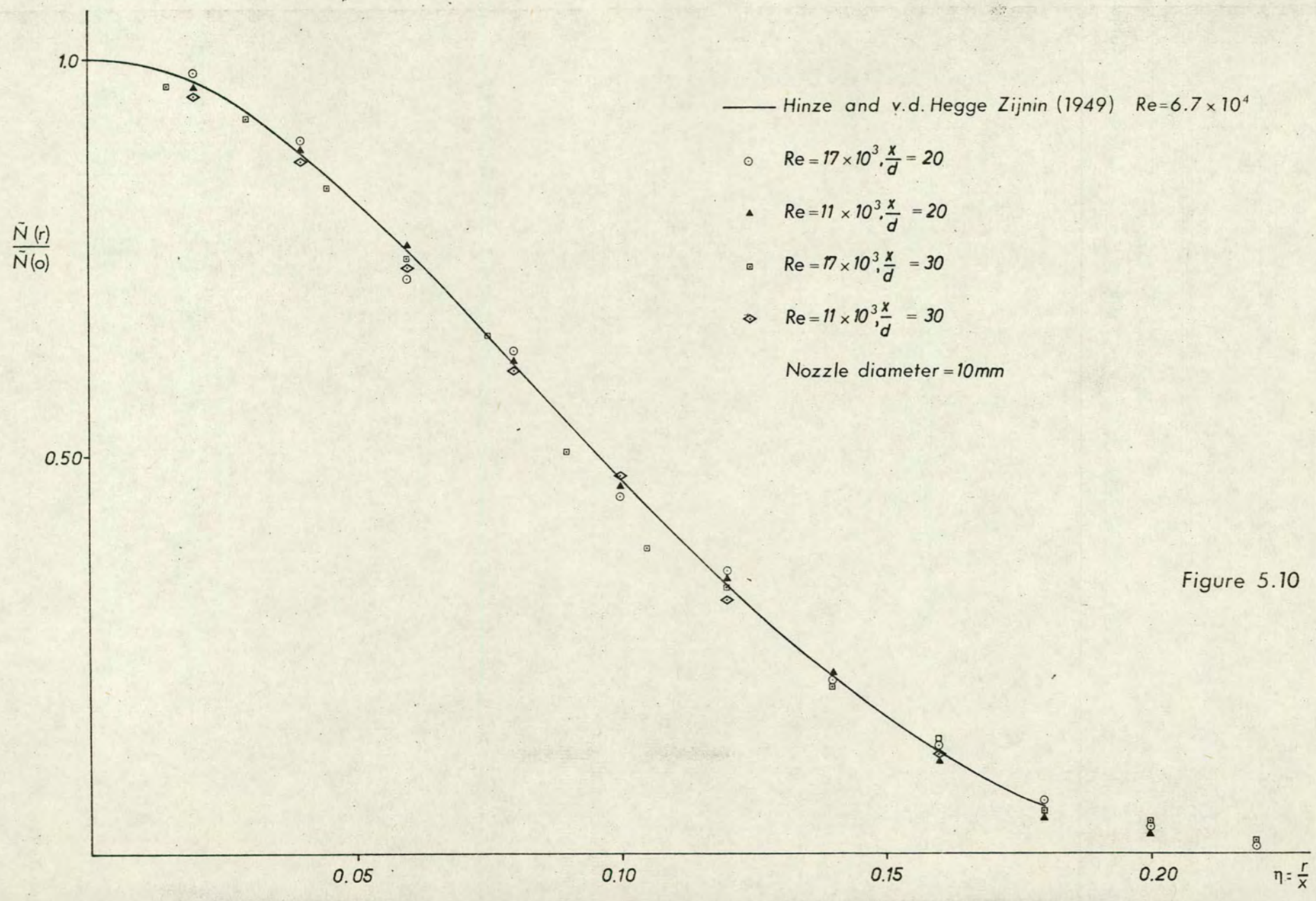
1.0
0.50
$\frac{\tilde{N}(r)}{\tilde{N}(o)}$
0.05
0.10
0.15
0.20
$\eta = \frac{r}{x}$
Hinze and v.d. Hegge Zijnin (1949) $Re = 6.7 \times 10^4$
$Re = 17 \times 10^3, \frac{x}{d} = 20$
$Re = 11 \times 10^3, \frac{x}{d} = 20$
$Re = 17 \times 10^3, \frac{x}{d} = 30$
$Re = 11 \times 10^3, \frac{x}{d} = 30$
Nozzle diameter = 10mm

Figure 5.10

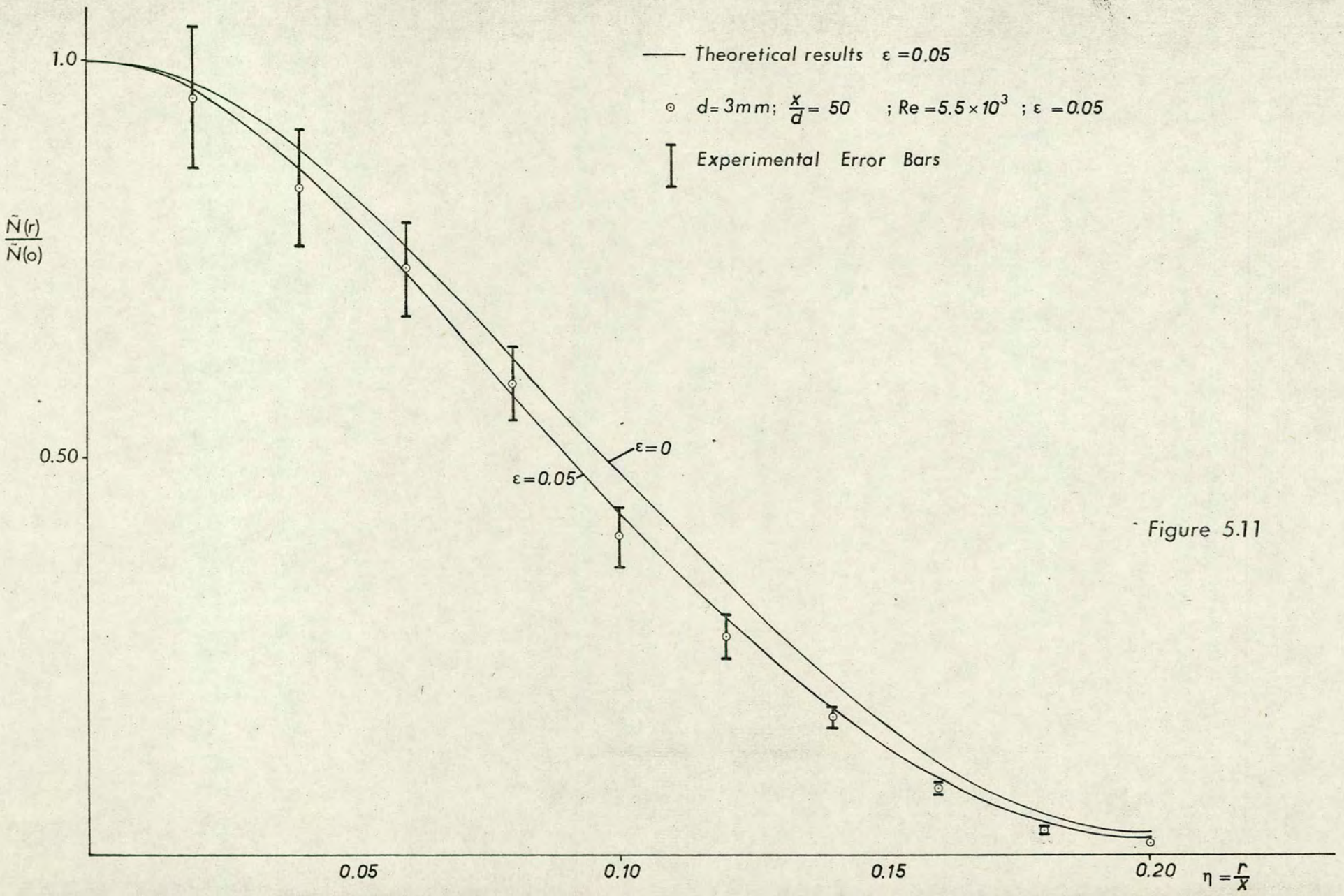
Theoretical results ε =0.05
d= 3mm; x/d= 50 ; Re =5.5×10^3 ; ε =0.05
Experimental Error Bars
1.0
0.50
N̄(r)/N̄(o)
ε=0
ε=0.05
0.05
0.10
0.15
0.20
η = r/x

Figure 5.11

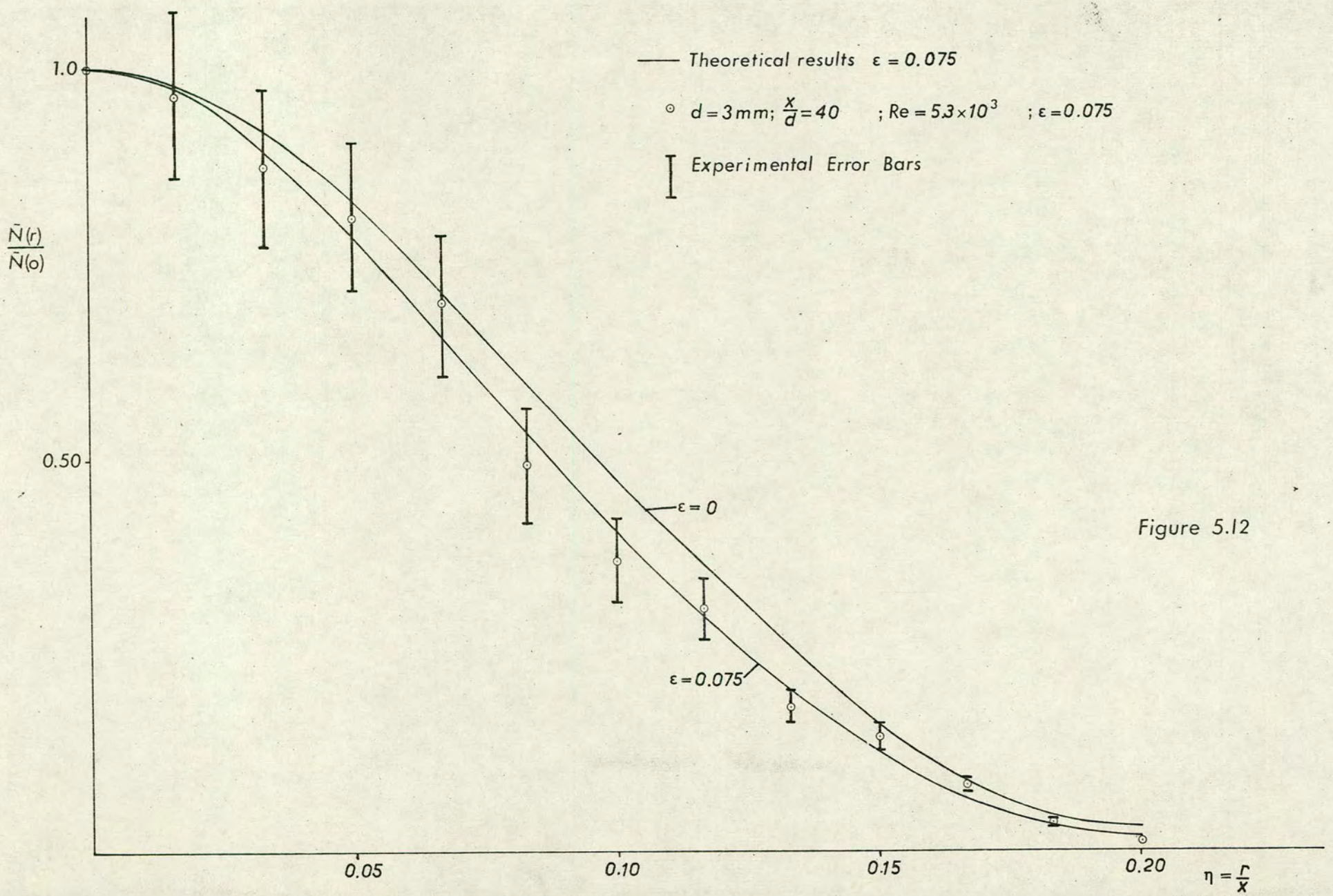
Theoretical results ε = 0.075
d = 3mm; x/d = 40 ; Re = 5.3×10³ ; ε = 0.075
Experimental Error Bars
1.0
0.50
N̄(r)/N̄(o)
ε = 0
ε = 0.075
0.05
0.10
0.15
0.20
η = r/x

Figure 5.12

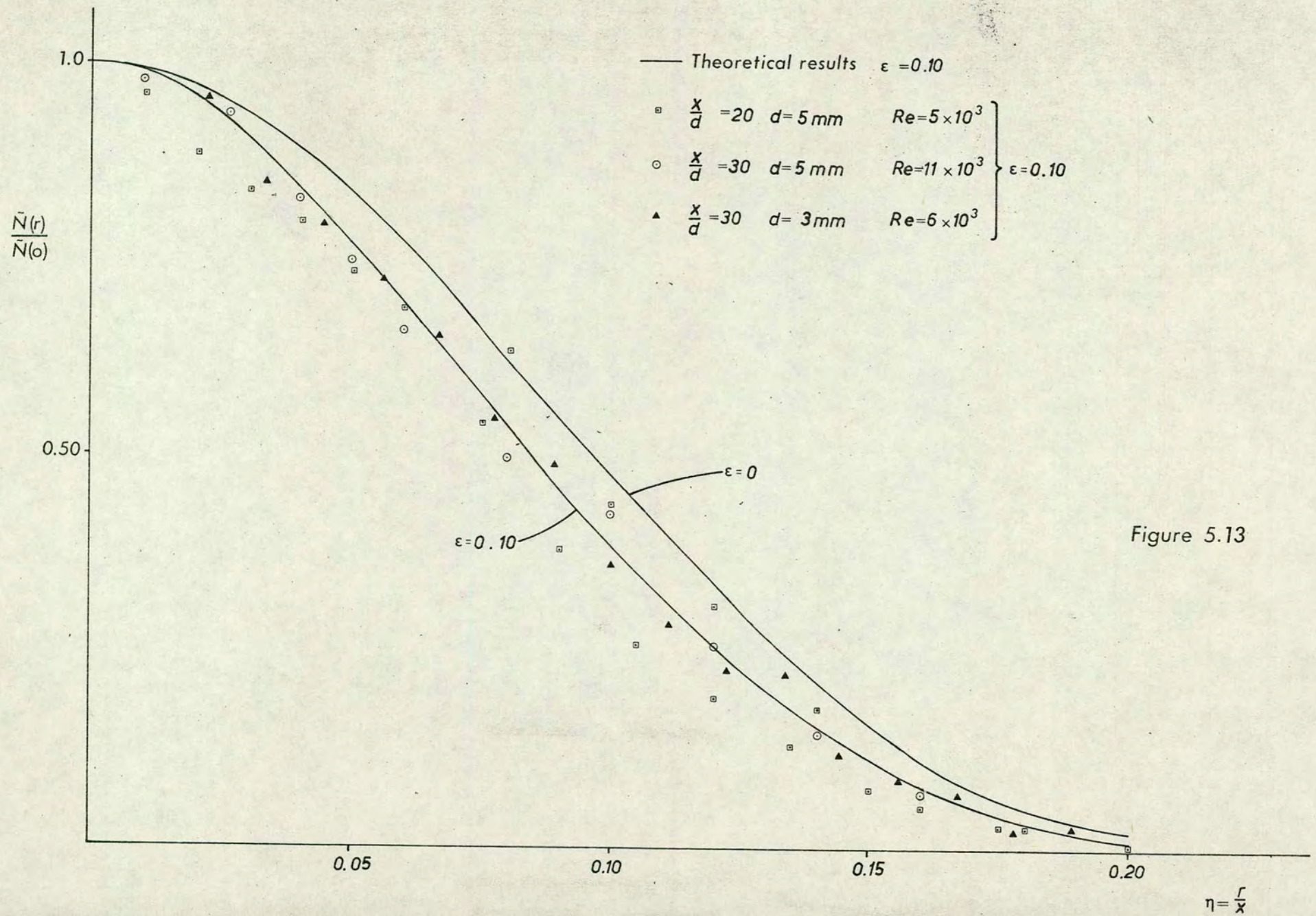
Theoretical results ε =0.10
x/d =20 d= 5 mm Re=5×10³
x/d =30 d=5 mm Re=11×10³
x/d =30 d= 3mm Re=6×10³
ε=0.10
1.0
0.50
N̄(r)/N̄(o)
ε=0
ε=0.10
0.05
0.10
0.15
0.20
η=r/x

Figure 5.13

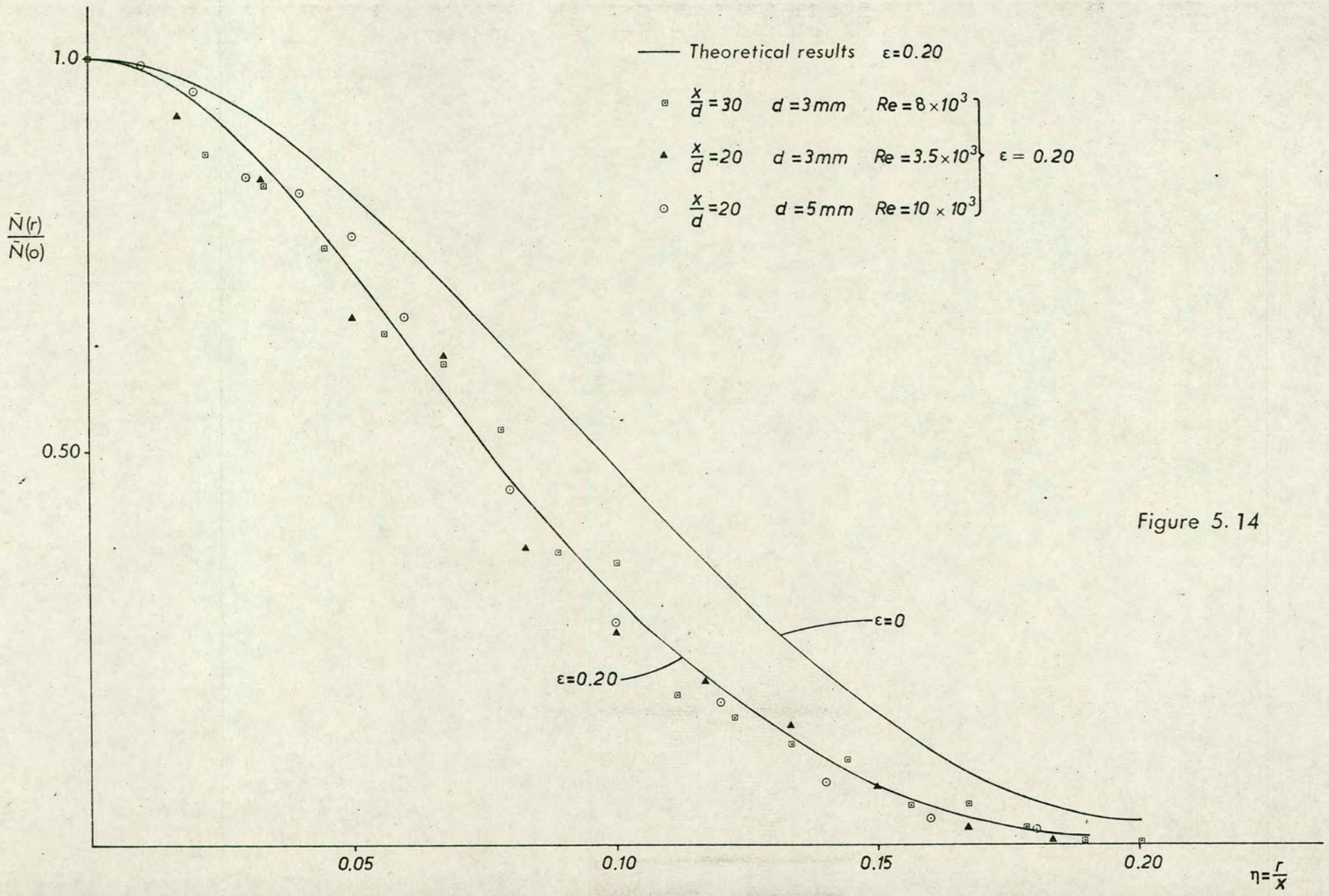
Theoretical results ε=0.20
x/d=30 d=3mm Re=8×10³
x/d=20 d=3mm Re=3.5×10³
x/d=20 d=5mm Re=10×10³
ε = 0.20
1.0
0.50
Ñ(r)/Ñ(o)
ε=0
ε=0.20
0.05
0.10
0.15
0.20
η=r/x

Figure 5.14

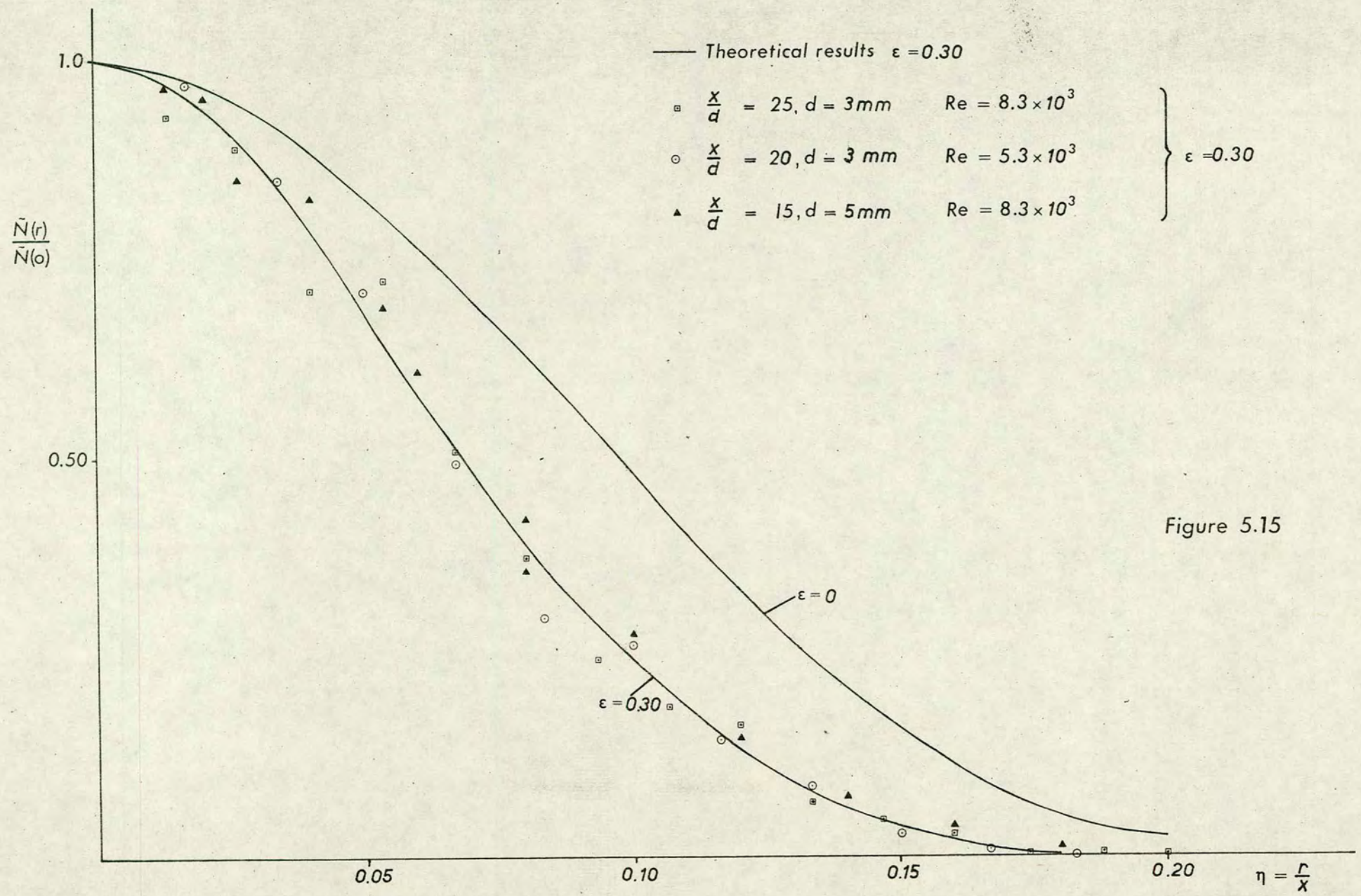
Theoretical results ε = 0.30
x/d = 25, d = 3mm Re = 8.3 × 10^3
x/d = 20, d = 3 mm Re = 5.3 × 10^3
x/d = 15, d = 5mm Re = 8.3 × 10^3
ε = 0.30
1.0
0.50
Ñ(r)/Ñ(o)
ε = 0
ε = 0.30
0.05
0.10
0.15
0.20
η = r/x

Figure 5.15

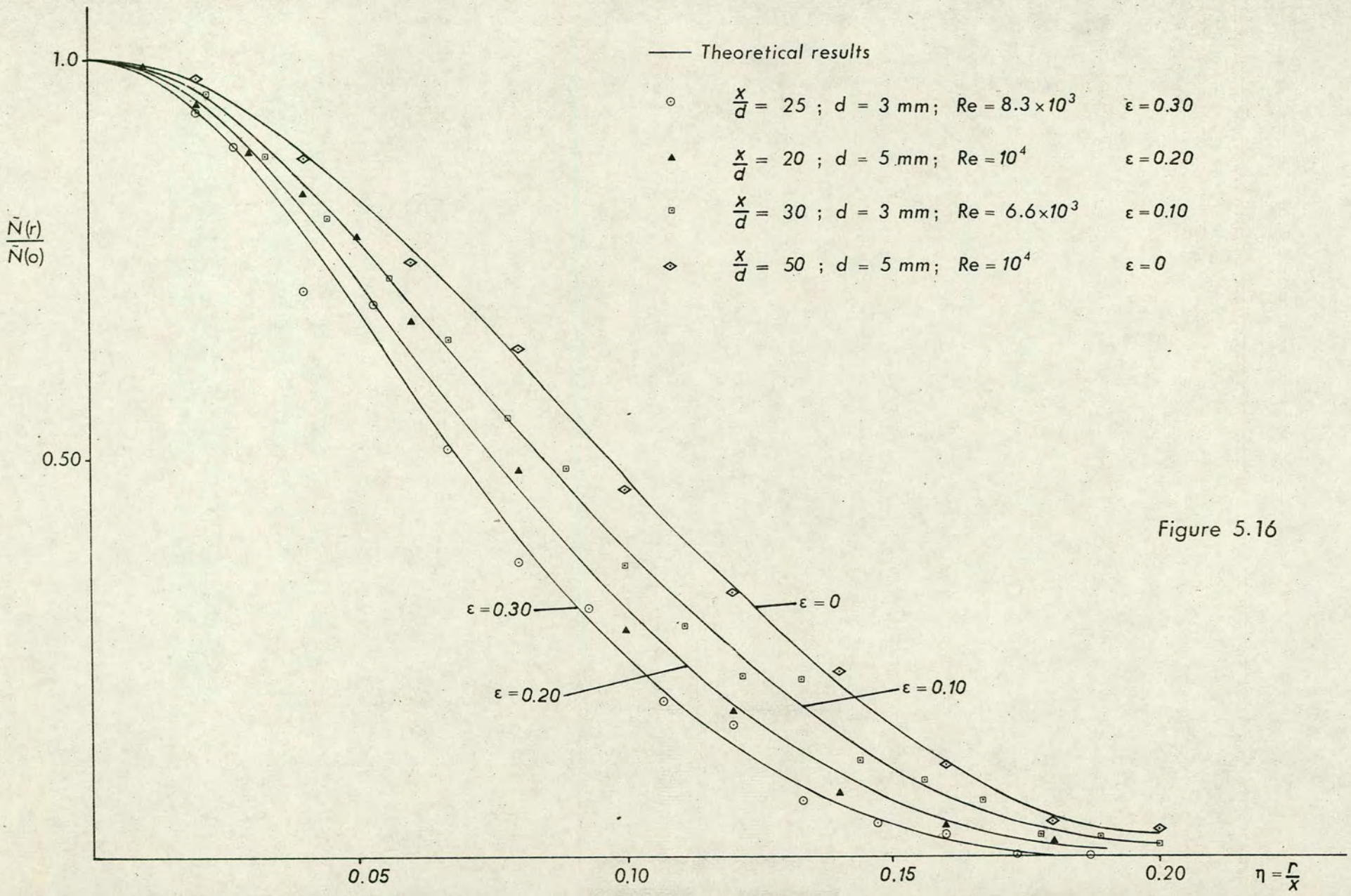
Theoretical results
x/d = 25 ; d = 3 mm; Re = 8.3×10³ ε = 0.30
x/d = 20 ; d = 5 mm; Re = 10⁴ ε = 0.20
x/d = 30 ; d = 3 mm; Re = 6.6×10³ ε = 0.10
x/d = 50 ; d = 5 mm; Re = 10⁴ ε = 0
1.0
0.50
N̄(r)/N̄(o)
0.05
0.10
0.15
0.20
η = r/x
ε = 0.30
ε = 0.20
ε = 0
ε = 0.10

Figure 5.16

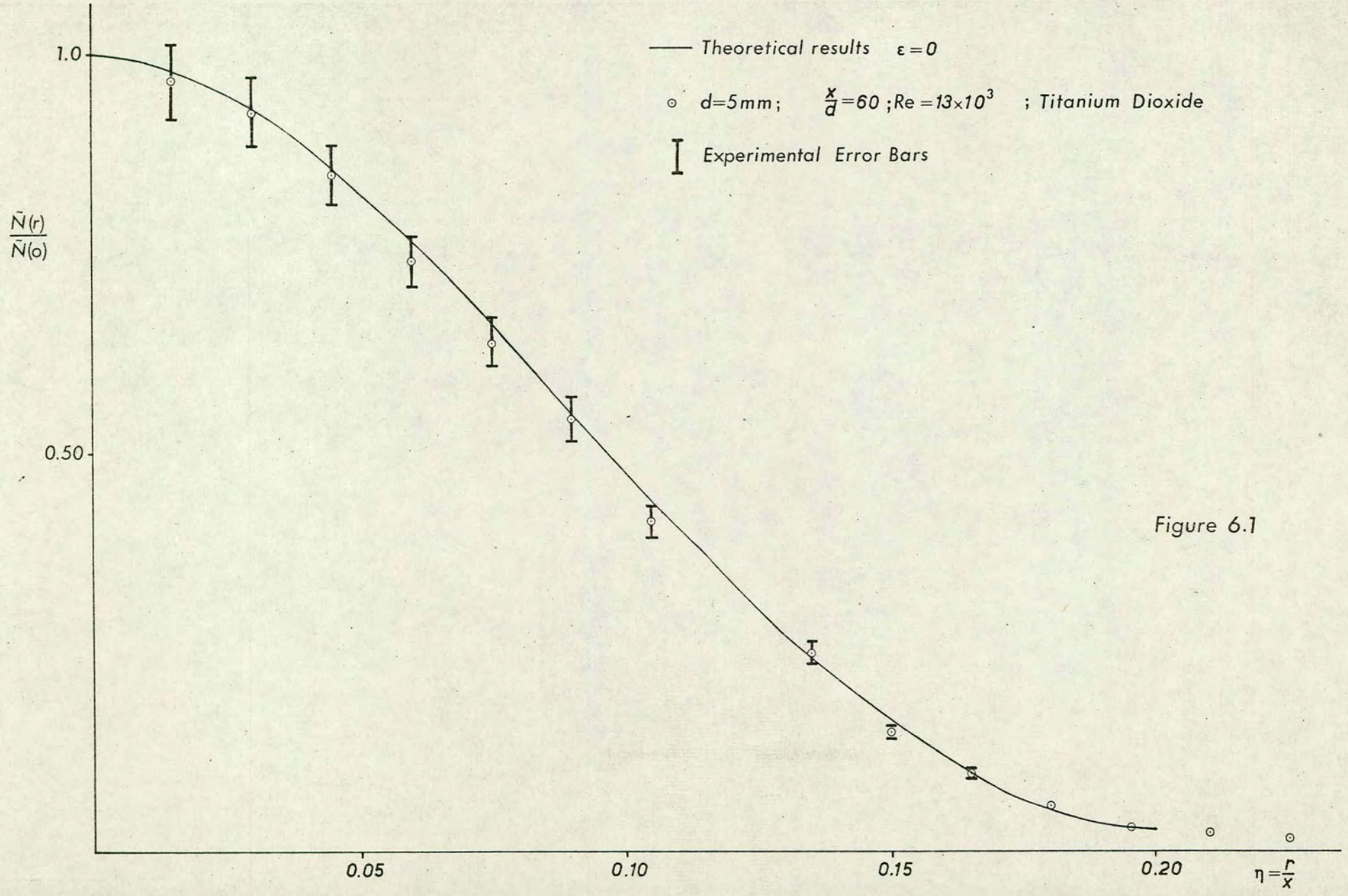
Theoretical results ε = 0
d=5mm; x/d=60 ; Re = 13×10^3 ; Titanium Dioxide
Experimental Error Bars
1.0
0.50
N̄(r)/N̄(o)
0.05
0.10
0.15
0.20
η = r/x

Figure 6.1

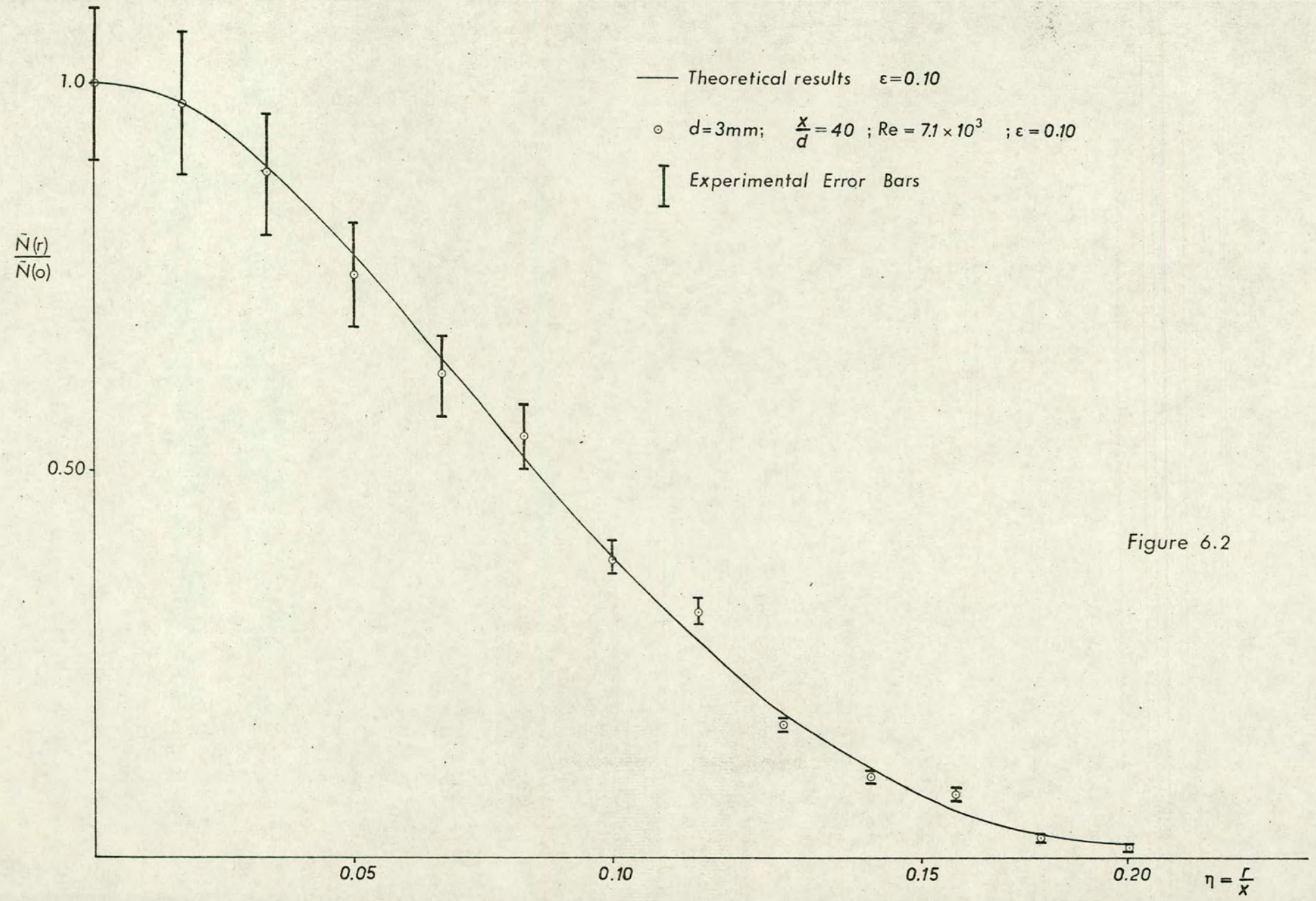
Theoretical results ε=0.10
d=3mm; x/d=40 ; Re = 7.1 × 10^3 ; ε = 0.10
Experimental Error Bars
1.0
0.50
N̄(r)/N̄(o)
0.05
0.10
0.15
0.20
η = r/x

Figure 6.2

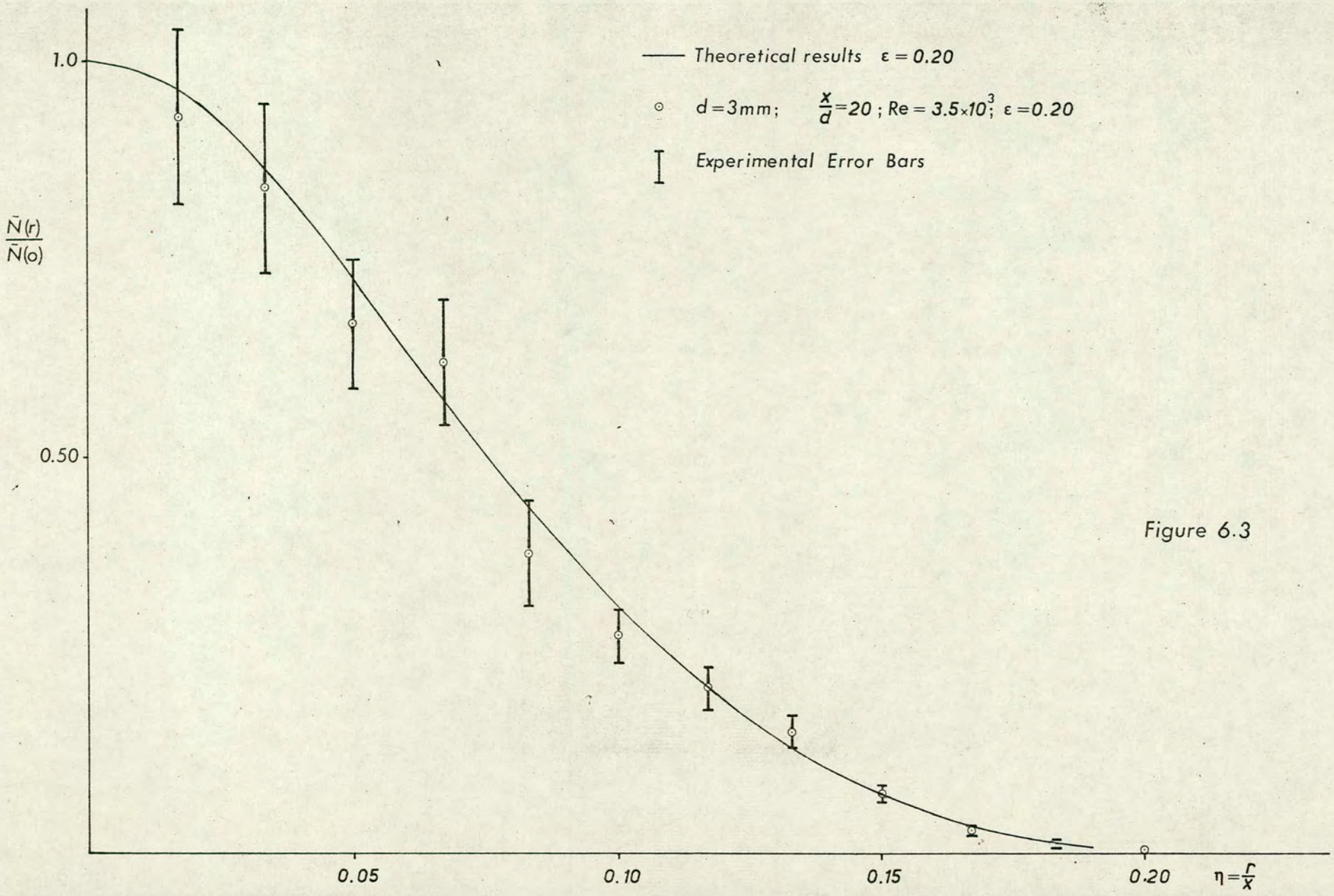
Theoretical results ε = 0.20
d = 3mm; x/d = 20 ; Re = 3.5×10^3; ε = 0.20
Experimental Error Bars
1.0
0.50
N̄(r)/N̄(o)
0.05
0.10
0.15
0.20
η = r/x

Figure 6.3

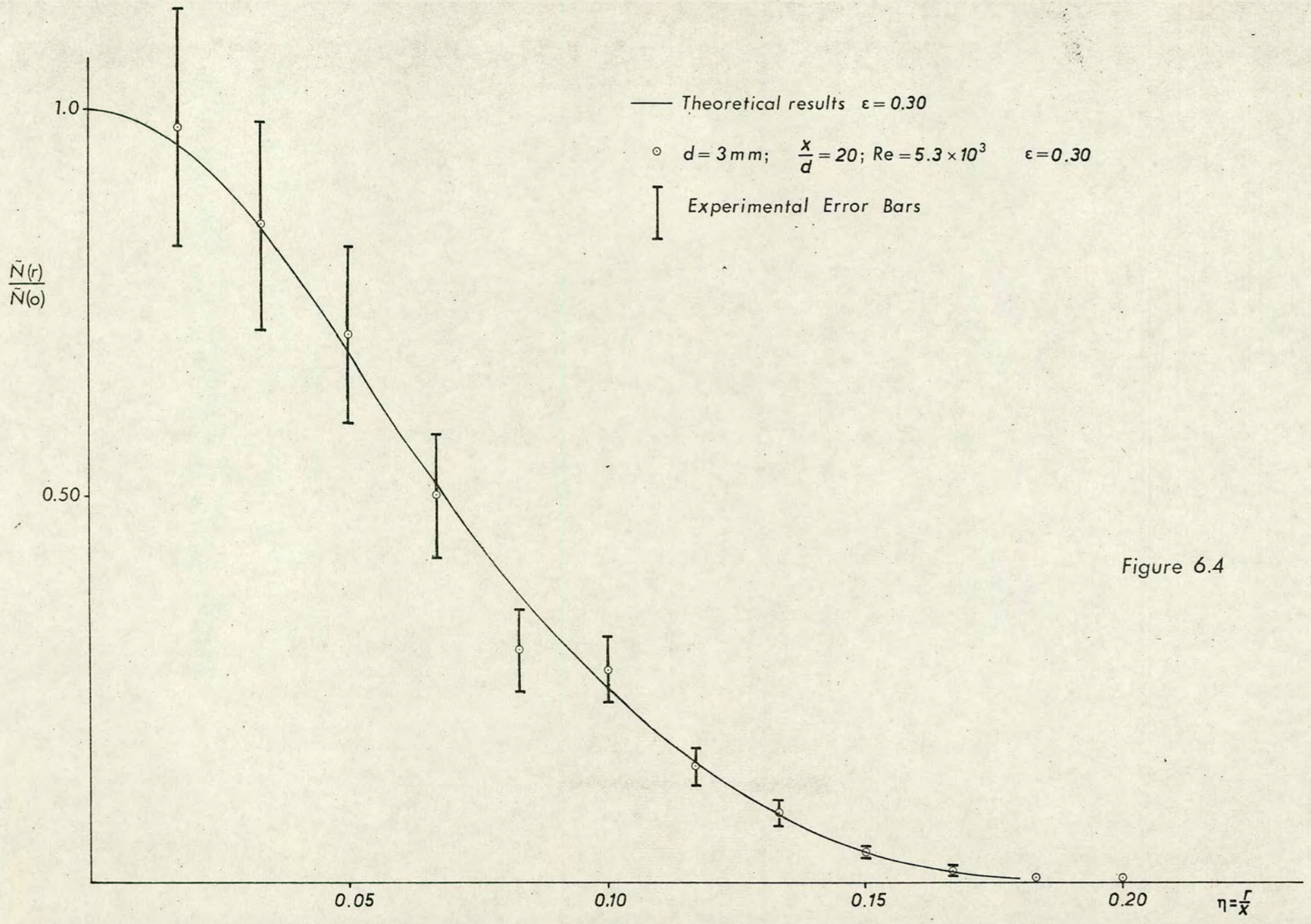
Theoretical results ε = 0.30
d = 3 mm; x/d = 20; Re = 5.3 × 10³ ε = 0.30
Experimental Error Bars
1.0
0.50
N̄(r)/N̄(o)
0.05
0.10
0.15
0.20
η = r/x

Figure 6.4

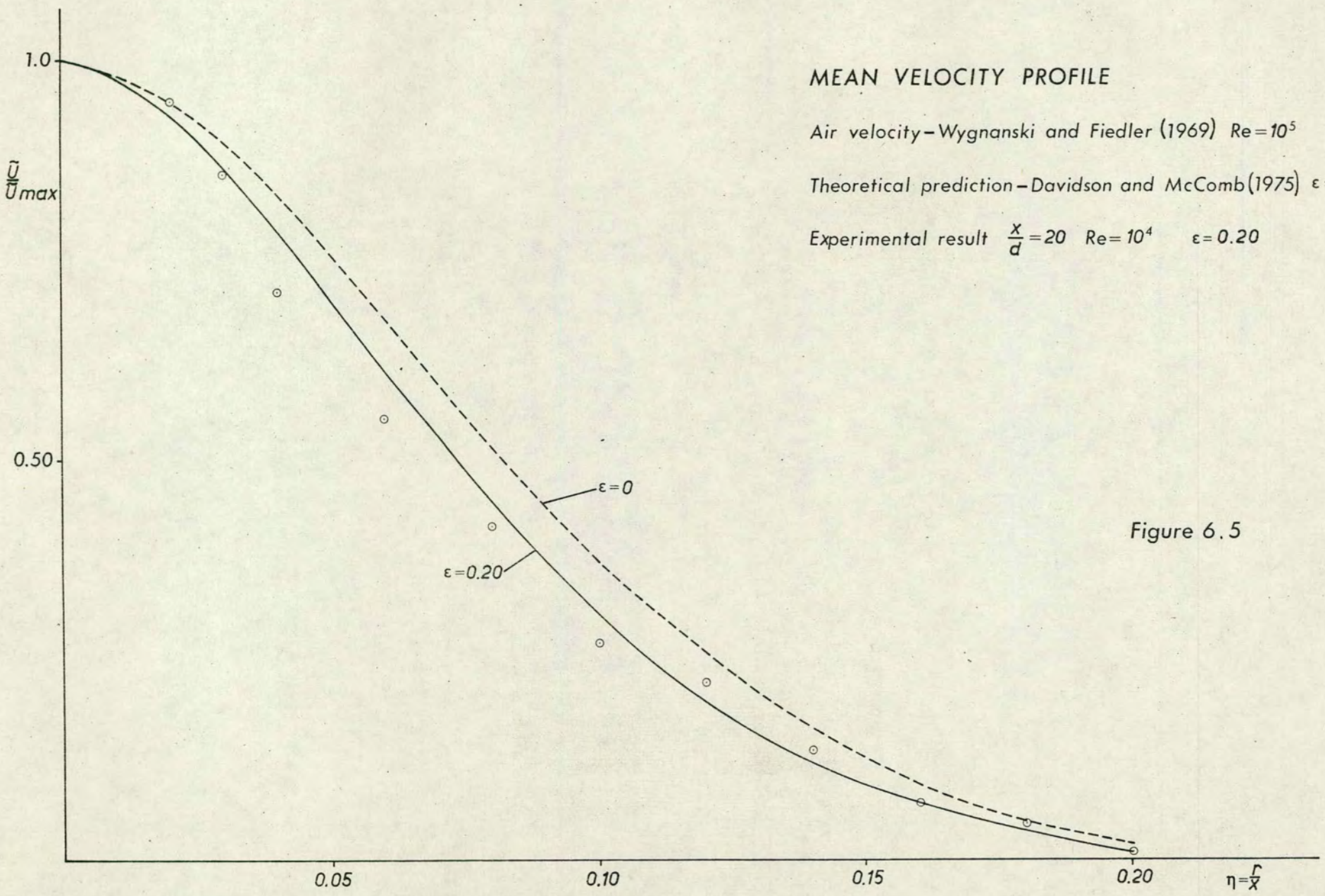
MEAN VELOCITY PROFILE
Air velocity – Wygnanski and Fiedler (1969) Re = 10^5
Theoretical prediction – Davidson and McComb (1975) ε = 0.20
Experimental result x/d = 20 Re = 10^4 ε = 0.20
1.0
0.50
Ũ/Ũmax
ε = 0
ε = 0.20
0.05
0.10
0.15
0.20
η = r/x

Figure 6.5